DNA Methylation of the POMC Gene:
Ontogenetic, Phylogenetic, and Functional Aspects

Dissertation

zur Erlangung des akademischen Grades
doctor rerum naturalium
(Dr. rer. nat.)
im Fach Biologie
eingereicht an der

Mathematisch-Naturwissenschaftlichen Fakultät I
der Humboldt-Universität zu Berlin

von

Diplom-Ernährungswissenschaftlerin Mona Mischke

Präsident der Humboldt-Universität zu Berlin
Prof. Dr. Jan-Hendrik Olbertz

Dekan der Mathematisch-Naturwissenschaftlichen Fakultät I
Prof. Dr. Andreas Herrmann

Gutachter/in: 1. Prof. Dr. Gudrun Brockmann
2. Prof. Dr. Heiko Krude
3. Prof. Dr. Werner Kloas

Datum der Einreichung: 14.07.2011
Datum der Promotion: 16.12.2011

Abstract deutsch

Adipositas ist eine polymorphe chronische Erkrankung mit epidemischer Prävalenz. Im katabolen Leptin-Melanocortin-Signalweg ist das Proopiomelanocortin Gen (POMC) ein zentrales Element, das bei Dysfunktion massive Adipositas bewirken kann. Auch eine kürzlich identifizierte intragenische Methylierungsvariante des POMC wurde mit Adipositas assoziiert und deutet somit auf eine mögliche epigenetische Modulation des Gewichtsphänotyps hin. Zur Aufklärung der Relevanz, Stabilität und Entwicklung dieser epigenetischen Modifikation wurden die Funktionalität, Ontogenese und Phylogenese der POMC DNA-Methylierung untersucht.

In vitro Analysen zeigten DNA-Methylierungsabhängige Promoteraktivität beider CpG-Inseln (CGIs) des POMC. Diese hier erstmals beschriebene Transkriptionsaktivität der intragenischen CGI weist auf einen alternativen Promoter des POMC hin.

Hinsichtlich der Ontogenese konnten in Mensch und Maus postnatal stabile DNA-Methylierungsmuster mit interindividueller Konservierung für beide CGIs des POMC identifiziert werden. Zusätzlich erwiesen sich Gewebeunabhängigkeit der DNA-Methylierungsmuster und ihre pränatale Ausbildung zwischen dem Blastocystenstadium und der frühen Organogenese in der Maus.

Die POMC DNA-Methylierungsmuster upstream des Exon3 unterscheiden sich in Mensch und Maus. Der mögliche Einfluss von primatenspezifischen Alu-Elementen im Intron2 des POMC hierauf wurde in verschiedenen Primatenfamilien analysiert. Die Ergebnisse zeigen eine bedingte Assoziation der Alu-Elemente mit der DNA-Methylierung in der entsprechenden Region, lassen jedoch auch weitere Einflussfaktoren vermuten.

Insgesamt zeigt diese Arbeit, dass die POMC DNA-Methylierung artspezifisch konserviert ist und in der frühen Embryogenese, vermutlich Alu-abhängig, ausgebildet wird. Dabei könnten stochastische Variationen der DNA-Methylierung die POMC-Aktivität beeinflussen und somit das Risiko für Adipositas erhöhen.

Schlagworte

Proopiomelanocortin (POMC), Adipositas, Epigenetik, DNA Methylierung, Alu-Elemente, alternativer Promoter, Pan troglodytes, Gorilla gorilla, Pongo pygmaeus, Papio hamadryas, Macaca mulatta, Callithrix jacchus, Galago senegalensis, Eulemur macaco

Abstract English

Obesity is a polymorphic chronic disease with epidemic prevalence. Within the catabolic leptin-melanocortin signaling pathway pre-proopiomelanocortin (POMC) is a pivotal element. Dysfunction of POMC, e.g. due to mutations, can cause severe obesity. Moreover, a recently identified intragenic methylation variant of POMC was found to be associated with obesity. Therefore, this indicates potential epigenetic modulation of the weight phenotype. To gain further insight into the relevance, stability, and origin of this epigenetic modification, the functionality, ontogenesis, and phylogenesis of the POMC DNA methylation patterns were analyzed.

In vitro analyses revealed DNA methylation-dependent promoter activity of both CpG islands (CGIs) of POMC. Thereby, the intragenic CGI was identified as a potential alternative promoter of *POMC*, which has not been described before.

Regarding the ontogenesis, postnatally stable POMC DNA methylation patterns with interindividual conservation were detected for both CGIs in humans and mice. In addition, it was observed that the POMC DNA methylation patterns are non-tissue-specific, stable upon long time administration of a high fat diet, and develop prenatally between the blastocystal stage and the early organogenesis.

The POMC DNA methylation pattern upstream of exon3 differs in humans and mice. A possible influence of primate-specific Alu elements within the intron2 region of POMC was analyzed in various primate families. Results evince a partial association of the Alu elements with the DNA methylation pattern in this particular region, but also suggest an influence of additional factors.

Overall, this work demonstrates that DNA methylation of the POMC locus is species-specific highly conserved, and that it is established during early embryogenesis, possibly Alu-triggered. In the course of this, stochastic variances of the POMC DNA methylation might influence the POMC activity and consequently alter the risk to develop obesity.

Keywords

pre-proopiomelanocortin (POMC), obesity, epigenetics, DNA methylation, Alu elements, alternative promoter, Pan troglodytes, Gorilla gorilla, Pongo pygmaeus, Papio hamadryas, Macaca mulatta, Callithrix jacchus, Galago senegalensis, Eulemur macaco

Danksagung

Mein Dank ist an alle gerichtet, die mich in den Jahren der Promotion aktiv und passiv unterstützt haben.

Ich danke Prof. Dr. Heiko Krude für die Überlassung des interessanten und herausfordernden Dissertationsthemas und seine zahlreichen Ideen und Anregungen.

Ein besonderer Dank gilt Prof. Dr. Gudrun Brockmann für die Bereitschaft, die vorliegende Arbeit offiziell zu betreuen und für die Bereitstellung von Maus-DNA-Proben.

Dr. Peter Kühnen danke ich herzlich für die aktive Betreuung meiner Arbeit, die Vielzahl eingebrachter Diskussions- und Lösungsansätze und das ergiebige Feedback während des Schreibprozesses.

Etliche Kooperationen haben zum Gelingen dieser Arbeit beigetragen, daher danke ich:

- → Dr. Christian Roos vom Deutschen Primaten Zentrum Göttingen, Christian Adams vom Centrum für Reproduktionsmedizin und Andrologie des Universitätsklinikums Münster und Prof. Dr. Torsten Schöneberg vom Institut für Biochemie der Universität Leipzig für die Zurverfügungstellung von Primaten-DNA-Proben.
- → Der Arbeitsgruppe Developmental Biology/Signal Transduction von Prof. Dr. Birchmeier-Kohler des Max-Delbrück-Centrum für Molekulare Medizin (MDC) in Berlin für die Bereitstellung von Maus-Blastocysten und dem Max Planck Institut für Molekulare Genetik für diverse Maus-Gewebeproben.
- → Maja Klug und dem Institut für Hämatologie und internistische Onkologie des Universitätsklinikums Regensburg für die Zurverfügungstellung des pCpGL- Vektors und den damit zusammenhängenden technischen Support.

Prof. Dr. Josef Köhrle danke ich ausdrücklich für die engagierte Leitung des Graduiertenkolleg 1208 der DFG (‚das mit der Nummer'), welches diese Arbeit finanziell ermöglichte und mir eine zusätzliche endokrinologische Ausbildung beschert hat

Prof. Dr. Lutz Schomburg, dem besten Co-Mentor, den ich mir vorstellen kann, danke ich dafür, daß er mir immer wieder das Licht im Forscherleben zeigen konnte.

Die Mithilfe und Unterstützung von PD Dr. Heike Biebermann in praktischen und formellen Fragen, Dr. Torsten Plösch als motivierende Zweitmeinung mit Rotstifteinsatz und Dr. Peter Hofmann bei spezifischen Problematiken waren maßgeblich für diese Arbeit. Vielen Dank hierfür.

Auch den Mitgliedern meiner animierenden und unterstützenden Arbeitsgruppe des Instituts für experimentelle Pädiatrische Endokrinologie möchte ich meinen herzlichsten Dank aussprechen: für die angenehme Arbeitsatmosphäre und gute Zusammenarbeit, die praktischen Hilfestellungen und theoretischen Diskussionen, die offenen Ohren und stützenden Schultern, die Aufrechterhaltung meines Koffeinpegels und die Bereitstellung quitschig-bunter Süßigkeiten.

Ein großer Dank von ganzem Herzen gilt meiner Familie für unendliche Unterstützung und Rückenstärken, und meinen Freunden, die mich nicht aufgegeben haben. Es ist wichtig zu wissen, daß es jemanden gibt, der an einen glaubt, und mit dem man lachen kann.

Last but not least I give my sincere and heartfelt thanks to my beloved partner Jeroen, who gave me more than I can put into words. I love you. – And I agree: the future is for us!

Index

1 Introduction

1.1 Obesity

Overweight is an expanding health problem worldwide. Nowadays obesity is considered a chronic disease and is defined as excessive fat deposition in the body storages accompanied by various co-morbidities. A simple numeric measure for estimating the weight status of a person is the body mass index (BMI = weight in kilograms divided by the square of height in meters [kg/m2]). For adults a BMI of 18.5 to 24.9 is considered optimal weight. BMI greater than 25 is considered as overweight, while a BMI larger than 30 and 40 indicate obesity and morbid obesity respectively (WHO, 2000). For children and adolescents BMI values are classified using age-related percentile charts (Kromeyer-Hauschild, 2001). Worldwide, it is observed that the prevalence and severity of obesity is increasing rapidly in children, adolescents, and adults (Chan and Woo, 2010; Wang and Lobstein, 2006). In Germany, more than 15% of the children and adolescents (3 – 17 years) were overweight in 2007, while even 6.3% were obese (Kurth and Schaffrath Rosario, 2007). In total that adds up to about 1.9 million children being overweight in Germany.

The associated co-morbidities of obesity, such as hypertension, dyslipidemia, and disturbed glucose tolerance are present in adults, adolescents, and children (I'Allemand et al., 2008; Mauras et al., 2010). Furthermore, childhood obesity is associated with an increased risk for coronary heart disease in adulthood with connected shortened lifespan (Baker et al., 2007; Biro and Wien, 2010; Reinehr and Wabitsch, 2010). The care for obese patients, to prevent further morbidity and mortality, is laborious but necessary and, therefore, the obesity-related health care costs are substantial (Ebbeling et al., 2002; John, 2010; Muller-Riemenschneider et al., 2008; Yach et al., 2006). For appropriate prevention and treatment of obesity and related health problems, knowledge of risk factors and contributing determinants is compulsive. This may also reduce the connected health care costs.

There is good evidence that individuals regulate their body weight constantly over long periods around a predetermined set point, despite minor short-term variations in the energy balance (Farias et al., 2010; Harris and Martin, 1984; Keesey and Hirvonen, 1997). For regulation of the body weight maintenance around this set point, the hypothalamus was identified to play a central role.

1.2 Hypothalamic body weight regulation

It is known for a long time that the hypothalamus is a crucial control node for the maintenance of energy homeostasis (Anand and Brobeck, 1951; Hetherington and Ranson, 1940). The hypothalamus receives and integrates neural, metabolic, and hormonal signals from the periphery. The signals converge in the hypothalamus, interconnect, and spread into respective brain areas (Coll et al., 2007; Schwartz et al., 2000). Especially the arcuate nucleus in the mediobasal hypothalamus receives hunger or satiety signals from beyond the blood-brain-barrier in the form of hormones, such as leptin, ghrelin, and insulin. The hormone stimuli regulate the expression of neuropeptides in the neurons of the arcuate nucleus. The neuropeptides transmit the information onto second order neurons by stimulating or antagonizing the respective receptors. In particular the arcuate nucleus neurons project onto second order neurons of the paraventricular nucleus and the lateral hypothalamus (Coll et al., 2004) that forward the signals further in order to maintain the body's energy homeostasis.

One subpopulation of the arcuate nucleus neurons are the neuropeptide Y (NPY) and agouti related peptide (AgRP) expressing neurons that represent the orexigenic (appetite-stimulating) pathway. They form a coordinated network with a second subpopulation of arcuate nucleus neurons, the

pre-proopiomelanocortin (in the further text referred to as POMC) expressing neurons, since both carry corresponding receptors (Cone, 2005). The POMC neurons are a pivotal link in the catabolic and anorexigenic (appetite-inhibiting) leptin-melanocortin pathway.

1.2.1 Leptin-melanocortin axis

The proteohormone leptin is secreted from white adipose tissue proportional to the body fat content and, therefore, is related to the body mass. Serum concentrations of leptin correlate well with BMI in both humans and rodents (Boston et al., 1997). Via the blood circuit, leptin reaches its target receptors (ObR/LepR) in the hypothalamic brain area, where the information of body fat conditions in the periphery is translated into central neuronal signals (Considine et al., 1996; Wang et al., 1998; Woods et al., 1998). Leptin stimulation of the anorexigenic POMC neurons in the *arcuate nucleus* induces POMC expression. On the other hand, decreased leptin levels due to fasting conditions result in lower POMC expression.

The biologically inactive polypeptide hormone precursor POMC is posttranslationally processed to generate a range of smaller biologically active peptides like the melanocyte-stimulating hormones (melanocortins; α-, β- and γ-MSH). This process depends on appropriate activity of prohormone convertases (PC)1 and PC2 (Coll et al., 2004; Seidah et al., 1999). α- and β-MSH activate the melanocortin 4 receptor (MC4R), which is a G protein-coupled seven transmembrane domain receptor (GPCR) located on the neurons of the *paraventricular nucleus*. After MC4R activation, subsequent signaling leads to a decreased food intake and increased metabolic rate (Figure 1) (Cone et al., 1996; Schwartz et al., 2000; Solomon, 1999). Possible mediators of this anorexigenic outcome are the brain-derived neurotropic factor (BDNF) and its receptor tyrosine kinase B receptor TrkB (Xu et al., 2003). α-, β-, and γ-MSH are also capable of activating the melanocortin 3 receptor (MC3R) that is expressed on the opposing POMC and NPY/AgRP neuron populations within the *arcuate nucleus*, forming a paracrine feedback loop (Bagnol, 2004). In addition to the control of food intake, it has been shown in rodents that the hypothalamic melanocortin system also participates in the regulation of peripheral energy expenditure and thermogenesis by influencing the brown adipose tissue sympathetic nerve activity (Yasuda et al., 2004).

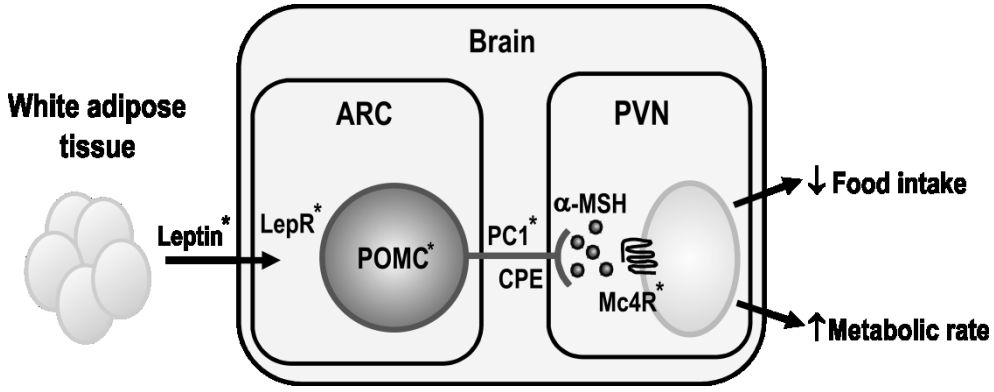

Figure 1: Catabolic leptin-melanocortin axis (Cummings and Schwartz, 2003). White adipose tissue secretes the peripheral hormone Leptin, which stimulates POMC expressing neurons in the arcuate nucleus (ARC) via the leptin receptor (LepR). POMC derived products, such as α-MSH, stimulate the MC4R in the paraventricular nucleus (PVN). Subsequent signaling of the MC4R, for example via BDFN and its receptor TrkB, leads to decreased food intake and increased energy expenditure. Mutations in *-marked genes can cause erly onset obesity in humans and rodents. PC1 = protein convertase 1, CPE = carboxypeptidase E.

Diverse factors can disturb this energy homeostasis-regulating system. Hence, obesity is not a single disorder but a heterogeneous group of conditions with multiple causes (Kopelman, 2000). Besides environmental and socio-cultural factors, also genetic determinants contribute to the development of obesity (Bouchard, 2009; Drewnowski, 2009; Maes et al., 1997; Yang et al., 2007). In most cases, obesity is a polygenic disease. Aberrant gene information and translation due to mutations or sequence variants like

single nucleotide polymorphisms (SNPs) of relevant genes can cause a disbalance in energy metabolism and shift the feeding behavior into pathological states (Coll et al., 2004). Studies in monozygotic and dizygotic twins showed that the heritability of the BMI is approximately 50 to 84% (Allison et al., 1996; Barsh et al., 2000; Stunkard et al., 1986). Besides genes involved in the differentiation of adipocytes and the thermogenesis, especially genes of the energy metabolism regulating system were identified in genome wide association (GWA) studies to be associated with the weight phenotype (Bouchard, 2009; Drewnowski, 2009; Maes et al., 1997; Speliotes et al., 2010; Thorleifsson et al., 2009; Yang et al., 2007).

For the majority of key genes of the leptin-melanocortin signaling pathway (Figure 1) gene mutations in rodents and humans were identified to lead to monogenic early onset obesity (Beales, 2010). Thereby, mutations within the MC4R are most commonly identified (Farooqi et al., 2003). In addition to seldom gene mutations, large scale GWAs also identified several SNPs that correlate with the weight phenotype. Among the latest identified SNPs is a sequence variant that lies near the POMC locus and might influence the POMC action (Speliotes et al., 2010).

1.3 Pre-proopiomelanocortin (POMC)

The human pre-proopiomelanocortin (POMC) gene is located on chromosome 2p23.3 and consists of three exons which enclose two introns (Figure 2A). Translation, starting within the second exon results in a complex, functionally inactive 32 kDA full-length precursor polypeptide. Posttranslationally, the inactive propeptide is proteolytically cleaved into smaller partially functional units (Coll et al., 2007) (Figure 2B). This processing occurs within secretory vesicles during the transport from the endoplasmatic reticulum through the Golgi apparatus towards the plasma membrane. The resulting repertoire of derived products is highly dependent on the particular tissue and its range of processing enzymes (Bertagna, 1994; Solomon, 1999).

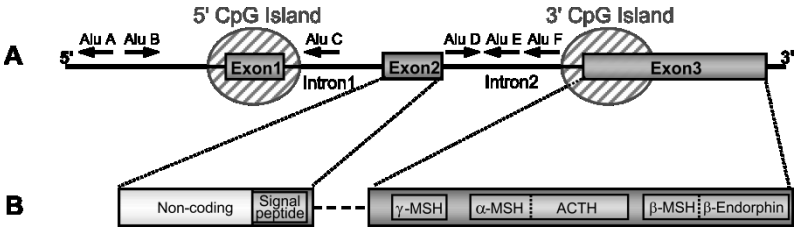

Figure 2: human POMC gene and precursor polypeptide structure. (A) Human POMC gene locus. Grey boxes indicate exons. Hatched ovals mark the location of CpG islands (CGIs). *Alu* element positions are marked by vertical arrows. (B) Full-length precursor polypeptide originating from exon2 and exon3. Repertoire of cleaving products depends on the present enzymes. ACTH = adrenocorticotropic hormone, MSH = melanocortin.

The majority of functional relevant POMC-derived peptides, including adrenocorticotropic hormone (ACTH), the endogenous opioid β-endorphin, and melanocyte-stimulating hormones (α-, β- and γ-MSH), are cleaved from the C-terminal region, which arises from the third exon (Coll et al., 2007). They all have a broad range of biological functions including roles in pigmentation, stress response, and the regulation of energy homeostasis (Adan and Gispen, 2000; Hadley et al., 1998; Yaswen et al., 1999). The exon2-derived N-terminal peptide solely forms the signal peptide and the N-terminal peptide.

A few hundred base pairs upstream of exon1 lies the promoter region with adjoining transcription start site (TSS) (Newell-Price et al., 2001). Further 10 to 12 kb upstream two evolutionary conserved neuronal enhancers, nPE1 and nPE2, are located. These neuronal enhancers are essential for expression in the hypothalamus but not for expression in the pituitary (de Souza et al., 2005). Within the gene region of the human *POMC* several domains can be distinguished based on their structure and function, including a

series of repetitive DNA units (Chang et al., 1980). Most of those repetitive DNA units are retrotransposable elements of the primate-specific *Alu* family (Whitfeld et al., 1982).

Except for the *Alu* elements, which do not have equipollents within the murine gene region, the POMC locus is highly conserved in mice and other species (Takahashi et al., 1983). Especially the exons and 3' terminal region of *POMC* show ample homology and, therefore, indicate an important physiological role of the gene product (Whitfeld et al., 1982).

The POMC sequence is coined by two CpG islands (CGIs). The 5' located CGI is associated with the promoter region and adjoining TSS. It is referred to as *5' CGI* or *first CGI*. Approximately 5 kb downstream a second CGI is located surrounding the intron2-exon3 junction. This CGI is referred to as *3' CGI* or *second CGI* (Gardiner-Garden and Frommer, 1994). The full-length transcripts of about 1200 bp initiate from a TSS within the 5' CGI. Only in skin cells, cells of the immune system, the anterior lobe of the pituitary, and neurons of the *arcuate nucleus* and *solitary nucleus* physiological significant levels of regular POMC transcripts can be detected (Coll et al., 2007; Wikberg, 1999). In mice POMC expressing cells in the anterior and intermedial pituitary are not detectable until the late stage of embryonic (E) day 12.5 and day E14.5, respectively (Elkabes et al., 1989). Beside the regular long transcripts also short POMC-related transcripts, approximately 800 bp in length, were detected in several peripheral tissues (Gardiner-Garden and Frommer, 1994). They might be initiated from alternative TSS within the 3' CGI of *POMC* (Gardiner-Garden and Frommer, 1994; Jeannotte et al., 1987; Lacaze-Masmonteil et al., 1987). This region also contains sequences matching the guidelines of *Kozak* (Lacaze-Masmonteil et al., 1987). Therefore, the translation of truncated peptides including the functional MSH peptides but lacking the signal peptide could be possible. Since the signal peptide is relevant for processing and secretion, the functionality of the resulting proteins is unclear. When the short transcripts are translated in *in vitro* systems, the truncated proteins are not secreted (Clark et al., 1990).

1.3.1 POMC action, gene dose, and obesity risk

Mutations in *POMC*, leading to improper transcription, translation, or posttranslational processing, can have extensive effects on the phenotype (Challis et al., 2002; Pritchard et al., 2002). In humans and rodents, a deficient POMC action is characterized by the development of obesity, hyperphagia, and increased linear growth. In addition, reddish hair, due to the lack of MSH at the MC1R receptor in skin and hair melanocytes, and secondary hypocortisolism caused by ACTH deficiency can be observedfrequently (Krude et al., 1998; Lee et al., 2006; Yaswen et al., 1999). Compound heterozygotes and homozygotes for complete loss-of-function mutations of the *POMC* show extreme phenotypes with early onset obesity. However, also heterozygous mutation carriers may show elevated body weight or even obesity (Farooqi et al., 2006; Krude et al., 2003). This implicates that POMC gene products contribute in a dosage-dependent fashion to the body weight regulation (Krude et al., 2003). Moreover, these findings suggest that factors, which only have subtle effects on the POMC action, could increase the risk of developing obesity (Farooqi et al., 2006).

The overall contribution of known genetic variants, including the identified mutations and SNP of the POMC locus, is estimated to account for less than 3% of the inherited variation of the weight phenotype (Li et al., 2010b; Loos et al., 2008). Therefore, novel strategies are needed to detect and elucidate further heritable factors that determine the individual weight phenotype. Since epigenetic events are also capable of altering gene expression and, therefore, hormonal signaling (Bird, 2007; Jaenisch and Bird, 2003; Wolffe and Matzke, 1999) this work is contributed to epigenetic mechanisms that may be involved in the development of the weight phenotype, particularly the DNA methylation of the POMC locus.

1.4 Epigenetics

Conrad Waddington introduced the term *epigenetics* it in the middle of the last century as the study of the mechanisms that convert genetic information into phenotypes (Waddington, 1957). Definitions that are more recent describe epigenetics as the potentially heritable structural adaptation of chromosomal regions to register, signal, or perpetuate altered gene activity states without alteration of the underlying DNA sequence (Bird, 2007; Portela and Esteller, 2010). For the establishment of this structural adaption corresponding signal and binding proteins, as well as enzymes and relevant substrates are reqired. The resulting so-called epigenetic modifications contribute to the phenomenon that genetically homogeneous organisms can show structural and functional heterogeneity of cells due to differential expression of genes in diverse tissues and developmental stages (Holliday and Pugh, 1975). Based on their mitotical and meiotical heritability (Riggs, 1975), epigenetic modifications could promote relatively fast adaption to the requirements of a changing environment without the need of changing the genetic backbone (Tang and Ho, 2007). Specifically, epigenetic modifications are mainly histone modifications, nucleosome positioning, and DNA methylation, which interact with each other. Histone modifications and nucleosome positioning are crucial in epigenetics but will not be discussed in detail in the following, since this work focuses on DNA methylation.

DNA methylation is a major epigenetic modification of the genome that regulates crucial aspects of its function and establishes heritable cellular memories (Reik, 2007). Although, it is likely, that DNA methylation has a conserved role in the regulation of gene expression and maintenance of genomic stability, manifestation of DNA methylation appears to vary among different organisms. However, covalent cytosine methylation at the C-5 position is a common feature found in most eukaryotic organisms including plants, animals, and fungi. The resulting 5-methylcytosine acts highly similar to a regular cytosine, for example forming hydrogen bonds with guanine. In animals the symmetric 5'- Cytosin-phosphatidyl-Guanin-3' (CpG) methylation on both strands is predominant (Feng et al., 2010; Lee et al., 2010).

The majority of cytosines in a CpG context are methylated in normal adult somatic tissues. Especially transposable elements and endogenous retroviruses, which are frequently found in intronic regions, are densely methylated (Yoder et al., 1997b). CpG residues in the context of CpG clusters in GC-rich regions, so called CpG islands (CGIs) (Gardiner-Garden and Frommer, 1987), form the exception. CGIs mostly remain methylation-free, particularly those in promoter regions of genes (5' CGIs) (Antequera and Bird, 1988). 5' CGIs make up approximately 50% of all occurring CGIs in the genome. Their methylation-free state is possibly mediated by specific sequence motifs closely related to transcription start sites (TSS) (Straussman et al., 2009). However, a small percentage of CGIs is methylated, preferentially inter- and intragenic CGIs, but also some 5' CGIs (Antequera and Bird, 1988; Shen et al., 2007; Yamada et al., 2004). Methylation of promoter-associated CGIs is a common feature of genomic imprinting and X chromosome inactivation and is generally associated with transcriptional silencing and gene dosage reduction, for example in differentiation processes (Costello and Plass, 2001; Feinberg and Tycko, 2004; Goll and Bestor, 2005; Jaenisch and Bird, 2003; Razin and Cedar, 1994; Shen et al., 2007). Artificial methylation of CGI promoters can decrease gene transcription, while the expression of genes with endogenous methylated CGIs can be restored by applying methylase inhibitors (Hansen and Gartler, 1990; Siegfried et al., 1999; Stein et al., 1982b). Methylation of intragenic CGIs may also effect transcriptional silencing in mammals, for example by initiating the formation of chromatin structures that reduce transcription efficiency (Lorincz et al., 2004).

1.4.1 Establishment and stable maintenance of DNA methylation

How the methylation of the genome and of gene-, tissue- and individual-specific patterns is established in detail has still to be resolved. However, it is known that a group of enzymes called *cytosine methyltransferases* mediates the process of CpG methylation. These enzymes have highly conserved sequences and functions, which indicate that DNA methylation is a critical process in an evolutionary sense (Bestor et al., 1988; Rodriguez-Osorio et al., 2010). In most eukaryotes DNA methyltransferases of the families 1 and 3 (DNMT1 and DNMT3) can be found in varying prevalence (Ponger and Li, 2005), while few eukaryotes, like *Caenorhabditis elegans* and *Saccharomyces cerevisiae*, do not possess any cytosine methyltransferases and henceforth lack cytosine methylation in their genomes (Goll and Bestor, 2005). All known DNMTs use S-adenosyl methionine (SAM) as methyl donor. For sufficient biosynthesis of SAM an adequate folate and folic acid (vitamin B9) uptake from the diet is essential (Trasler et al., 2003).

DNMTs can be divided into two groups: (1) *de novo* DNMTs and (2) maintenance DNMTs. *De novo* DNMTs initiate the DNA methylation pattern on unmethylated DNA double strands. How *de novo* DNA methyltransferases are attracted and activated by non-methylated DNA has not been discovered so far. They are expressed mainly in early embryo development where they initially set up the pattern of DNA methylation (Bestor, 2000; Santos et al., 2005; Vertino et al., 1996). In mammals the three DNMT3 homologues DNMT3A, DNMT3B and DNMT3L represent the *de novo* DNA methyltransferases (Okano et al., 1999). However, DNMT3L lacks cytosine methylase activity but shows regulatory functions in germ cells.

Maintenance DNMTs methylate the unmethylated strand of asymmetric, heterogeneously methylated DNA to achieve a symmetric methylation pattern. In this way maintenance DNMTs are responsible for preservation of the epigenetic code in the process of semiconservative DNA replication (Stein et al., 1982a). The DNMT1 affinity to heterogeneously methylated DNA is 5 to 30 times greater than to unmethylated DNA. Hence, it is considered as maintenance DNA methyltransferase (Stein et al., 1982a; Yoder et al., 1997a). Mutations in the mouse DNMT1 gene lead to dysregulation of DNA methylation which are lethal to the mouse embryo (Li et al., 1992). DNMT2 shares strong sequence similarities with the other DNMTs, but methylates tRNA instead of DNA (Goll et al., 2006).

DNA methylation is crucial for the phenotypic manifestation of the genetic code. Even tough, DNA methylation patterns in differentiated cells are generally stable (Bestor, 2000; Bird, 2002) genome wide DNA methylation reprogramming occurs at least at two developmental periods in mammals. Then a substantial part of the genome is demethylated and afterward newly methylated in a tissue- or cell-specific pattern.

One large-scale epigenetic reprogramming phase takes place periconceptionally (Figure 3A). During the preimplantation phase both parental genomes are demethylated to a certain extend. The loss of the specific DNA methylation of the paternal genome is fast and seems to be active since it occurs in the absence of DNA replication. Within six hours after fertilization the lowest methylation status of the paternal genome is reached in mice (Mayer et al., 2000). The maternal methylation is more resistant and remains intact during the first cell cycle (Santos et al., 2002). In the subsequent cell cycles the maternal DNA methylation vanishes passively as a consequence of a lack of DNMT1 in the nucleus, which results in a lack of maintenance DNA methylation (Rougier et al., 1998). The nadir of DNA methylationis reached at the morula stage (Dean et al., 2003). Subsequent remethylation establishes individual-specific DNA methylation at first instance (Santos et al., 2005). In mice, the *de novo* methylation wave is observed between the morula and blastocystal stage of the germ, just before implantation. At this point, DNA methylation is mainly involved in the repression of lineage-specific genes that are later demethylated during terminal differentiation. In contrast, regions that are unmethylated at the time of implantation can

become *de novo* methylated in a tissue-specific manner and may be involved in gene regulation (Santos et al., 2002; Straussman et al., 2009).

In the early post-implantation embryo, during the development of primordial germ cells (PGCs), another reprogramming phase takes place (Figure 3B), which probably has a more general role in the restoration of totipotency (Mitalipov and Wolf, 2009). Thereby the parent-of-origin specific markings of the alleles are erased. Afterwards, uniform imprinting marks are established for both alleles in all PGCs. In the case of fertilization, those uniform imprinting marks are transferred to the offspring as parent-of-origin specific marks (Hajkova et al., 2002; Lee et al., 2002). In mice, demethylation of the PGCs is finished around E13 to E14 when they have entered the gonads (Monk et al., 1987). Remethylation occurs in the male germ line in the prospermatogonial stage starting at day E16. In the female germ line, remethylation takes place only after birth and during the growth of the oocyte (Reik et al., 2001). The described flow of reprogramming and the consequent DNA methylation patterning seems to be evolutionary conserved.

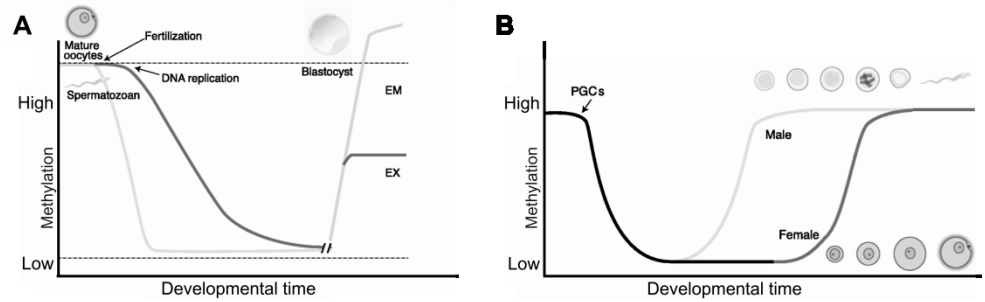

Figure 3: Methylation reprogramming during early embryogenesis and in germ line cells. Reprinted by permission (Reik et al., 2001). (A) Methylation reprogramming during early embryogenesis. The paternal genome (blue) is demethylated immediately after fertilization. The maternal genome (red) is demethylated by a passive mechanism that depends on DNA replication. Both are remethylated around the time of implantation to different extents in embryonic (EM) and extraembryonic (EX) lineages. Some methylated imprinted genes and repeat sequences (upper dashed line) are not demethylated. (B) Methylation reprogramming in the germ line. Primordial germ cells (PGCs) in the mouse become demethylated early in development. Remethylation begins in prospermatogonia on E16 in male germ cells, and after birth in growing oocytes. Some stages of germ cell development are shown.

Despite these evolutionary conserved mechanisms of reprogramming, also examples of epigenetic inheritance are described. The mechanism of direct transgenerational transmission of DNA methylation - the escape from the post-fertilization DNA methylation reprogramming process and instead direct inheritance of the DNA methylation of the parental gametes - was firstly suggested for the A^{vy} (viable yellow agouti) and $Axin^{Fu}$ (axin fused) loci (Morgan et al., 1999; Rakyan et al., 2003; Youngson and Whitelaw, 2008). However, it was not specifically shown for these loci, but for endogenous retrovirus-like intracisternal A-particles (IAPs) in general (Lane et al., 2003). Thus, the DNA methylation and connected suppression of transposable IAP elements is maintained in order to prevent uncontrolled transposition and linked genomic rearrangements (Reik, 2007; Walsh et al., 1998). Recently, also specific genes were identified that show direct transgenerational transmission of DNA methylation, such as the somatic expressed genes *Rrh* (retina) or *Cd4* and *Fyb* (hematopoietic cells) (Borgel et al., 2010).

Besides reprogramming, longitudinal changes in DNA methylation of individuals are detectable but seem to occur seldom (Eckhardt et al., 2006). In 2008, Bjornsson *et al.* showed global methylation changes over time in two independent cohorts. These findings have recently been supported by various studies (Bollati et al., 2009; Christensen et al., 2009). Some changes happen to be locus-specific, intraindividual, and family-related. Hence, the data suggest that methylation maintenance, for at least specific loci, may be under genetic control (Bjornsson et al., 2008; Heijmans et al., 2007). The identified sex-association to DNA methylation, as well as the connection to single nucleotide polymorphisms supports this theory (Boks et al., 2009; Fuke et al., 2004). In addition, Talens *et al.* demonstrated that the variability and stability of the

DNA methylation depends fundamentally on the locus itself, despite methylation variability over time (Talens et al., 2010). It is discussed that some loci with longitudinal DNA methylation stability and interindividual variability could add up to a personalized epigenetic signature which may be related to the risk of common diseases (Feinberg et al., 2010).

1.4.2 Environmental and stochastic alterations of DNA methylation

DNA methylation has a strong evolutionary determination with heritable components, which cause a certain stability of manifestation and maintenance of epigenetic marks. However, stochastic, environmental, or age-related components to epigenetic variation can be observed.

For a few genes it was shown to date that the phenotype of genetically identical cells is correlated with the epigenetic status of the locus, in particular the DNA methylation. These loci are called genes with metastable epialleles. The DNA methylation of metastable epialleles can be changed intrauterine by environmental factors, for example methyl donor supplementation of the mother's diet (Dolinoy et al., 2006; Waterland and Jirtle, 2003). Two genes with metastable epialleles are A^{vy} and $Axin^{Fu}$ (Jirtle and Skinner, 2007) which both contain a retrotransposable IAP sequence in their promoter region (Duhl et al., 1994; Vasicek et al., 1997). The epigenetic state of these loci can be inherited transgenerationally (Rakyan et al., 2003) and their allelic expression is correlated with the methylation status of the IAP retrotransposon in their promoter region. More studies support the notion of relationships between early environmental exposures and alterations in the epigenome (Waterland et al., 2011; Waterland et al., 2008; Wolff et al., 1998), of which some are potentially reversible (Weaver et al., 2004). Thereby, the timing of exposure seems to be crucial (Heijmans et al., 2008; Waterland, 2009a).

As observed in twin cohort studies, changes in DNA methylation can also occur postnatally. Older identical twins showed greater differences in global methylation than younger twin pairs (Fraga et al., 2005). In addition, considerable intraindividual differences in DNA methylation of various tissues were observed in newborn twins. Additional interindividual discordances of DNA methylation patterning of specific loci within twin pairs occurred. These differences were more pronounced in dizygotic twin pairs than in monozygotic (Kaminsky et al., 2009; Ollikainen et al., 2010).

Altogether, these results imply that genetic and stochastic factors, as well as the prenatal environment may contribute to the establishment of the epigenome. Research approaches that focus on stochastic components of methylation changes within a lifetime – to which the maintenance DNMT1 contributes to due to an error rate of 5% (Goyal et al., 2006; Whitelaw and Whitelaw, 2006) – underline this impression.

1.4.3 Alterations of DNA methylation and pathophysiological states

In the past, it was assumed that the susceptibility of diseases is determined solely by inheritable information carried in the primary sequence of the DNA. However, recently it has become clear that epigenetic disruption of gene expression plays an equally important role in the development of diseases (Godfrey et al., 2007; Jiang et al., 2004; Tang and Ho, 2007). The observed connections of epigenetic changes with human diseases are diverse and DNA methylation in particular can be associated with various diseases. In the context of imprinting, DNA methylation abnormalities can cause clinical syndromes like the Prader-Willi syndrome or the Angelman syndrome. These two imprinting disorders are reciprocally inherited and are associated with the inactivation of the chromosomal region 15q11-13 (Knoll et al., 1989). Thereby, the incorrectly imprinted allele often carries the imprinting marks of the opposite parental origin (Walter and Paulsen, 2003). Imprinting mainly regulates and affects embryonic growth and development but also inhibits aberrant growth in later life. Therefore, abnormal expression of a gene due to an imprinting defect may result in carcinogenesis, as observed in Wilms' tumors (Jelinic and

Shaw, 2007). Imprinting changes in DNA repair systems and tumor suppressor genes may promote carcinogenesis (Esteller, 2005; Robertson, 2005).

Besides imprinting disorders, dissimilar forms of epigenetic alterations are also associated with pathological states such as cancer. A range of silenced genes in cancer cells, including tumor-suppressor and cell cycle-regulating genes, were identified to promote tumorigenesis due to aberrant hypermethylation within their promoter regions (Esteller, 2005; Jones, 2002; Santos et al., 2005). In addition, hypomethylation seems to contribute to cell transformation, for example by inducing genomic instability and by deregulation of transposable elements (Berdasco and Esteller, 2010; Wilson et al., 2007).

Recent studies also show relationships between DNA methylation changes and neurodegenerative, neurological, and autoimmune diseases (Portela and Esteller, 2010). Both, aberrant hypomethylation or hypermethylation of specific gene promoters have been observed, for instance in multiple sclerosis patients and in cases of Alzheimer's disease respectively (Urdinguio et al., 2009). For rheumatoid arthritis it is suggested that partial hypomethylation of promoter regions of repetitive elements are associated with reactivation of the mobile elements causing genomic instability (Karouzakis et al., 2009). Furthermore, transposon-induced epigenetic variations causing transcriptional interferences have been described as in X-linked dystonia-parkinsonism. In this movement disorder a disease-specific retrotransposable insertion of a SVA (short interspersed nuclear element, variable number of tandem repeats, and *Alu* composite) element was detected, which induces abnormal DNA methylation. This is assumed responsible for decreased expression of the subsequent gene and hence involved in the disease genesis (Makino et al., 2007). Transposable elements seem to have a close relation to DNA methylation in the genome and contribute to genome organization, gene expression, and related disorders in various ways.

1.5 Transposable elements

Transposons are a group of genetic elements that are mobile in the genome, meaning that they can translocate to new loci. They are abundant in the genomes of most eukaryotic organisms. Transposons can act as endogenous mutagens altering genes and their expression, promote genomic rearrangements and may contribute to the speciation of organisms (Mills et al., 2007). They are considered important for several reasons. One reason is the space they occupy. The group of transposons and transposon-like elements constitutes approximately 44% of the human genome sequence (Lander et al., 2001). Another reason is their ability for transposition within the genome and consequentially the related mutational potential, even though some are not known to be active (Smit, 1999; Smit and Riggs, 1996). Depending on their strategy for transposition, transposons are divided into two subgroups (Figure 4): (1) DNA transposons, which transpose via DNA intermediates, and (2) retrotransposons (Biemont and Vieira, 2006).

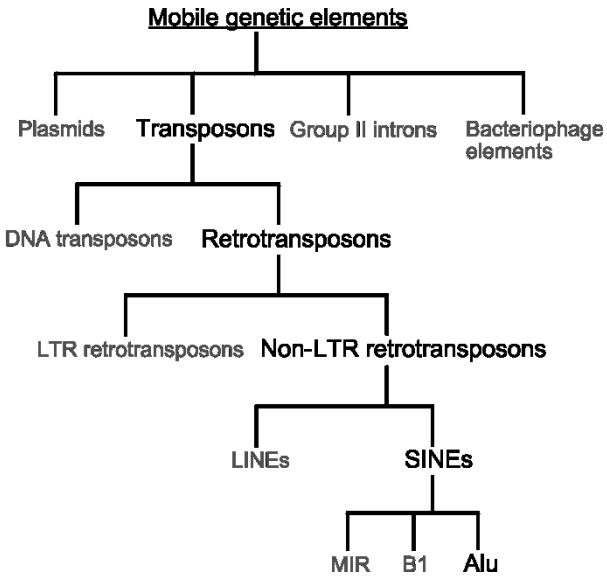

Figure 4: Tree of mobile genetic elements. *Alu* = primate *Alu* element; B1 = rodent B1 element; LINE = long interspersed repetitive element; LTR = long terminal repeats; MIR = mammalian-wide interspersed repeat; SINE = short interspersed repetitive element.

Retrotransposons transpose via RNA intermediate elements generated by RNA polymerase. The RNA intermediates are transcribed by reverse transcriptase into cDNA, which is subsequently integrated in the genome. The retroposition mechanism of retrotransposons is always replicational ("copy & paste") and, therefore, increases the number of mobile elements in the genome (Cordaux and Batzer, 2009).

The group of retrotransposons consists of two sub-types, the ones possessing long terminal repeats (LTR retrotransposons) and the non-LTR retrotransposons (Deininger et al., 2003). Long interspersed nuclear elements (LINEs) and short interspersed nuclear elements (SINEs) are the two subgroups of the non-LTR retrotransposons.

SINEs are usually up to 500 bp. Their retroposition is catalyzed by RNA polymerase III and reverse transcriptase. Since SINEs do not encode for the enzymes themselves, they rely on the apparatus of other mobile elements for transposition, such as of the LINEs. SINE families in primates and rodents are related and originate from the 7SL RNA gene of the signal recognition particle (Kriegs et al., 2007). They have been identified in primates, scandentians (tree shrews), and rodents (Krayev et al., 1980; Nishihara et al., 2002).

1.5.1 *Alu* elements

The most abundant primate-specific representatives of SINEs are the *Alu* elements that are named after the restriction enzyme AluI. AluI cleaves *Alu* elements into two distinct fragments of approximately 130 bp and 170 bp lengths. *Alu* elements compose 11% of the human genome (Cordaux and Batzer, 2009). As other SINEs, they have no coding capacity and make use of the retroposition machinery encoded by L1 elements (Dewannieux et al., 2003). Therefore, they are considered non-autonomous. Their retroposition mechanism is replicative ("copy & paste") via RNA intermediate elements (Figure 5B).

Alu elements are approximately 300 bp long and consist of two related monomers (fossil left *Alu* monomers C = FLAM-C and fossil right *Alu* monomers = FRAM) which both arose from the 7SL RNA gene (Gal-Mark et al., 2008; Kriegs et al., 2007; Ullu and Tschudi, 1984). The monomers are separated by an A-rich linker region (Gal-Mark et al., 2008). The left monomer comprises a RNA polymerase III-promoter. The element ends with an oligo(dA)-rich tail of variable length (Batzer and Deininger, 2002). *Alu*s can be directed in either sense or anti-sense orientation. In the human genome both directions are almost equally represented with 45% of *Alu*s in sense and 55% *Alu*s in anti-sense orientation (Gal-Mark et al., 2008). As

Alu elements do not possess termination signals for RNA polymerase III, their transcripts extend into the vicinal 3' region until a terminator sequence is encoded (Shaikh et al., 1997). Due to the retroposition mechanism, usually the 3' overhang is not integrated in the target site (Figure 5C).

Alu elements can be classified into three lines depending on their structure and age, namely the *Alu*J, *Alu*S, and *Alu*Y. *Alu*J is the most ancient line (circa 65 Ma) and inactive in humans (Batzer et al., 1996; Bennett et al., 2008). The second oldest line, *Alu*S, is approximately 30 Ma years old. This is the major group of *Alu*s and constitutes up to 80% of all *Alu* representatives in humans, and some subfamilies are still active, meaning retroposition can be detected (Batzer et al., 1996; Bennett et al., 2008). *Alu*Y elements form the most modern line, which is active in retroposition (Batzer et al., 1996; Bennett et al., 2008). The genomic distribution of *Alu* elements is not uniform, but is characterized by a strong bias towards gene-rich regions. Approximately 70% of *Alu*s reside within intronic sequences in protein coding regions (Gal-Mark et al., 2008).

Organisms beside primates do not possess dimeric SINEs like the *Alu* elements. However, monomeric SINEs can be found, which are related to *Alu* elements and originate from the same precursor as FLAM-C, which is called rodent proto-B1 element (PB1) or fossil left *Alu* monomers A (FLAM-A) (Quentin, 1994). For example the murine B1 elements (B1) and the Tu-type SINEs found in tree shrews descended from the PB1/FLAM-A precursor, too, and are therefore equipollents of the *Alu* elements (Kramerov and Vassetzky, 2005; Krayev et al., 1980; Nishihara et al., 2002; Singer, 1982). This kind of relationships in combination with information about type and location of trace mobile elements makes it possible to establish a phylogenetic framework for species (Kriegs et al., 2007), for instance a primate cladogram.

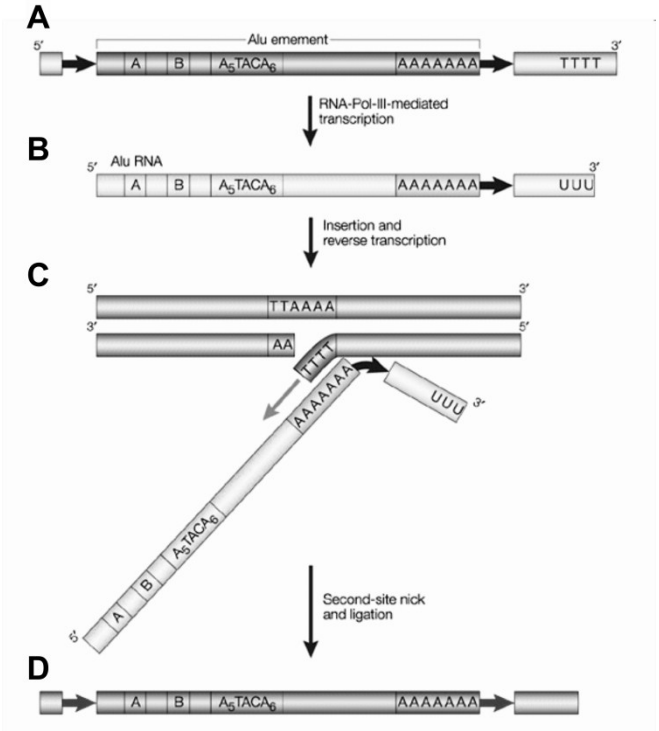

Figure 5: A typical human *Alu* element and its retroposition. Reprinted by permission from Macmillan Publishers Ltd: Nature Reviews Genetics (Batzer and Deininger, 2002), copyright 2002. (A) A typical human *Alu* element: approximately 300 bp long, built of two monomers connected by an A-rich linker. The 5' monomer contains a RNA polymerase III-promoter (box A and B). The 3' terminus is a poly-A tail. (B) For retroposition, the *Alu* element is transcribed by RNA polymerase III. (C) It has been proposed that the run of As at the 3' terminus of the *Alu* RNA might anneal directly at the site of integration and a target-primed reverse transcription (mauve arrow) is performed. The first nick at the insertion site is most likely made by the L1 endonuclease at the TTAAAA consensus site. (D) A new set of direct repeats (red arrows) is created during the insertion of the new *Alu* element.

1.5.1.1 *Alu* elements in primate phylogeny

Alu elements are used for elucidating human population genetics and for unraveling the phylogeny of the primate family. They suite this purpose of tracing the complex patterns of duplication and rearrangements in genomes taking place during evolution of the primate family (Rowold and Herrera, 2000), since:

- → *Alu* elements evolved around the same time as primates developed within the supraprimates clade, approximately 65 Ma years ago (Singer, 1982), hence are primate-specific.
- → They have a defined ancestral state and are rarely lost completely during retroposition (Roy-Engel et al., 2001).
- → The distribution of *Alu* elements is free from homoplasy since independent but identical retroposition is very unlikely (Batzer and Deininger, 1991).
- → Some *Alu* copies are still actively retroposing and can help unravel kinships that are more recent.

Even though the retroposition rate in humans is reduced drastically compared to its peak in early primate evolution (Shen et al., 1991), frequent *Alu* insertion can be detected. Until 2006, *Alu*-retroposition rates were estimated, using exclusively evolutionary approaches, on approximately one insertion per 200 births. The advancement of *method by mutation information* corrected the estimation to the occurrence of one new *Alu* insertion per 20 births in humans (Cordaux et al., 2006).

Figure 6: Genus-level phylogenetic cladogram of the primate branch based on the study of mobile elements. Reprinted by permission (Xing et al., 2007). Numbers beside the branches indicate the number of mobile element insertions supporting each node.

Even though, approximately 7,000 *Alu* insertions are unique for humans (Chimpanzee-Sequencing-and-Analysis-Consortium, 2005) many of the 1.1 million human *Alu* element insertions can be found in the corresponding positions in the genomes of other primates. However, only human-specific copies of the *Alu*S and *Alu*Y have been identified, but not of the *Alu*J line, suggesting that *Alu*J elements have not been active since the branching of humans (Hedges et al., 2004; Mills et al., 2006). Compared to humans, a much larger variability of *Alu*s is observed in the chimpanzee genome, even though there are almost twice as much *Alu* insertions in the human genome, which indicates contemporary retroposition activity (Lander et al., 2001). For the lemur, a member of the strepsirrhini, seven lineage-specific *Alu* subfamilies have been

identified which are distinctly different from their human counterparts. For comparison, only one lineage-specific *Alu* subfamily each has been identified for the platyrrhine (marmoset) and catarrhine (baboon and macaque) families. In combination with the information about distribution-divergences of *Alu* elements in the various primate genomes, this indicates a steady rate of *Alu*-retroposition activity among strepsirrhini and declining rates of *Alu* activity among the hominoid lineage of evolution (Liu et al., 2009). Concluding, the primate-specific *Alu* elements show varying activity in different primate genomes and, therefore, are present to different extends and distribution.

Alu elements not only aid the unraveling of primate phylogeny (Figure 6) but also have the potential to participate actively in primate evolution itself. Over the 65 Ma that *Alu* elements exist, they have been accumulating in primate genomes. The acute *Alu*-insertion-rate in humans is estimated to be one new insertion per 20 births (Cordaux et al., 2006). Therefore, some *Alu* insertions are so recent that they are classified as polymorphic for their presence/absence (Roy-Engel et al., 2001).

Extrapolating the rate of one *Alu* per 20 births to the global population of six billion people, it gets clear that new *Alu* insertions must have an impact on human genetics, biology, and diseases (Batzer and Deininger, 2002; Belancio et al., 2008; Mills et al., 2007). Various kinds of genomic rearrangements are caused by *Alu* insertion and are partly integrated into the functional apparatus of the genome (Babich et al., 1999; Faulkner et al., 2009; Hasler and Strub, 2006; Lee et al., 2008). However, the variety of possible genomic rearrangements, as deletion of genomic sequences (Belancio et al., 2008), mutagenesis (Gal-Mark et al., 2008; Sorek et al., 2002), microsatellite seeding (Arcot et al., 1995; Kelkar et al., 2008), and ectopic recombination (Sen et al., 2006), will not be discussed in detail in the following. This work focuses on epigenetic effects, possibly triggered by *Alu*s. *Alu* insertion into the promoter of a gene might change its expression, either through disruption/addition of regulatory sequences, promoter effects of the *Alu* itself, or by changes of the DNA methylation status and, therefore, of the epigenetic regulation of the gene (Borchert et al., 2006; Britten, 1996; Chen et al., 2008; Norris et al., 1995).

1.5.1.2 *Alu* elements and epigenetics

The epigenetic silencing of transposon activity through DNA methylation is an important defense mechanism for the cell to prevent genomic instability. Transcription of *Alu* elements can be inhibited by CpG methylation (Kochanek et al., 1993). Defense mechanisms like this became essential for organisms because of the massive increase in transposon copy numbers (Yoder et al., 1997b). Hence, highly conserved high levels of transposon methylation are found in land plants and vertebrates (!!! INVALID CITATION !!!). About one third of all genomic CpG sites in humans are accumulated in *Alu* elements (Rubin et al., 1994) and most of these sites are methylated *in vivo* in somatic cells (Schmid, 1991). However, distinct differences in the levels of methylation and even hypomethylated *Alu* elements have been found. The differences in methylation patterning depend on the type of *Alu* sequence, as well as on the type of tissue (Hellmann-Blumberg et al., 1993; Xie et al., 2009). These tissue-specific differences in pattern are in concordance with the methylation observed for the surrounding sequences.

It is suggested that variation in the methylation level of *Alu* elements not only regulates their own expression, but also modifies gene expression of other genes (Batzer and Deininger, 2002; Liu et al., 1994; Liu and Schmid, 1993). The methylation levels of *Alu*s, as well as the *Alu* structure itself, influence the positioning of nucleosomes, even in neighboring regions (Englander and Howard, 1995). This can compress chromatin to inactive heterochromatin causing repression of transcription of *Alu* elements and adjacent genes (Buttinelli et al., 1995; Englander et al., 1993).

Alu elements are found at significantly low densities in imprinted regions of the genome. The prevention of retrotransposon accumulation in imprinted regions might be actively mediated. This could be for the reason that *Alu*s attract and spread DNA methylation and heterochromatin. *Alu*-induced silencing of the

single active allele in an imprinted locus could lead to deleterious consequences for embryonic growth and survival (Greally, 2002; Khatib et al., 2007).

As already mentioned, sequence- and tissue-specific differences can occur in *Alu* methylation. However, other factors, like sex and alcohol consumption, may influence the methylation patterns, too (Zhu et al., 2010). As for the global DNA methylation in age (Bjornsson et al., 2008; Wilson and Jones, 1983; Wilson et al., 1987) also a decrease of *Alu* element methylation in particular has been described for ageing (Bollati et al., 2009; Jintaridth and Mutirangura, 2010; Zhu et al., 2010). Likewise, influences of *Alu* elements on cancer development and other diseases have been reported.

1.5.1.3 *Alu* elements in human disease

All genetic and epigenetic effects of *Alu* elements, which are mentioned and described above, have the potential to disrupt the genome or the gene expression regulation in a way that could lead to various diseases or cancer (Deininger and Batzer, 1999). Well-known examples for *Alu* insertion genetic disorders are neurofibromatosis, hemophilia, breast cancer, cholinesterase deficiency and the Apert syndrome (Deininger and Batzer, 1999; Miki et al., 1996; Muratani et al., 1991; Oldridge et al., 1999; Vidaud et al., 1993; Wallace et al., 1991). Disorders and cancers to which *Alu*-mediated recombination contribute include insulin-resistant diabetes type II, familial hypercholesterolemia, acute myelogenous leukaemia, and the Ewing sarcoma (Chae et al., 1997; Onno et al., 1992; Shimada et al., 1990; Strout et al., 1998). These are only some examples of how *Alu* elements contribute to a significant portion of human genetic diseases. Disease-causing alleles have been reported to carry *Alu*s of the S and Y line but not the *Alu*J line (Batzer and Deininger, 2002; Bennett et al., 2004; Mills et al., 2007). Beyond causing the disease, *Alu* elements can also act as a marker for the disease, segregating with the particular affected allele.

Not only retroposition of *Alu*s disturbing the new locus can cause diseases. Since *Alu* elements determine methylation of their vicinity, they are expected to influence expression of adjacent genes. Hence, also *Alu*-induced epigenetic changes, causing aberrant expression of pivotal genes, can induce disease genesis, as described for the X-linked dystonia parkinsonism (Paragraph 1.4.3). A similar effect was observed for ependymomas. There the DNA methylation of *Alu* elements and their vicinity is aberrant (Xie et al., 2010).

The mechanism of transposon insertion-induced methylation spreading has not only been observed in disease states, but also in other contexts. In melon, for example, a mechanism like this determinates the sex of the flowers. This contributes to the evolution of the species since the transposon-induced alteration are forwarded to the next generation (Martin et al., 2009). The other way around, this heritable and, therefore, stable alteration could possibly be used as indicator for sex ascertainment in the flowers of melon.

Recently it was observed that stable alterations of the DNA methylation occur more commonly and may serve as *personalized epigenetic signature*. Some were identified to co-vary consistently with certain phenotypes or diseases, such as the weight phenotype (Feinberg et al., 2010). Since DNA methylation has an impact on gene expression, the variances in DNA methylation might not only correlate with a certain phenotype but account for it. This hypothesis was tested by Kuehnen *et al.* by investigating the DNA methylation of POMC as candidate gene for obesity.

1.6 DNA methylation of the POMC locus

The promoter-associated 5' CGI of the POMC locus is better investigated to date than the 3' CGI. This first CGI of POMC was found to be specifically unmethylated in POMC expressing tissues (Mizoguchi et al., 2007; Newell-Price et al., 2001; Ye et al., 2005). Moreover, DNA methylation of the region inhibits POMC expression in a manner that suggests that the specific location rather than the quantity of methylated CpG

dinucleotides are crucial (Newell-Price, 2003). Since (i) short POMC transcripts are possibly initiated from an alternative TSS within the 3' CGI (Gardiner-Garden and Frommer, 1994) and (ii) already minor changes of the POMC dose can stimulate the development of POMC-associated syndromes like obesity, the assessment of the DNA methylation state of the 3' CGI and its involvement in POMC expression becomes significant.

Kuehnen *et al.* investigated the POMC DNA methylation of both CGIs in search for CpG methylation variants that correlate with childhood obesity (Kuehnen et al., in revision). In human peripheral blood cells (PBC) and β-MSH positive cells from the human hypothalamus, which are both POMC-expressing but originate from different germ layers, equivalent DNA methylation patterns were detected for both CGIs (Figure 7A and B). Thereby, the 5' CGI was found to be primarily hypomethylated, as common for promoter-associated CGIs and described by (Newell-Price et al., 2001), while the 3' CGI showed a more prominent particular sharp pattern of hypermethylation in intron2 and hypomethylation in exon3.

In obese children, the sharp border between hypermethylation in intron2 and hypomethylation in exon3 of the 3' CGI was found to be significantly shifted into the exon3 region (Figure 7C and D), while the 5' CGI pattern remained unchanged. The stability of this changed POMC methylation pattern in obese individuals was verified in longitudinal samples, revealing that the aberrant methylation in the 3' CGI exists before the development of obesity occurs. Moreover, the binding of the transcription enhancing p300 complex, as well as the POMC expression in PBC is reduced in obese children with altered methylation (Kuehnen et al., in revision). These data reflect a correlation of methylation status of the POMC locus with the weight phenotype and possibly the gene function. These findings raise of course more questions and hypotheses of which several were investigated and answered in the scope of this thesis work.

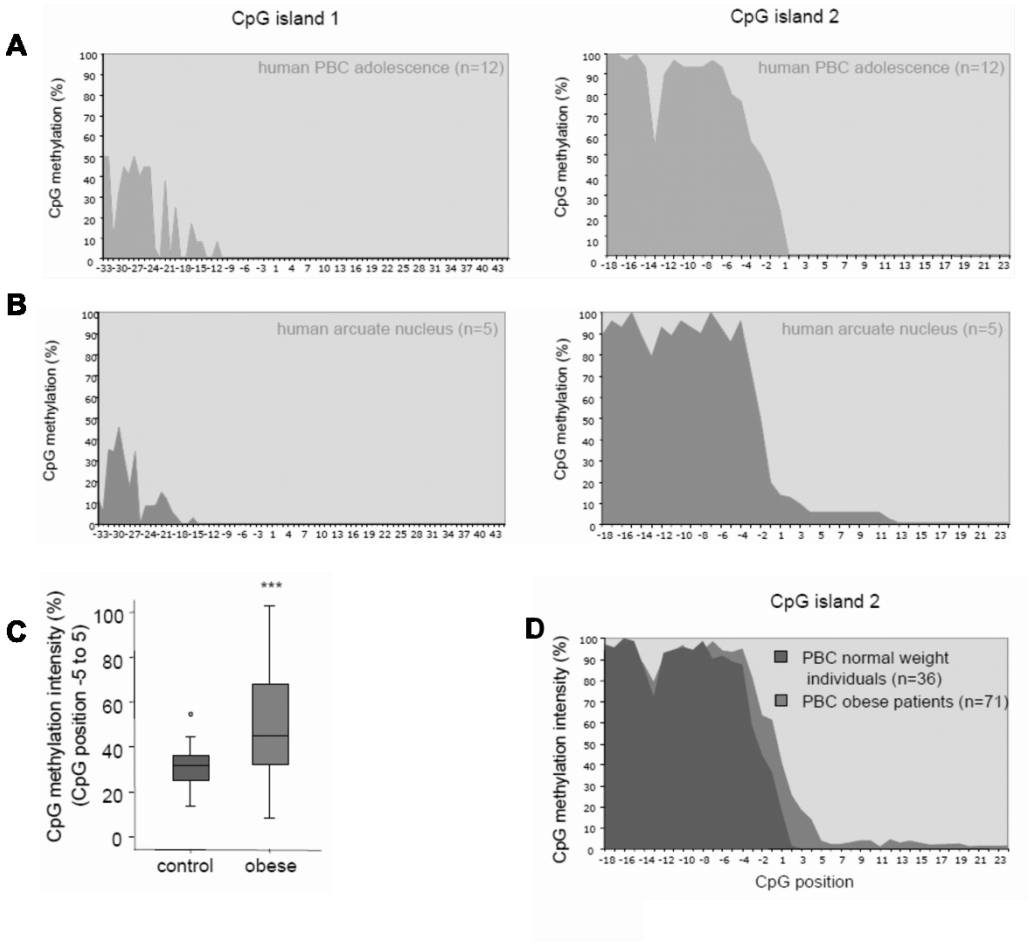

Figure 7: DNA methylation pattern of the human POMC locus (Kuehnen et al., in revision). (A) and (B) POMC DNA methylation patterns of CGI 1 and 2 (5' CGI and 3' CGI respectively) in peripheral blood cells (PBC) of normal weight adolescents (n = 12) and microdissected ß-MSH positive cells of human *arcuate nucleus* (n = 5). (C) Box plots analysis represents the statistic differences from the mean CpG methylation intensity (in %) of CpG position -5 to +5 (relative to exon3 start) in normal weight individuals and obese patients ($p < 0.001$). (D) POMC DNA methylation intensity (in %) of CGI 2 in PBC of normal weight and obese individuals (red and blue curve respectively). CpG positions are numbered according to their relative position to the next exon start.

1.7 Aim of this thesis

Obesity is classified as a chronic disease with severe organic co-morbidities. Childhood obesity is associated with an increased risk for coronary heart disease in adulthood and premature death (Baker et al., 2007; Reinehr and Wabitsch, 2010). Moreover, the obesity prevalence worldwide is epidemic-like and causes substantial costs for health care systems. The genesis of obesity is multiplex based on individual predisposition and environmental factors.

Even though approximately 50 to 84% of the BMI can be accounted to heritability (Allison et al., 1996; Barsh et al., 2000; Stunkard et al., 1986) only about 10% of the severe cases with early onset, which are therby likely inherited, can be explained by concrete genetic defects, which mostly constitute insufficiencies within the leptin-melanocortin pathway (Speliotes et al., 2010). The origin of the majority of cases remains unclear.

Epigenetic modifications, like DNA methylation, are heritably metastable and capable of changing gene expression without changing the DNA itself. Therefore, it is conceivable that, in the context of body weight regulation, epigenetic changes of involved genes can lead to disruption of the minute control of food intake and the energy expenditure equilibrium. For the human POMC gene, which is a central pivot in the

catabolic leptin-melanocortin-axis, a significant change in the DNA methylation pattern, associated with obesity, was detected. For a better understanding and estimation of the role of POMC DNA methylation in pathogenesis of obesity, it is important to get insights in its function and development. Therefore, the aim of the thesis was to analyze the functional relevance of the POMC CGIs and effects of POMC DNA methylation changes on its gene expression. Moreover, the ontogenetic development of the POMC DNA methylation patterns and possible influencing factors were examined, as well as the phylogenetic origin of the POMC methylation patterns. This was done based on the following four hypotheses:

1) The DNA methylation status of POMC influences its gene expression.

   Constructs containing variations of either the 5' or 3' CGI of the human POMC gene were created using a CpG-free luciferase-containing vector backbone.

   Functional analysis, based on dual luciferase assays applying those vector constructs in different methylation states, were performed.

2) The DNA methylation patterns of *POMC* are stably established early during ontogenesis.

   The DNA methylation patterns of *POMC* were determined in sundry prenatal stages and in various tissues postnatally.

   DNA methylation of newborn humans was compared to the pattern of adult humans.

3) The DNA methylation patterns of *POMC* are stable postnatally.

   The DNA methylation patterns of *POMC* were determined in mice receiving a high fat diet for 29 weeks.

4) The phylogenetic development of *POMC* DNA methylation is associated with *Alu* element incidence within the intron2 region.

   This hypothesis was tested by establishing the incidence of *Alu* elements in the POMC locus of various primate families.

   Alu element incidence was correlated to the DNA methylation patterns in the gene region of interest.

2 Materials and Methods

2.1 Materials

2.1.1 Index of manufacturers

Manufacturer	Location
Affymetrix	Santa Clara, CA, USA
Applied Biosystems	Foster City, CA, USA
Berthold Technologies GmbH & Co. KG	Bad Wildbad, Germany
BINDER Inc.	Bohemia, NY, USA
Biochrom AG	Berlin, Germany
Biometra GmbH	Goettingen, Germany
Bio San Laboratories Inc.	Derry, NH, USA
BRAND GMBH + CO KG	Wertheim, Germany
Braun biotech = Sartorius AG	Goettingen, Germany
Carl Zeiss AG	Oberkochen, Germany
Eppendorf	Hamburg, Germany
Fried Electric	Haifa, Israel
Heraeus Holding GmbH	Hanau, Germany
IKA® Werke GmbH & Co. KG	Staufen, Germany
Invitrogen	Carlsbad, CA, USA
ITW Dynatec	Hendersonville, TN, USA
KNF Neuberger GmbH	Freiburg, Germany
Leica Camera AG	Solms, Germany
Liebherr-Hausgeräte Ochsenhausen GmbH	Ochsenhausen, Germany
MACHEREY-NAGEL GmbH & Co. KG	Dueren, Germany
MAG Biosystems	Exton, PA, USA
Mettler-Toledo GmbH	Giessen, Germany
Millipore Headquarters	Billerica, MA, USA
New England Biolabs	Ipswich, MA, USA
Peqlab	Erlangen, Germany
Promega GmbH	Mannheim, Germany
QIAGEN	Hilden, Germany
Sartorius AG	Goettingen, Germany
Seegene	Rockville, MD, USA
Siegma-Aldrich	St. Louis, MO, USA
Stratagene	La Jolla, USA
Syngene	Cambridge, UK
Thermo Fisher Scientific Inc.	Waltham, MA, USA
ZIEGRA Eism aschinen GmbH	Isernhagen, Germany

2.1.2 Antibiotics

For the plasmid and cell culture work of this thesis, the following antibiotics were used:

Antibiotic	Manufacturer
Ampicillin	Sigma-Aldrich
Penicillin- Streptavidin	Biochrome
Zeocin (Phleomycin D1)	Invitrogen

2.1.3 Enzymes

The following enzymes were used for the plasmid and cell culture work described in this work:

Enzyme	Manufacturer
ExonucleaseI	New England Biolabs
Methyltransferase	
HhaI	New England Biolabs
HpaII	New England Biolabs
M.SssI	New England Biolabs
Polymerase	
AmpliTaq® DNA Polymerase	Applied Biosystems
BIOTAQ™ DNA Polymerase	Bioline
MangoTaq™ DNA Polymerase	Bioline
PfuTurbo® DNA polymerase	Stratagene
Restriction endonuclease	New England Biolabs
BamHI	
EcoRI	
NcoI	
Shrimps Alkaline Phosphatase	Affymetrix
T4-DNA- Ligase	New England Biolabs

2.1.4 Buffer and media

For the experimental work of this thesis, the following media and buffer were used:

Buffer/medium	Composition/manufacturer
For bacterial culture	
LB medium according to Miller*, pH 7.0	1% tryptone, 0,5% yeast extract, 1% NaCl H_2O, sterilized
LB agar culture plates*	1,5% agar in LB medium, in culture dishes, stored at 4°C
* The antibiotics were added in a final concentration of 50 µg/ml (ampicillin) and 25 µg/ml (zeocin)	
SOB medium, pH 7.4	2% tryptone, 0,5% yeast extract, 0.05% NaCl in 2.5 mM
SOC medium	20 mM $MgCl_2$, 20 mM glucose in sterilized SOB medium
X-gal	40 mg/ml X-gal in dimethylformamide
For cell culture	
Dulbecco`s Modified Eagle Medium	Biochrome
Phosphate buffered saline (PBS)	Biochrome
Furthermore	
Ammonium acetate	10 M ammonium acetate in H_2O_{HPLC}
5x TBE, pH 8.3	0.45 M tris-borate, 1 mM EDTA in H_2O

2.1.5 Equipment

For this thesis work, following apparatus and software were used:

Hardware/device	Specification	Manufacturer
Automated Nucleic Acid Extraction System		
	Maxwell® 16 System	Promega
Centrifuge		
	Refrigerated Microcentrifuge 5417 R	Eppendorf
	Non-refrigerated Microcentrifuge 5417 C	Eppendorf
	Sorvall® RC 6™ Plus Superspeed-Centrifuge	Thermo Scientific

	Labofuge® 200 Centrifuge	Thermo Scientific
Gel documentation system		
	Gene Flash gel documentation system	Syngene
Gel Electrophoresis Apparatus		
	Agagel Midi-Wide Horizontal	Biometra
	Compact XS/S Horizontal	Biometra
Ice machine		
	ChipIce Machine ZBE 70-35	Ziegra
Incubator		
	CO_2 incubator B 6120	Heraeus
	Drying oven T6030	Heraeus
	Drying oven APT.line™	Binder
	Thermomixer compact	Eppendorf
	Ceromat® BS-1 incubation shaker	B. Braun Biotech
Laminarflow cabinet		
	LaminAir® HBB 2448	Heraeus
Magnetic stirrer		
	RCT basic IKAMAG® safety control	IKA
Microscope and imaging system		
	Axiovert 10	Zeiss
	DV2™ Dual-Channel	MAG Biosystems
	Stereomikroskope MZ 6, MZ 12.5	Leica
Multimode microplate reader		
	Mithras LB 940	Berthold Technologies
pH meter		
	S20-SevenEasy™ pH	Mettler-Toledo
Pipette		
	Research® Adjustable-volume Pipette series	Eppendorf
	Research® Multichannel Pipette	Eppendorf
	HandyStep® repetitive pipette	Brand
	Accu-jet® pro pipette controller	Brand
Scale		
	Analytical Balance CPA 2235-OCE	Sartorius
	Precision Balance MC1 LC2200P	Sartorius
Sequencer		
	ABI 3130 Genetic Analyzer	Applied Biosystems
Shaker		
	Vortex Genius	IKA
	BioVortex V1 Plus	Biosan
	Microtiter plate Vari-Shaker	ITW Dynatech
	CombiSpin FVL-2400N	peqlab
Software		
	In vitro search tool for transcription factor binding sites	
	In vitro sequence screen tool for repetitive elements	
Spectrophotometer		
	BioPhotometer 6131	Eppendorf
	NanoDrop 3300	Thermo Scientific
Sterilizer		
	VARIOKLAV® Steam Sterilizer 75 S	Thermo Scientific

Hardware/device	Specification	Manufacturer
Thermocycler		
	Mastercycler ep gradient S	Eppendorf
	Mastercycler gradient	Eppendorf
	UNO-Thermoblock	Biometra
Vacuum Pump		
	LABOPORT	KNF Neuberger
Water Bath		
	Thermostatic Water Bath (WBS)	Fried Electric
Water Purification System		
	Elix 5 Water Purification System	Millipore

2.1.6 Kits

The preassembled reaction systems (kits) used for this thesis work are listed below:

Kit	Application	Manufacturer
BigDye® Terminator v3.1 Cycle Sequencing Kit	Sequencing	Applied Biosystems
DNA IQ™ Casework Sample Kit for Maxwell® 16	DNA extraction	Promega
DNA Walking SpeedUp™ Kit II	Amplification	Seegene
Dual-Luciferase® Reporter Assay System	Reporter gene assay	Promega
Effectene Transfection Reagent	Transfection	Qiagen
Maxwell® 16 Tissue DNA Purification Kit	DNA extraction	Promega
Omniscript™ RT Kit	RT-PCR	Qiagen
Plasmid DNA Purification NucleoBond® Xtra Midi System	Midi preparation	Macherey Nagel
PureYield™ Plasmid Miniprep System	Mini preparation	Promega
TOPO TA Cloning® Kit (pCR®2.1-TOPO-Vektor)	TOPO cloning	Invitrogen
TRIzol® Reagent	RNA isolation	Invitrogen
Wizard® SV Gel and PCR Clean-Up System	DNA purification	Promega

2.1.7 Primers

All oligonucleotide primers used in this thesis were synthesized either by TIB MOLBIOL, Berlin, Germany, or by Invitrogen GmbH, Darmstadt, Germany.

2.1.7.1 Bisulfite sequencing, mouse

Bisulfite sequencing mouse		
Primer	Sequence	Fragment size
mPOMC-F1-for-out	5'-GGTATAGAAGGATATTTGTTTTGAAATA-3'	342 bp
mPOMC-F1-rev-out	5'-TCCACTTAAAACTAAACAAAAACTTAAC-3'	
mPOMC-F1-for-in	5'-TTTATTTTAAAAGGTAGTTTGTTTTGGG-3'	243 bp
mPOMC-F1-rev-in	5'-CAAACCTAATTCTAAAATCTTACAAATC-3'	
mPOMC-F2-for-out	5'-GATTTGTAAGATTTTAGAATTAGGTTTG-3'	541 bp
mPOMC-F2-rev-out	5'-CCCATCTCAAAAATTTAAAAAAAAATCAA-3'	
mPOMC-F2-for-in	5'-GTTAAGTTTTTGTTTAGTTTTAAGTGGA-3'	421 bp
mPOMC-F2-rev-in	5'-CCAATCTACTAAAAATCCCAAAATCC-3'	
mPOMC-F3-for-out	5'-GTTTATGTTTGTTTTGGATTTAAATAG-3'	421 bp
mPOMC-F3-rev	5'-CAACACTACTACTATTCCTAAAAC-3'	
mPOMC-F3-for-in	5'-GTAAGATTTTGTTAGTAAGAGTTAAG-3'	396 bp
mPOMC-F4-for-out	5'-GGAGATGAATAGTTTTTGATTGAAAAT-3'	604 bp

Bisulfite sequencing mouse		
Primer	Sequence	Fragment size
mPOMC-F4-rev-out	5'-CCTAACACAAATAACTCTAAAAAAC-3'	
mPOMC-F4-for-in	5'-GGAGATGAATAGTTTTTGATTGAAAAT-3'	494 bp
mPOMC-F4-rev-in	5'-CCCATACAAAAAAAAAACCTTAAAAT-3'	

2.1.7.2 Bisulfite sequencing, human

Bisulfite sequencing human		
Primer	Sequence	Fragment size
hPOMC_F1 for-out	5'-ttttaaagtggaatagagagaatatga-3'	484 bp
hPOMC_F1 rev-out	5'-ctcctctatccttatatacttacc-3'	
hPOMC_F1 rev-in	5'-acaacacaaaaaacaacTccc-3'	416 bp
hPOMC_F1 for-in	5'-gtggaatagagagaatatgatttttt-3'	
hPOMC_F2 for	5'-GTAAGTATATAAGGATAGAGGAG–3'	
hPOMC_F2 rev-out	5'-CTCTCCAACATAAACAACAAAAAC–3'	499 bp
hPOMC_F2 rev-in	5'-AATTATCCCAAAACCTCCTAACAA–3'	442 bp
hPOMC-F3-for-out	5'-TTAGATAAATTATGGAATGGGA-3'	687 bp
hPOMC-F3-rev-out	5'-AAACTCCAAAAAAAAAACCTC-3'	
hPOMC-F3-for-in	5'-GTGGTAAGATTTTAGATGTTT-3'	513 bp
hPOMC-F3-rev-in	5'-AAAATACTCCATAAAATAAAAAC-3'	

2.1.7.3 Bisulfite sequencing, non-human primates

Bisulfite sequencing non-human primates		
Primer	Sequence	Fragment size
Eulemur macaco		
t-POMC-F14-for_out	5'–AGAAGTATGTAGGGGTATAGGGA-3'	341 bp
t-POMC-F14-R-rev	5'–CTAAAATTCRCCCTTAAAATAACCC-3'	
t-POMC-F14-for_in	5'–GGTGAGTTTTAGGAGTTGTTTATTAG-3'	300 bp
Galago senegalensis		
t-POMC-F14-for_out	5'–AGAAGTATGTAGGGGTATAGGGA-3'	316 bp
t-POMC-F14-R-rev	5'–CTAAAATTCRCCCTTAAAATAACCC-3'	
t-POMC-F13-for_in	5'–GGGTATAGGGAATAAGAGTGATG-3'	291 bp
Macaca mulatta		
t-POMC-F29-for-out	5'–GTTAGATAAATTATGGAATGGGATGG-3'	687 bp
t-POMC-F29-rev-out	5'–AAAATACTCCATAAAATAAAAA-3'	
t-POMC-F29-for-in	5'–GGTGGTAAGATTTTAGATGTTTA-3'	506 bp
t-POMC-F29-rev-in	5'–CTCTTAAACTCCAAAAAAAAAACCTC-3'	
tPOMC-F29-seq-mitte	5'–GGAGTGTATTYGGGTTTGTAAG-3'	
Papio hamadryas		
t-POMC-F44-for-out	5'–TAGTTGTTAGGTAGAAGTATGTAGG-3'	382 bp
t-POMC-F44-R-rev	5'–CTAAAATTCRCCCTTAAAATAACCC-3'	
t-POMC-F44-for-in	5'–GGAATAAAAGAGTGGTGGTAAGATT-3'	353 bp
Callithrix jacchus		
t-POMC-F51-for-out	5'–TGTTAGATATAATAGTAGGATT-3'	758 bp
t-POMC-F51-rev-out	5'–AAACTCCAAAAAAAAAACCTC-3'	
t-POMC-F51-for-in	5'–GGTGGTAAGATTTTAGATGTTT-3'	522 bp
t-POMC-F51-rev-in	5'–AAAATACTCCATAAAATAAAAAC-3'	

2.1.7.4 Sequencing POMC intron2-region in non-human primates

Sequencing POMC intron2-region in non-human primates		
Primer	Sequence	Fragment size
Amplification of gene region		
hPOMC_Alu_for_out	5'-CCACAATAGAGTCCTCTAGG-3'	1,066 bp
hPOMC_Alu_rev_out	5'-GCATCTAAGATCTTGCCACTG-3'	
hPOMC_Alu_for_in	5'-CAAGGAGCAGAGACACAG-3'	1,022 bp
hPOMC_Alu_rev_in	5'-CTCTTTTGTCCCATCCCC-3'	
hPOMC_Intron2_for5	5'-TCAGGACCTCACCACGGAA-3'	3,078 bp
hPOMC_Intron2_rev5	5'-GAAGTGGCCCATGACGTACT-3'	
Sequencing		
Galago senegalensis		
Midi13-1-seq-for1	5'-CACTCTGTATTGCTTCCTC-3'	
Midi13-1-seq-for2	5'-GTAGTTCCACGAATTACCTC-3'	
Midi13-1-int-for3	5'-GTGGAACCATAACCAGGTC-3'	
Midi13-1-int-for4	5'-ACCACACACAGAGGCCATGA-3'	
Eulemur macacoI		
Midi14-2-seq-for1	5'-GTCTGCTAGGTAGTTCCACA-3'	
Midi14-2-seq-for2	5'-AGGGGAAAAAGGAAAAACCAAG-3'	
Midi14-2-int-for3	5'-CAGAACCCATGGGTTCTAG-3'	
Midi14-2-int-for4	5'-TGCAGTTCCCAGGTCACTG-3'	
Midi14-2-seq-rev1	5'-AGGCCTGGATGCACTCCT-3'	
Midi14-2-int_rev2	5'-AGCCCTATCCCTGCACTAT-3'	
Midi14-2-int_rev3	5'-CTGAACTGATATCCCTGTAC-3'	
Eulemur macacoII		
Midi16-3-seq-for1	5'-GTCTGCTAGGTAGTTCCACA-3'	
Midi16-3-seq-for2	5'-AGGAAAAACCAAGTCACCA-3'	
Midi16-3-int_for3	5'-GACACAGAACAGGTTTCACG-3'	
Midi16-3-int_for4	5'-GAGACCCAAGAGTTTCTCGA-3'	
Papio hamadryas		
Midi44a-int-for1	5'-GCTCATATCACTTGCCATTTTCA-3'	
Midi44a-int-for2	5'-CAAATCATCTCTGGAAGAAGGAA-3'	
Midi44a-int-for3	5'-GGTGCCAAATGTCTCATGCTAC-3'	
Midi44a-int-for4	5'-CCAGTTGCAAAACCAGCCAGG-3'	
Midi44a-int-for5	5'-TAAGAAATGGGAGAAGGAATGAGGG-3'	
Midi44a-int-for6	5'-GGTTGAGTCCACAATTTCTGTTTAG-3'	
Midi44a-seq-rev1	5'-TTGGCACTCGTGGGCATCTAA-3'	
Midi44a-seq-rev2	5'-CTTCCCTACAGAGCAGGTCT-3'	
Midi44a-int-rev3	5'-CCTCAGTGATGGAAAACCTAC-3'	
Midi44a-int-rev4	5'-TCACGACTTCTAAGCTGATC-3'	
Midi44a-int-rev5	5'-CTCTTGGGTCTTTTCTGAACT-3'	
Midi44a-int-rev6	5'-TCCCTGGTGAGCTGTGCAGT-3'	
Midi44a-int-rev7	5'-TCCCCTGGATGGATAATGAAAC-3'	
Midi44a-int-rev8	5'-GGACTAGAACCCATGTGTCCTG-3'	
Midi44a-int-rev9	5'-TCAAGCAATCCTCCCACCTTAGC-3'	
Midi44a-int-rev10	5'-TGTGACCTCAAACTCTTGGCCTCA-3'	

2.1.7.5 Site-directed mutagenesis

Site-directed mutagenesis	
Primer	Sequence
pCpGL-Isand2 long-construct	
Insel2-del-for	5'-CGCGTCTTCCCCCAGTGCATCCGGGCCTGC-3'
Insel2-del-rev	5'-GCAGGCCCGGATGCACTGGGGGAAGACGCG-3'
Insel2-mut-for	5'-CGCGTCTTCCCCCAGCTCTGCATCCGGGCCTGC-3'
Insel2-mut-rev	5'-GCAGGCCCGGATGCAGAGCTGGGGGAAGACGCG-3'
Insel2-mut-CpG-for	5'-CCCAGGAGTGCATCTGGGCCTGCAAGCCCG-3'
Insel2-mut-CpG-rev	5'-CGGGCTTGCAGGCCCAGATGCACTCCTGGG-3'

2.1.7.6 Cloning

Cloning		
Primer	Sequence	Fragment size
pCR®2.1-TOPO® vector		
M13_for	5'-GTAAAACGACGGCCAG-3'	
M13_rev	5'-CAGGAAACAGCTATGAC-3'	
pCpGL vector		
pCpGL-basic_for	5'-GAGCAAACAGCAGATTAAAAGG-3'	
pCpGL-basic_rev2	5'-GCCATCTTCCAGAGGGTAGAA-3'	
hPOMC_Prom1a_for	5'-CGAT**GGATCC**CCCCAAAGTGGAACAGAGAG-3'	592 bp
hPOMC_Prom1a_rev	5'-CGATCCATGGCTGCGCCCTTACCTGTCTC-3'	
hPOMC-Insel2-lang_for	5'-CGAT**GGATCC**GCAGTTGCCAGGCAGAAGCA-3'	550 bp
hPOMC-Insel2-lang_rev	5'-CGATCCATGGAGTAGGAGCGCTTGCCCTCG-3'	
hPOMC-Insel2-mittel_for	5'-CGAT**GGATCC**GCAGTTGCCAGGCAGAAGCA-3'	294 bp
hPOMC-Insel2-mittel_rev	5'-CGATCCATGGGAGAGGTCGGGCTTGCAGGC-3'	
hPOMC-Insel2-kurz_for	5'-CGAT**GGATCC**GCAGTTGCCAGGCAGAAGCA-3'	247 bp
hPOMC-Insel2-kurz_rev	5'-CGATCCATGGGACGCGAGGGCATGAGGGCA-3'	
hPOMC-Insel2-mut_for	5'-CGCGTCTTCCCCCAGCTCTGCATCCGGGCCTGC-3'	550 bp
hPOMC-Insel2-mut_rev	5'-GCAGGCCCGGATGCAGAGCTGGGGGAAGACGCG-3'	
hPOMC-Insel2-mut-CpG_for	5'-CCCAGGAGTGCATCTGGGCCTGCAAGCCCG-3'	550 bp
hPOMC-Insel2-mut-CpG_rev	5'-CGGGCTTGCAGGCCCAGATGCACTCCTGGG-3'	
hPOMC-Insel2-del_for	5'-CGCGTCTTCCCCCAGTGCATCCGGGCCTGC-3'	547 bp
hPOMC-Insel2-del_rev	5'-GCAGGCCCGGATGCACTGGGGGAAGACGCG-3'	

BamHI-Schnittstelle

NcoI-Schnittstelle

2.1.7.7 RT-PCR

RT-PCR from GT1-7 RNA		
Primer	Sequence	Fragment size
β-Actin-RT-for	5'-CGACAACGGCTCCGGCATG-3'	159 bp
β-Actin-RT-rev	5'-CCTCTCTTGCTCTGGGCCTCG-3'	
mPOMC_RT_for	5'-GTTGCTGGCCCTCCTGCTTC-3'	216 bp
mPOMC_RT_rev	5'-CAGCGGAAGTGACCCATGACG-3'	
mEp300-RT_for	5'-AACCAGCAGATGCTCAACCT-3'	238 bp

Primer	Sequence	Fragment size
mEp300-RT_rev	5'-CGGTAAAGTGCCTCCAATGT-3'	
mGATA1-RT-for	5'-AGCCCAGGTTCAACCCCAGTGT-3'	487 bp
mGATA1-RT-rev	5'-GCAGGCAGTGCAGTCCCCAG-3'	

2.2 Methods

2.2.1 Extraction of genomic DNA

Genomic DNA from samples was extracted using the *Maxwell® 16 System* (Promega). Depending on the type of sample, different protocols were applied.

2.2.1.1 DNA extraction from blood and tissue samples

For DNA extraction from EDTA blood (peripheral blood cells, PBCs) and tissue samples the *Maxwell® 16 Tissue DNA Purification Kit* (Promega) was used according to the manufacturer's instructions (Henry, 2001; Promega, 2010c). Up to 50 µg of tissue sample or 350 – 500 µl EDTA blood was processed directly with the *tissue program*. The extracted DNA was eluted with 270 – 350 µl H_2O_{HPLC} and stored at 4°C afterwards.

2.2.1.2 DNA extraction from Guthrie spots (blood on newborn screening cards)

Newborn screening cards (Whatman Protein Saver™ 903® cards) were punched (diameter = 3.2 mm). Four punches per sample (= 8.04 mm^2) were applied for DNA extraction from blood (peripheral blood cells, PBCs) using the *DNA IQ™ Casework Sample Kit for Maxwell® 16* (Promega) according to the manufacturer's instructions (Promega, 2010a). The punches were pre-incubated in 200 µl lysis buffer containing 10 mM DTT (60 min, 350 rpm, 70°C) and then cooled on ice for 2 min. Afterwards the samples were centrifuged (2 min, 14,000 rpm, rt) in DNA IQ™ Spin Baskets (Promega). The filtrate was transferred to the forensic kit cartridge and processed with the *tissue program*. The extracted DNA was eluted with 50 µl elution buffer and stored at 4°C.

2.2.2 Determination of genomic DNA concentration

DNA concentrations of samples were determined by measuring the optical density (OD) at a wavelength of 260 nm. Measurements were performed either with diluted samples (1:25) using the *Biophotometer 6131* (Eppendorf), or the undiluted samples were measured using the *NanoDrop 3300* (Thermo Scientific). Purity of genomic DNA was assessed by determining the $OD_{260\ nm}/OD_{280\ nm}$-ratio. $OD_{260\ nm/280\ nm}$ values of 1.8 - 2.0 were considered as sufficient.

2.2.3 Polymerase chain reaction (PCR)

The polymerase chain reaction (PCR) enables exponential amplification of selected genomic regions of interest from genomic or plasmid DNA by utilization of pairs of sequence specific oligonucleotide primers, as well as a thermo stable Taq or Pfu DNA polymerase (Erlich, 1989; Lundberg et al., 1991). For this thesis, various PCR methods were applied, of which the specificities are outlined in the following paragraphs. For accurate pipetting schemes and PCR run protocols, see Appendix Table A1 and A3.

2.2.3.1 Bisulfite PCR amplification

Genomic regions of interest were amplified from bisulfite-treated DNA (Paragraph 2.2.12) or blastocysts using the thermo stable *AmpliTaq® DNA Polymerase* (Applied Biosystems). For examining the methylation status of specific regions, oligonucleotide primers were designed flanking the regions of interest. Primer landing site sequences did not contain CpG dinucleotides, and therefore their nucleotide sequences remained independent of the methylation state during bisulfite treatment. As a result, both methylated

and unmethylated DNA could be proportionally amplified in the same reaction. To achieve higher yields and reduced contamination by unspecific amplification products, all bisulfite PCRs were designed as nested or half-nested PCRs. Nested polymerase chain reactions involve two sets of primers used in two successive polymerase chain reaction runs. Hereby the second set is intended to amplify a secondary target within the first amplification product (Figure 8).

A suitable amount of bisulfite-treated DNA or a washed agarose bead (Paragraph 2.2.12) was used for each PCR reaction. The PCR mix contained 1x *AmpliTaq® buffer*, 1.5 mM $MgCl_2$, 1 M betaine, 100 µM dNTPs, 200 nM forward primer 'out', 200 nM reverse primer 'out', and *AmpliTaq® DNA Polymerase*. The reaction was started in a PCR block with preheated lid (105°C). After initial denaturation for 5 min (95°C), 40 cycles of 45 s denaturation (95°C), 45 s primer annealing, and 60 s elongation (72°C) were performed. The final elongation time was 8 min at 72°C. The primer annealing temperature depended on the primers used.

With the product of the first PCR, a second PCR run was implemented using the same PCR run protocol and a similar PCR mix as for the first PCR. Only the 'out' primers were replaced by the corresponding 'in' primer pair. The product of the second PCR was loaded on an agarose gel for analysis. Samples showing the expected size of PCR product were either directly applied to an Exo/SAP-reaction and subsequent sequencing (Paragraph 0) with gene region specific primers, or the fragments were purified from the gel, TOPO cloned (Paragraph 2.2.7.1) and sequenced after colony PCR as described below.

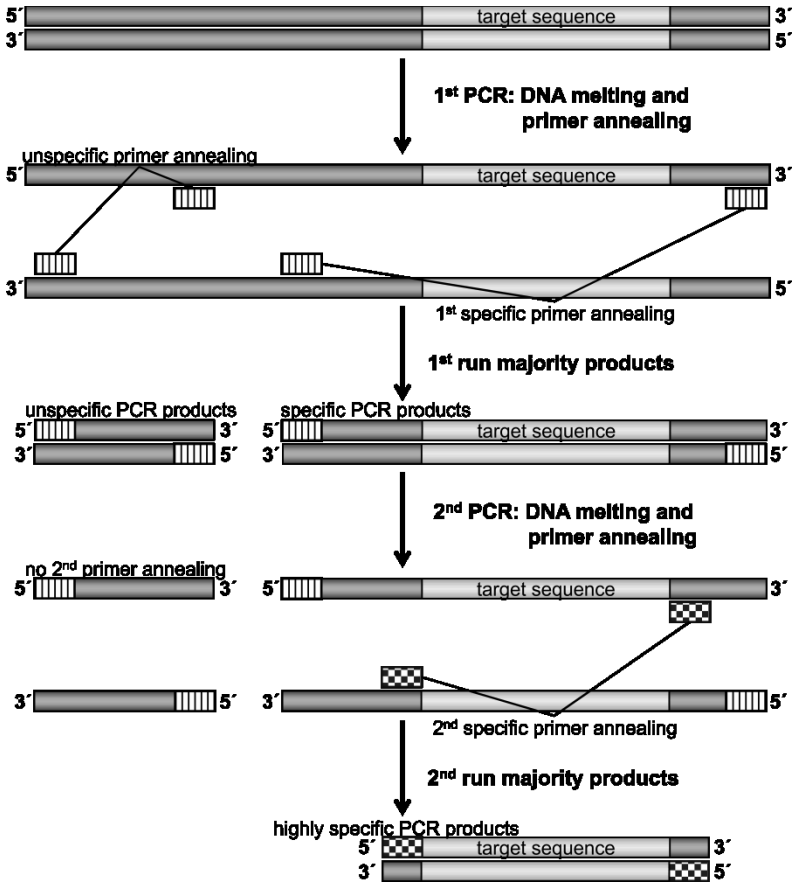

Figure 8: Principle of nested PCR.

2.2.3.2 Colony PCR amplification

When the transformants of TOPO cloning reactions were analyzed by PCR amplification, single colonies were picked and dissolved in 10 µl H_2O_{HPLC}. Using this solution as template, the cloned fragments were amplified by PCR using *pCR®2.1-TOPO®* vector-specific M13 primers (333 nM each). Beside the primers, the PCR mixture contained 1x *NH_4 Reaction Buffer*, 1.5 mM $MgCl_2$, 100 µM dNTPs, and *BIOTAQ™ DNA Polymerase*. After initial denaturation for 10 min (95°C), 30 cycles of 30 s denaturation (95°C), 30 s primer annealing (55°C), and 45 s elongation (72°C) were performed. The final elongation time was 8 min at 72°C.The PCR products were analyzed by agarose gel electrophoresis. When the DNA bands in the gel showed the right size, the PCR amplification product was applied to an Exo/SAP-reaction and subsequently sequenced (Paragraph 0) with gene specific primers.

2.2.3.3 PCR amplification of unknown POMC fragments for sequencing

For comparative sequence and methylation analyses of the different primate POMC loci, the respective gene region of various primates had to be determined. Therefore, the DNA fragment of interest was PCR amplified using primers that had their landing sequence in highly conserved regions of the POMC locus (Paragraph 0).

- → The POMC-Intron2 regions were determined for *Pongo pygmaeus* (orangutan), *Papio hamadryas* (baboon), *Galago senegalensis* (galago), and *Eulemur macaco* (lemur) with genomic DNA kindly provided by the *Deutsches Primaten Zentrum* (DPZ), Göttingen, Germany.
- → The POMC-*Alu* region was amplified from *Gorilla gorilla* (gorilla) DNA (DPZ) with a nested PCR approach (Figure 8).

The PCR mixes contained DNA in suitable amounts, 1x *AmpliTaq® buffer*, 1.5 mM $MgCl_2$, 1 M betaine, 100 µM dNTPs, 200 nM respective forward primer, 200 nM respective reverse primer, and *AmpliTaq® DNA Polymerase*. The reaction was started in a PCR block with preheated lid (105°C). After initial denaturation for 5 min (95°C), 40 cycles of 45 s denaturation (95°C), 45 s primer annealing, and 1 - 4 min elongation (72°C) were performed. The final elongation time was 10 min at 72°C. The primer annealing temperature depended on the primers used. The PCR products were validated by agarose gel electrophoresis, and the DNA bands were cut from the gel. The purification product from the agarose gel slices were TOPO cloned (Paragraph 2.2.7.1). Resulting plasmid vector preparations were applied for sequencing procedures with respective sequencing primers (Paragraph 0).

2.2.3.4 PCR amplification of POMC fragments for functional analysis

For functional analysis of the 5' CGI and the 3' CGI region of the human POMC gene, appropriate fragments were amplified from human genomic DNA. Therefore, restriction site-containing oligonucleotide primers were used, to substitute the fragments with a BamHI restriction site upstream and an NcoI restriction site downstream (Paragraph 0).

The PCR mixes contained DNA in suitable amounts, 1x *AmpliTaq® buffer*, 1.5 mM $MgCl_2$, 1 M betaine, 100 µM dNTPs, 200 nM forward primer, 200 nM reverse primer, and *AmpliTaq® DNA Polymerase*. The reaction was started in a PCR block with preheated lid (105°C). After initial denaturation for 5 min (95°C), 40 cycles of 45 s denaturation (95°C), 45 s primer annealing, and 4 min elongation (72°C) were performed. The final elongation time was 10 min at 72°C. The primer annealing temperature depended on the primers used. The PCR products were validated by agarose gel electrophoresis, and the DNA bands were cut from the gel. The purification product from the agarose gel slices were TOPO cloned and sequenced (Paragraph 2.2.7.1 and 0). For *trans*-cloning from the TOPO vector into the pCpGL vector the TOPO constructs were BamHI and NcoI restricted and the resulting restriction fragments were ligated into the likewise restricted pCpGL vector (Paragraph 2.2.7.2).

2.2.3.5 Site-directed mutagenesis PCR

For further analysis of the 3' CGI region of the human POMC gene, the pCpGL-Island2 long-construct (obtained in pCpGL cloning, Paragraph 2.2.7.2) was mutated and deleted by site-directed mutagenesis PCR with corresponding primer pairs (Paragraph 0). Respective complementary primer pairs were designed containing desired mutation or deletion (up to three nucleotides were mutated or deleted).

The PCR mix was prepared on ice and contained pCpGL-Island2 long-construct DNA in suitable amounts, 1x *Cloned Pfu DNA polymerase reaction buffer*, 1.5 mM $MgCl_2$, 1 M betaine, 200 µM dNTPs, 300 nM forward primer, 300 nM reverse primer, and *PfuTurbo® DNA polymerase* (Stratagene). The reaction was started in a PCR block with preheated lid (105°C). After initial denaturation for 30 s (95°C), 18 cycles of 30 s denaturation (95°C), 60 s primer annealing (55°C), and 6 - 8 min elongation (68°C) were performed. The final elongation time was 10 min at 72°C. After the PCR amplification, the samples were further processed as described in Paragraph 2.2.8.

2.2.4 RT-PCR for determination of gene expression in GT1-7 cells

For semi-quantitative determination of the occurrence of specific mRNAs within a cell line or tissue as a measure of gene expression, a technique called reverse transcription PCR (RT-PCR) is applied. Firstly whole RNA isolated from cells or tissues and secondly RT-PCR is performed using primer pairs that have their landing sites within two different exons of one gene, to avoid false-positive results by genomic DNA-contamination. RNA extracted from GT1-7 cells (Paragraph 2.2.13) was tested for expression of *POMC*, *Ep300* (E1A binding protein p300), *GATA1*, and *Actb* of β-actin as control.

2.2.4.1 Extraction of total RNA from GT 1-7 cells

Total RNA of GT1-7 cells was isolated applying the *TRIzol® Reagent* (Invitrogen) according to the manufacturer's instructions (Invitrogen, 2010) after trypsination of the adherent cells. The RNA was resuspended in 30 µl DEPC H_2O and stored at -80°C until use for RT-PCR procedures.

2.2.4.2 RT-PCR

The RT-PCR is a variant of PCR, in which a RNA strand is reverse transcribed into its DNA complement (cDNA) by the enzyme reverse transcriptase. Then the resulting cDNA is amplified using standard PCR.

a) cDNA generation:

An oligo-dT-Primers was used in combination with the *Omniscript™ RT Kit* (Qiagen) according to the manufacturer's instructions (Qiagen, 2010) to generate cDNA from the extracted RNA from GT1-7 cells.

b) PCR amplification of desired cDNA fragments:

Corresponding primer pairs (Paragraph 0) were used to amplify desired fragments from cDNA in a PCR mix that contained 1x *MangoTaq colored reaction buffer*, 1.5 mM $MgCl_2$, 1 M betaine, 50 µM dNTPs, 200 nM forward primer, 200 nM reverse primer, and *MangoTaq™ DNA Polymerase* (Bioline). The reaction was started in a PCR block with preheated lid (105°C). After initial denaturation for 5 min (95°C), 40 cycles of 30 s denaturation (95°C), 30 s primer annealing, and 60 s elongation (72°C) were performed. The final elongation time was 7 min at 72°C. The primer annealing temperature depended on the primers used. The PCR products were validated by agarose gel electrophoresis (Paragraph 2.2.5).

2.2.5 Agarose gel electrophoresis

Agarose gel electrophoresis (1 - 2% agarose in 0.5 TBE buffer) was used to separate nucleic acid fragments by length. Application of an electric field (80 - 100 V) moves negatively charged molecules, such as DNA, through the agarose matrix. Thereby, shorter molecules move faster through the pores of the gel and migrate farther than longer molecules (Aaij and Borst, 1972). The gels were supplemented with

ethidium bromide (EtBr, 0.4 µg/ml) which fluoresces when intercalated into nucleic acids. Hence, ethidium bromide makes DNA (and RNA) visible in UV light.

After gelatinizing, the gels were transferred into TBE (0.5x) containing horizontal electrophoresis chambers. Before loading, the samples were substituted with negatively charged 6x loading buffer (containing 0.25% xylene cyanol and 0.25% bromphenol blue which co-sediment with nucleic acids) for visualization in visible light. In each well 7 – 30 µl of one sample or 2 – 4 µl of size marker were loaded. DNA marker, *Quick-Load® 100 bp DNA Ladder* (New England Biolabs), *1 Kb DNA Ladder* (Invitrogen), were used as standards to estimate the fragment sizes. After electrophoresis, the gels were assessed with the *Gene Flash gel documentation system* (Syngene).

2.2.6 Purification of DNA fragments or PCR products

For some applications, it is suitable to purify DNA fragments or PCR products to remove buffers, primer residues, enzymes, or other disturbing substances. For purification of PCR products or of DNA fragments from agarose gel slices the *Wizard® SV Gel and PCR Clean-Up System* (Promega) was used according to the manufacturer's instructions for the centrifugation strategy (Betz and Strader, 2002; Promega, 2009b) with following modifications:

- → Gel slices were dissolved at 65°C and 500 rpm.
- → No evaporation step with open centrifuge lid was carried out.
- → DNA was eluted with 40 µl nuclease-free water.

2.2.7 Molecular cloning

Cloning is commonly used as method to save and amplify DNA fragments for further application in molecular biological experiments, such as sequencing, gene (-fragment) characterization, and protein production. With the molecular cloning approach, the DNA amplification takes place in a living organism. Therefore, the DNA fragment of interest has to be ligated into a vehicle (plasmid vector), which exhibits certain features, such as an origin of replication. Then living cells, for example bacteria, are transformed with the vector construct to propagate the DNA fragment of interest.

2.2.7.1 TOPO cloning

By TOPO cloning, Taq polymerase-amplified DNA fragments can be directly inserted into specific plasmid vectors without the requirement of restriction sites, restriction enzymes, or ligases. The TOPO vector is equipped with covalently bound topoisomerase and 3´ thymidine (T)-overhangs. The T-overhangs match the 3' adenine (A)-overhangs at the Taq polymerase-amplified DNA fragment and the topoisomerase catalyzes the covalent binding of the TOPO vector and the DNA fragment (Shuman, 1994).

The *TOPO® TA Cloning® Kit* (Invitrogen) was used in combination with *One Shot® TOP10* chemically competent *Escherichia coli* (*E. coli*) (Invitrogen) for DNA fragments amplified in PCRs using *AmpliTaq® DNA Polymerase* (Applied Biosystems).

i. For sequencing, PCR products from bisulfite PCRs and fragments containing the POMC-Intron2 region of various monkeys were cloned into the pCR®2.1-TOPO® vector.
ii. For functional analysis the pCR®2.1-TOPO® vector was used as a vehicle for necessary DNA fragments for further cloning steps into the target vector pCpGL.

a) PCR amplification of fragment of interest:

Fragments of interest were amplified in respective PCRs, separated by agarose gel electrophoresis, and purified from the gel (Paragraph 2.2.3, 2.2.5, and 2.2.6).

b) Cloning reaction:

The cloning reaction was carried out according to the manufacturer's instructions (Invitrogen, 2006) using 4 µl of purified PCR product (Paragraph 2.2.6), 1 µl salt solution and 1 µl of the *pCR®2.1-TOPO®* vector.

c) Transformation of *TOP10* competent cells:

TOP10 competent cells were transformed according to the manufacturer's instructions (Cohen et al., 1972; Invitrogen, 2006) with following modifications:

- → The total amount of 6 µl TOPO cloning reaction mix was added to the cells.
- → The cells were heat-shocked for 45 s.
- → 200 µl of each transformation was spread onto one culture plate.

d) Selection:

For dual selection, LB plates containing 50 µg/ml ampicillin were additionally spread with 40 µl X-gal (Table 1). The ampicillin in the agar confirms the transformation of the bacteria. Since the *pCR®2.1-TOPO®* vector encodes ampicillin-resistance, only successfully transformed bacteria can grow in this environment. The X-gal application is to distinguish bacteria transformed with an empty vector from bacteria transformed with an insert-containing vector. The insertion of a fragment into the vector disrupts its LacZ gene. Thus, the bacteria cannot metabolize X-gal anymore and appear white instead of blue.

e) Analysis of transformants:

The transformants were analyzed by either:

- → Mini preparation and restriction cut analysis (Paragraph 2.2.9.1 and 2.2.10).
- → Colony PCR (Paragraph 2.2.3.2).

Table 1: Composition of LB medium, LB agar culture plates and X-gal used in the cloning procedure. The LB medium and LB agar were substituted with the antibiotics ampicillin or zeocin in the concentrations of 50 µg/ml or 25 µg/ml respectively.

Solution/buffer	Composition
LB medium according to Miller,pH 7.0	1% tryptone, 0,5% yeast extract, 1% NaCl H_2O, sterilized
LB agar culture plates	1.5% agar in LB medium, in culture dishes, stored at 4°C
X-gal	40 mg/ml X-gal in dimethylformamide

→

2.2.7.2 pCpGL cloning

The promoter activity of the 5' CGI and 3' CGI of the human POMC locus were analyzed in this thesis. Therfore, vector constructs that contained 5' CGI- or 3' CGI-fragments were made (Table 2). All fragments were substituted upstream with a BamHI restriction site and downstream with an NcoI restriction site for fragment insertion. The pCpGL vector is a luciferase-containing plasmid vector with a CpG-free backbone (Figure 9).

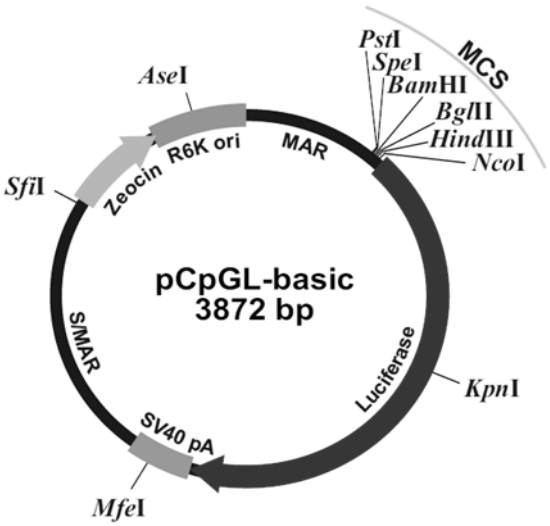

Figure 9: Map of the CpG-free reporter vector: pCpGL. Reprinted by permission (Klug and Rehli, 2006). The vector, including its multiple cloning site (MCS), is completely free of CpG dinucleotides. It contains a zeocin resistance gene and the R6K origin of replication. The plasmid is propagated in bacteria expressing the PIR gene.

The CpG-free vector backbone is of importance for methylation experiments, since effects of backbone CpG-methylation can distort the results. The pCpGL-basic as well as the pCpGL-CMV/EF1 vector construct, which can be used as positive control, was kindly provided by the working group of Dr. Rehli from the *Institut für Hämatologie und internistische Onkologie*, Universitätsklinikum Regensburg, Regensburg, Germany. The transformation was performed with *One Shot® PIR1* chemically competent *E. coli* (Invitrogen). The selection was carried out using zeocin-containing LB culture plates.

a) PCR amplification of fragment of interest:

Fragments of interest were amplified in respective PCRs, separated by agarose gel electrophoresis, and purified from the gel (Paragraph 2.2.3, 2.2.5, and 2.2.6). If necessary, they were TOPO cloned before further use (Paragraph 2.2.7.1).

b) Restriction of DNA fragments of interest and of the pCpGL vector:

The DNA fragment of interest containing necessary restriction sites – as purified PCR product or as TOPO construct - and the pCpGL-basic vector were restricted overnight (37°C). The BamHI and NcoI enzymes (New England Biolabs) were applied simultaneously in a mix containing 1x the corresponding buffer NEB3 and 10x BSA (Appendix Table A2). Afterwards, the enzymes were heat inactivated (20 min, 85°C).

c) Purification:

The *Wizard® SV Gel and PCR Clean-Up System* (Promega) was used as described in Paragraph 2.2.6, to remove small nucleotide fragments, the buffer, and the enzymes (i) directly the pCpGL vector-restriction reaction mixture, (ii) the PCR product-restriction after agarose gel electrophoresis.

d) Ligation:

The restricted DNA fragment of interest (15 µl) was ligated into the corresponding restriction sites of the pCpGL vector (2 µl) using 1 µl of a T4 DNA ligase (400 u/µl; New England Biolabs). The T4 DNA ligase catalyzes the formation of a phosphodiester bond between juxtaposed 5' phosphate and 3' hydroxyl termini in duplex DNA (Sambrook and Russel, 2001). The ligation reaction was carried out at room temperature in 1x T4 DNA ligase reaction buffer (4 h).

e) Transformation of *PIR1* competent cells:

The pCpGL vector contains the R6K origin of replication. For transformation, *PIR1* competent cells (Invitrogen) are suitable. They express the protein *pi* that is needed for the activation of the R6K origin of replication. *PIR1* competent cells were transformed according to the manufacturer's instructions (Invitrogen, 2004) with following modifications:

- → The total volume of 20 µl pCpGL ligation reaction was added to the cells.
- → The cells were heat shocked for 60 s.
- → 200 µl of each transformation was spread onto the culture plates.

f) Selection:

LB plates containing 25 µg/ml zeocin were used to select transformed bacteria (Table 1). The pCpGL vector encodes for zeocin-resistance. Therefore, only transformed *PIR1* bacteria can grow on zeocin containing LB agar culture plates.

g) Analysis of transformants:

The transformants were analyzed by mini preparation, restriction cut analysis and sequencing.

h) Amplification of correct transformants:

To obtain a larger amount of plasmid for further usage, the correct transformants were amplified by midi preparation (Paragraph 2.2.9.2).

Table 2: pCpGL vector-constructs obtained from pCpGL cloning procedures and applied in dual-luciferase reporter gene assays. The noted fragments were obtained from human genomic DNA by PCR amplification of POMC fragments for functional analysis.

Name	Inserted fragment of the human POMC gene
pCpGL-PromI	-493 bp to + 98 bp relative to exon1 start
pCpGL-Island2 long	-256 bp to +294 bp relative to exon3 start
pCpGL-Island2 medium	-256 bp to +32 bp relative to exon3 start
pCpGL-Island2 short	-256 bp to -10 bp relative to exon3 start

2.2.8 Site-directed mutagenesis of pCpGL vector-constructs

Site-directed mutagenesis is a technique in which a mutation is created at a defined site in a DNA molecule using polymerase chain reaction (PCR) with oligonucleotide primers that contain the desired mutation (Braman et al., 1996). For plasmid manipulations, a pair of complementary mutagenic primers is used to amplify the entire plasmid. Resulting nicked, circular DNA is mended by the endogenous bacterial repair machinery after transformation. To separate the mutated DNA from the non-mutated template plasmid, enzymatic digestion with a methyl-sensitive restriction enzyme can be applied. The biosynthesized template DNA carries specific methylation marks but not the *in vitro* generated mutated plasmid. Therefore, template DNA is eliminated by digestion, while the mutated DNA is preserved and can be used for amplification in bacteria cells. This method was applied to the pCpGL-Island2 long-construct to obtain mutated and deleted constructs (Table 3) for further analysis of the p300 binding site.

a) Site-directed mutagenesis PCR:

The pCpGL-Island2 long-fragments were PCR amplified using corresponding primers for insertion of the desired mutations and deletions (Paragraph 2.2.3.5).

b) Elimination of template plasmid:

The methylated template plasmid was restricted by the methyl-sensitive DpnI enzyme (1 h, 37°C). Therefore, a sufficient amount of enzyme (1 µl) was added directly to the sample after PCR amplification.

c) Purification and precipitation:

To remove buffer and enzymes, the samples were mixed with phenol/chloroform (1 : 1) and centrifuged (10 min, 14,000 rpm, 4°C). After centrifugation, from the uppermost of the three phases the DNA was precipitated overnight (-80°C) using 1/5 of the sample volume of 1.5 M sodium acetate (pH 5.5) and 2.2 times the sample volume of 100% ethanol. To pellet the DNA, the samples were centrifuged (25 min, 14,000 rpm, 10°C). The pellet was washed with 70% ethanol (20 min, 14,000 rpm, 10°C), subsequently dried at 37°C, and resuspended in 30 µl H_2O (HPLC quality).

d) Transformation of *PIR1* competent cells:

For ligation of the nick in the circular DNA and for amplification, *PIR1* competent cells were transformed with the mutated or deleted pCpGL-Island2 long-constructs The transformation of *PIR1* competent cells was performed according to the manufacturer's instructions (Invitrogen, 2004) with following modifications:

- → 10 µl of mutated or deleted pCpGL-Island2 long-constructs was added to the cells.
- → The cells were heat shocked for 60 s.
- → 200 µl of each transformation was spread onto the culture plates.

Selection, analysis of transformants and amplification of correct transformants was performed according to the procedure described in Paragraph 2.2.7.2.

Table 3: Deleted and mutated pCpGL-Island2 long-constructs obtained from site-directed mutagenesis. The noted positions are relative to the exon3 start of the human POMC gene. Construcs were applid in reporter gene assays.

Name	Position (relative to exon3 start)	Deletion or mutation
pCpGL-Island2 long-del	+1 to +3 bp	GAG were deleted
pCpGL-Island2 long-mut	+1 to +3 bp	GAG → CTC
pCpGL-Island2 long-mut CpG	+10 bp	C → T

2.2.9 Plasmid vector preparation

To amplify the plasmid vector DNA for further experiments, such as sequencing, secondary cloning steps, or for functional analysis, LB medium containing ampicillin (50 µg/ml) or zeocin (25 µl/ml) was inoculated with a single bacterial colony picked from a culture plate and incubated overnight (220 rpm, 37°C). Depending on the plasmid DNA yield that should be achieved, either 4 ml (mini preparation) or 250 ml (midi preparation) medium was used. In the case of midi preparations, glycerol stocks were produced for backup. Therefore, bacteria culture was mixed with glycerol (1:1) and stored at -80°C. To isolate the plasmid vector DNA from the cultured bacteria the *PureYield™ Plasmid Miniprep System* (Promega) or the *Plasmid DNA Purification NucleoBond® Xtra Midi Syste*" (Macherey Nagel) was used.

2.2.9.1 Mini preparation (miniprep)

The *PureYield™ Plasmid Miniprep System* (Promega) provides a rapid method to purify plasmid DNA using a silica membrane column. Initially, the 4 ml bacteria culture was centrifuged (10 min, 4,000 rpm, rt) and the supernatant was removed. Afterwards, the kit was used according to the manufacturer's instructions (Promega, 2009a). The purified plasmid DNA was eluted with 30 µl elution buffer and stored at 4°C. The correctness of the inserts was verified by enzymatic restriction and subsequent sequencing (Paragraphes 2.2.10 and 0).

2.2.9.2 Midi preparation (midiprep)

Larger amounts of plasmid DNA were produced in larger volumes of culture charging stock (250 ml). The purification was performed using the *Plasmid DNA Purification NucleoBond® Xtra Midi System* (Macherey Nagel) according to the manufacturer's instructions for the centrifugation strategy (MachereyNagel, 2010). The purified plasmid DNA was eluted with 200 - 400 µl H_2O_{HPLC} and stored at 4°C. The correctness of the inserts was verified by enzymatic restriction and subsequent sequencing (Paragraph 2.2.10 and 0).

2.2.10 Enzymatic plasmid vector restriction

To verify the inserts by length, the plasmid DNA preparations were restricted (1 h, 37°C) using appropriate enzymes (Table 4) and separated by agarose gel electrophoresis (Sambrook and Russel, 2001). The cloning site of the *pCR®2.1-TOPO®* vector is flanked up- and downstream by EcoRI restriction sites and, therefore, a restriction with EcoRI (New England Biolabs) releases the DNA insert from the vector. The pCpGL vector constructs were restricted by simultaneous use of BamHI and NcoI. Vectors containing inserts of expected sizes were Sanger sequenced by capillary electrophoresis (Paragraph 0).

Table 4: Pipetting scheme for restriction analysis of plasmid DNA preparations. The appropriate restriction enzymes - EcoRI for TOPO vector constructs and BamHI/NcoI for pCpGL vector constructs - and buffers were applied.

EcoRI restriction		BamHI and NcoI restriction	
pCR®2.1-TOPO® vector preparation	2 µl	pCpGL vector preparation	2 µl
10x EcoRI buffer	1 µl	10x NEBuffer 3	1 µl
		100x BSA	1 µl
EcoRI (100 u/µl)	0.25 µl	BamHI (20 u/µl)	0.5 µl
		NcoI (20 u/µl)	0.5 µl
H_2O_{HPLC}	6.75 µl	H_2O_{HPLC}	5 µl
Total volume	10 ul	Total volume	10 ul

2.2.11 Sequencing

To determine the sequence of nucleotides within a DNA fragment of interest, samples were Sanger sequenced using the *ABI 3130 Genetic Analyzer* which works with capillary electrophoresis (Sanger et al., 1977). For sequencing PCR products without a preceding cloning step, the primer leftovers of the PCR reaction had to be eliminated by restriction with exonuclease I (Exo, New England Biolabs) and shrimp alkaline phosphatase (SAP, Affymetrix), the so called Exo/SAP restriction. Afterwards, the samples were prepared for sequencing in a sequencing reaction. Plasmid DNA, which did not contain primer residues, was applied directly to the sequencing reaction without preceding Exo/SAP reaction.

2.2.11.1 Exo/SAP restriction

PCR products (8 µl) were incubated with 0.18 µl ExoI (20 u/µl) and 0.32 µl SAP (1 u/µl) in a final volume of 11 µl (35 min; 37°C) followed by heat inactivation of the enzymes (15 min, 80°C).

2.2.11.2 Sequencing reaction

Pretreated PCR products and plasmid DNA were applied in sequencing reactions using fragment-specific or vector-specific primers and luminescent dNTPs in the *BigDye®*-Sequencingmix (Table 5). After initial denaturation (1 min, 95°C) the sequencing reaction was performed with 30 cycles of 30 s denaturation (95°C), 15 s primer annealing (55°C) and 4 min elongation (60°C). The final elongation step was 8 min (60°). The products of this reaction were precipitated using 1/5 of the sample volume of 1.5 M sodium acetate (pH 5.5) and twice the sample volume of 100% ethanol (25 min, 14,000 rpm, 10°C). The pellet was

washed with 70% ethanol (20 min, 14,000 rpm, 10°C), subsequently dried at 60°C and resuspended in 10 µl H_2O (HPLC quality) preceding to the application to capillary electrophoresis sequencing in the ABI 3130 Genetic Analyzer.

Table 5: Pipetting scheme for sequencing reactions either of Exo/SAP products or of plasmid DNA.

Sequencing reaction of Exo/SAP product		Sequencing reaction of plasmid DNA	
Exo/SAP product	5 µl	Plasmid DNA	1 µl
5x BigDye sequencing buffer	1.5 µl	5x BigDye sequencing buffer	1.5 µl
Primer (5 µM)	1 µl	Primer (5 µM)	1 µl
BigDye®-Sequencingmix	0.75 µl	*BigDye*®-Sequencingmix	0.75 µl
H_2O_{HPLC}	1.75 µl	H_2O_{HPLC}	5.75 µl
Total volume	10 µl	Total volume	10 µl

2.2.12 Bisulfite genomic sequencing for DNA methylation analysis

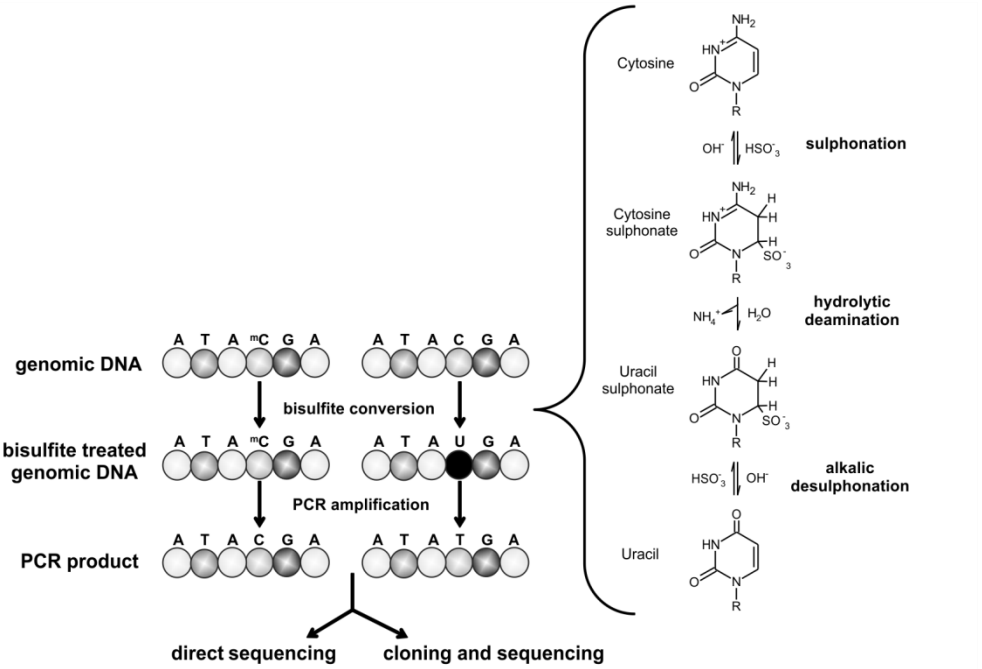

Figure 10: The principle of bisulfite genomic sequencing. In genomic DNA, methylated (^{m}C) and non-methylated cytosines (C) are present. Treatment with bisulfite changes latter in three steps to uracil (U): 1. sulphonation, 2. hydrolytic deamination, 3. alkali desulphonation. In PCR, uracil is translated to thymine, while cytosine remains cytosine. This can be demonstrated by sequencing.

To determine the DNA methylation status in single CpG resolution, genomic DNA was bisulfite converted by standard techniques (Clark et al., 2006; Frommer et al., 1992). Non-methylated cytosines of the DNA are converted into uracil, while methylated cytosines remain unchanged (Figure 10). In subsequent PCR amplification, uracils are transformed into thymines. Consequently, methylated and non-methylated cytosines can be distinguished after sequencing, since the latter causes a thymine signal instead of a cytosine signal.This method was applied to various samples from mice, humans, and non-human primates (Table 6). All animal experiments were performed in accordance with the German animal welfare act.

Table 6: Compilation of samples to which the bisulfite genomic sequencing method was applied. Genomic DNA was extracted from all samples, except from blastocysts, and applied to bisulfite genomic sequencing.

Samples for bisulfite genomic sequencing				
Organism	Specification	Type/tissue	Age/stage	Number
Feeding experiment[1,#]				
Mouse	BFMI860 strain	Blood – control diet	10 weeks	9
		Blood – high fat diet	10 weeks	10
		Blood – control diet	32 weeks	9
		Blood – high fat diet	32 weeks	10
	B6 strain	Blood – control diet	10 weeks	10
		Blood – high fat diet	10 weeks	10
		Blood – control diet	32 weeks	10
		Blood – high fat diet	32 weeks	10
Ontogenesis				
Mouse	NMRI strain[2]	Blood	adult	1
		Various tissues[*]	adult	[*]
[*] 1 x adrenal, 3 x brain (whole), 1 x heart, 1 x kidney, 3 x liver, 1 x lung, 1 x ovary, 1 x pancreas, 3 x spleen and 1 x thymus				
Mouse	NMRI strain[2]	Whole embryo	E8.0	3
		Whole embryo	E8.5	1
		Whole embryo	E9.5	3
		Whole embryo	E10.5	3
		Whole embryo	E11.5	3
		Whole embryo	E14.5	1
Mouse	B6 strain[2]	Blood	adult	20
		Various tissues[**]	adult	[**]
[**] 1 x brain, 1 x heart, 3 x hypothalamus, 1 x kidney, 1 x liver, 1 x lung, 1 x muscle, 1 x pancreas, 1 x spleen and 1 x white adipose tissue				
		Whole blastocysts[3]	blastocyst	11
Human[4]		Blood	newborn	8
Phylogenesis				
Primate	Pan troglodytes[5]	Blood	adult	5
	Gorilla gorilla[5]	Blood	adult	5
	Macaca mulatta[5]	Blood	adult	5
	Papio hamadryas[5]	Blood	adult	5
	Callithrix jacchus[6]	Blood	adult	4
	Eulemur macaco[5]	Muscle tissue	adult	4
	Galago senegalensis[5]	Muscle tissue	adult	4

[1] The samples were kindly provided by the working group of Prof. Brockmann from the *Institut für Züchtungsbiologie und molekulare Tierzüchtung*, Humboldt-Universität zu Berlin, Berlin, Germany.[#]

[2] The samples were kindly provided by the Max Planck Institute for Molecular Genetics, Berlin, Germany. Noon of the day that the mating plug was observed was considered embryonic day 0.5 (E0.5) of development.

[3] The samples were kindly provided by the research group '*Developmental Biology / Signal Transduction*' of Prof. Birchmeier-Kohler, Max-Delbrück-Centrum für Molekulare Medizin (MDC), Berlin, Germany.

[4] For the analysis of the newborn blood samples parents gave special informed consent.

[5] The samples were kindly provided by the *Deutsches Primaten Zentrum* (DPZ), Göttingen, Germany.

[6] The samples were kindly provided by Christian Adams of the *Centrum für Reproduktionsmedizin und Andrologie*, Universitätsklinikum Münster, Münster, Germany.

[#] The long-term feeding study, from which this samples of the working group of Prof. Brockmann are obtained, is extensively described by Widiker *et al.* (Widiker et al., 2010). To describe the study in short:

Mice of two mouse strains

a) obese Berlin Fat Mouse Inbred (BFMI) line 860 of the Institute of Animal Sciences, Humboldt-University, Berlin, Germany (Meyer et al., 2009; Wagener et al., 2006)

b) lean C57BL/6NCrl (B6) mouse line (Charles River Laboratories, Sulzfeld, Germany)

were divided into 8 groups of 4 - 5 mice of the same mouse strain and sex. They were fed either a standard maintenance diet (SMD; V1534-000 ssniff R/M-H) or high fat diet (HFD; S8074-E010 ssniff EF R/M, both *ssniff Spezialdiäten GmbH*, Soest, Germany, Table 7) for 29 weeks (starting week 3 after weening until week 32). Water consume was *ad libidum*. They were caged at room temperature with a light-dark cycle of 12 h.

Blood samples were collected at week 10 and week 32. Genomic DNA was extracted with the *NucleoSpin Tissue Kit* (Macherey-Nagel GmbH & Co., Duren, Germany). The animal experiments were in accordance with the German Animal Welfare Act (approval no. G0152/04).

Table 7: Compositions of the standard maintenance diet and high fat diet used in the mouse feeding experiment.

Content			
		Standard maintenance diet SMD	High fat diet HFD
Metabolizable energy		12.8 MJ/kg	19.1 MJ/kg
Energy from	* Fat	9%	45%
	* Protein	33%	24%
	* Carbohydrates	58%	31%

2.2.12.1 Bisulfite conversion of DNA samples

a) Denaturation:

Approximately 1 µg genomic DNA in a total volume of 50 µl was chemically denatured by incubation with 5.7 µl freshly prepared 3 M sodium hydroxide solution (NaOH) (15 min, 500 rpm, 37°C) followed by a thermal denaturation step (5 min, 500 rpm, 95°C). The DNA containing tubes were immediately placed on ice to ensure that the DNA remained denatured.

b) Sulfonation and hydrolytic deamination:

The bisulfite solution was always freshly prepared by mixing one aliquot 5% hydroquinone solution with 3.25 aliquots saturated sodium metabisulfite solution (Table 8). Thereof 563 µl were added to each sample. Then the samples were incubated (12 h, 50°C). To avoid oxidation, preparation of the solution, as well as the bisulfite conversion incubation were performed protected from light.

c) Purification:

The samples were desalted using the *Wizard® SV Gel and PCR Clean-Up System* (Promega) according to the manufacturer's instructions (Promega, 2009b) and eluted with 50 µl nuclease-free water.

d) Alkali desulfonation:

The final alkali desulfonation was achieved by incubating with 5.7 µl 3 M NaOH (15 min, 500 rpm, 37°C).

e) Neutralization and precipitation:

To neutralize the samples and precipitate the DNA, 1 µl of glycogen solution (10 mg/ml), 17 µl 7.5 M ammonium acetate, and 450 µl 100% ethanol were added, followed by overnight precipitation at -80°C. The DNA was centrifuged (25 min, 14,000 rpm, 10°C) and washed with 500 µl ice cold 70% ethanol (20 min, 14,000 rpm, 10°C). Afterwards, all traces of supernatant were removed and the samples were air dried for approximately 20 min (37°C). Finally, the DNA was resuspended in 35 µl H_2O_{HPLC} and either used directly for PCR amplification procedures (Paragraph 2.2.3.1) or stored at 4°C.

Table 8: Composition of solutions used for the bisulfite conversion of genomic DNA samples.

Solution/buffer	Composition
3 M NaOH	1.2 g NaOH pellets in 10 ml H_2O_{HPLC}
5% hydroquinone solution	50 mg hydroquinone crystals dissolved in 1 ml
Saturated sodium metabisulfite solution, pH	1.9 g sodium metabisulfite in 3.25 ml 0.46 M NaOH

2.2.12.2 Bisulfite conversion of blastocysts

This protocol is suitable for small amounts of tissue or cells without prior DNA extraction.

a) Preparation of single blastocyst-containing agarose beads:

Single blastocysts were mixed with 6 µl of 2% *SeaPlaque® Agarose* (Lonza), equilibrated twice with 50 µl 1x EcoRI buffer (New England Biolabs, 15 min, on ice) and then incubated overnight with 100 µl EcoRI restriction-mix (37°C).

b) Denaturation:

The EcoRI restriction-mix was removed and the agarose beads were washed with 50 µl 0.4 M NaOH (2 x 15 min, rt) and 50 µl 0.1 M NaOH (5 min, rt). After complete removal of the NaOH, the beads were overlaid with 500 µl heavy mineral oil and heated to destroy the cells and to denature the DNA (30 min, 95°C). Next, the samples were put on ice for approximately 20 min. until the agarose was getting solid again, hereby enclosing the denatured DNA in the beads.

c) Sulfonation and hydrolytic deamination:

Bisulfite solution was always freshly prepared by mixing 1 aliquot 10% hydroquinone solution with 6.5 aliquots saturated sodium metabisulfite solution and put on ice to cool (Table 9). 800 µl ice cold bisulfite solution was added to each sample in such a way that the bead was located in the watery bisulfite phase, and incubated (12 h, 50°C). To avoid oxidation, preparation of the solution, as well as the bisulfite conversion incubation were performed protected from light.

Table 9: Composition of solutions and buffer used for the conversion of blastocysts.

Solution/buffer	Composition
2% SeaPlaque® Agarose	20 mg *SeaPlaque® Agarose* powder in 1 ml H_2O_{HPLC}
EcoRI restriction-mix	20 units EcoRI in 100 µl 1x EcoRI buffer
2 M NaOH	0.8 g NaOH pellets in 10 ml H_2O_{HPLC}
10% hydroquinone solution	5 mg hydroquinone crystals dissolved in 0.5 ml
Saturated sodium metabisulfite	1.9 g sodium metabisulfite powder in 3.25 ml 0.31 M
1x TE, pH 8.0	10 mM Tris-HCl, 1mM EDTA in H_2O

d) Purification and alkali desulfonation:

After sulfonation and deamination, the mineral oil and bisulfite solution were carefully removed and the beads were washed with 500 µl 1x TE buffer (3 x 10 min, rt), 500 µl 0.2 M NaOH (3 x 10 min, rt) and

500 µl 1x TE buffer (3 x 10 min, rt) respectively. The beads were either used immediately for PCR amplification procedures (Paragraph 2.2.3.1) or stored at 4°C in 1x TE buffer.

2.2.12.3 Translation of bisulfite genomic sequencing results

The bisulfite converted DNA samples were PCR amplified (Paragraph 2.2.3.1). The resulting fragments were either directly applied to Exo/SAP and sequencing reaction (Paragraphs 0), or only after TOPO cloning and colony PCR (Paragraphs 2.2.7.1 and 2.2.3.2). Afterwards, sequences were evaluated and translated into (i) color-code for lollipop diagrams and (ii) number-code for methylation intensity plots. Response codes were used to translate the sequencing curves as stated below (Table 10 and Figure 11). Thereby cytosine-thymine double peaks were always interpreted as 'heterogeneously methylated' independent of their relation of heights.

Table 10: Response code for interpreting and translating methylation data from sequences.

Translation and coding of methylation status			
Base	Methylation status	Color-code	Number-code
Cytosine	methylated	black	100%
Thymine	non-methylated	white	0%
cytosine-thymine	heterogeneously methylated	grey	50%

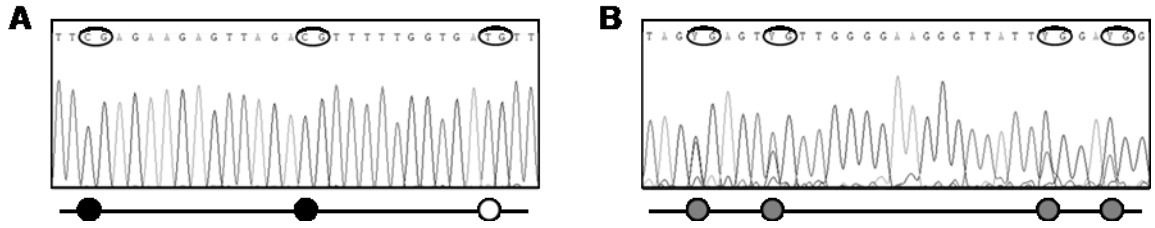

Figure 11: Translation of bisulfite sequences into the methylation status with respective lollipop figures. (A) Sequence with single cytosine = C and thymine = T peaks that are interpreted as 'methylated' or 'non-methylated' respectively and translated into black or white circles respectively. (B) Sequence with double peaks of cytosine-thymine = Y that are all interpreted in the same way as 'heterogeneously methylated' and translated into grey circles.

2.2.13 Functional analysis of the pCpGL vector constructs in GT1-7 cells

The promoter activity of the 5' CGI and 3' CGI of the human POMC locus was analyzed in dual luciferase reporter gene assays. Therefore, GT1-7 cells were transiently transfected with the luciferase-containing pCpGL vector constructs (Paragraph 2.2.7.2) and a renilla vector as transfection control.

2.2.13.1 Culturing GT1-7 cells

The GT1-7 cell line, developed by Mellon *et al.* (Mellon et al., 1990), is a mouse cell line obtained from anterior hypothalamic tumors with neuronal morphology. They were constructed and used for studies related to GnRH. However, it is one of the most utilized neuronal cell models for studies of basic neuronal function as they represent one of the few appropriate neuronal models available (Mayer et al., 2009).

GT1-7 cells were adherently cultured in *Dulbecco's Modified Eagle's Medium* (DMEM; Biochrom) containing 4.5 mg/l glucose, 548 mg/l L-glutamine, 10% fetal bovine serum (FBS), and 100 U/ml penicillin-streptavidin antibiotics, in a 4 – 5% CO_2 environment in 37°C. Once a week cells were trypsinized with 1 x Trypsin/EDTA solution (T/E) and passed through 1: 5 or used for seeding.

2.2.13.2 Transfection of GT1-7 cells

The GT1-7 cells were transfected with both a pCpGL construct and the pGL4.74 renilla vector using the *Effectene Transfection Reagent* (QIAGEN) according to the manufacturer's instructions (QIAGEN, 2002). Cells were seeded in 12-well plates at a cell density of 1.5 x 10^5 cells/well. The transfection was performed 24 h after the seeding. Per well 300 ng of the pCpGL construct and 0.12 ng of the renilla vector were added for transfection (1: 2500) using 2.4 µl *Enhancer* solution and 6 µl *Effectene* reagent. The pCpGL vector constructs were applied either unmethylated or after *in vitro* methylation with the methyltransferases M.SssI, HhaI, HpaII.

2.2.13.3 *In vitro* methylation of pCpGL vector constructs

Methyltransferase M.SssI was applied for complete methylation of each CpG position within the fragment. For partial methylation of the fragments, side specific methylases HhaI and HpaII were used. For detailed information about the specific methylation sites, see the Results section 3.1. Each microgram of vector construct was incubated (16 h, 37°C) in 1x buffer (NEB2 for M.SssI, HhaI buffer for HhaI, and HpaII buffer for HpaII), S-adenosylmethyonine (SAM, 160 µM for M.SssI and 80 µM for HhaI or HpaII), and the respective enzyme (enzymes, buffers and SAM obtained from New England Biolabs). To stop the enzymatic reaction, samples were purified using the centrifugation strategy (Promega, 2009b) of the *Wizard® SV Gel and PCR Clean-Up System* (Promega) with following modifications:

- → No evaporation step with open centrifuge lid was carried out.
- → DNA was eluted with 60 µl nuclease-free water.

After purification, DNA concentrations of the samples were determined by NanoDrop, so the right amount could be deployed for transfection. For the mock controls, the same sample processing protocol was followed without the addition of SAM. The unmethylated vector was also exposed to the same incubation, cleaning and measuring steps for control.

2.2.13.4 Dual-luciferase reporter gene assay

The dual-luciferase reporter gene assay is based on two different luciferase reporter enzymes, which are simultaneously expressed after transfection into the cell. The *firefly* luciferase and the *renilla* (sea pansy) luciferase have different bioluminescence substrates and do not cross-activate (Sherf et al., 1996). The dual-luciferase assay was applied for functional analysis of the pCpGL vector constructs (Table 2 and Table 3). These fragments are assumed to have promoter function, hence to be capable of activating gene transcription and expression of the firefly luciferase gene, which is located downstream of the multiple cloning site of the pCpGL vector. By transfecting constant ratios of the firefly luciferase vector constructs (pCpGL) and the renilla luciferase vector (pGL4.74), the independently measured light signals can be used to (i) detect gene expression activation due to the cloned fragments by measuring the firefly luciferase signal and (ii) adjust the data for transfection efficiency by the renilla luciferase signal.

a) Cell lysis:

The GT1-7 cells were lysed 48 h hours after transfection in two steps. First, the medium was substituted by 250 µl of 1x passive lysis buffer (PLB, Promega) and the plates were shaked (15 min, 500 rpm, rt). Secondly, the cells were frozen (at least 1 h, -20°C) after the shaking procedure.

b) Measurement of both luciferase signals:

After thawing, 3 x 20 µl, the cell lysate was measurement using the *Dual-Luciferase® Reporter Assay System* from Promega (Promega, 2010b) with the microplate reader *Mithras LB 940* (Berthold).

2.2.14 Statistical analysis

The statistical analyses (exploratory data analysis and non-parametric statistics) of the bisulfite genomic sequencing results of the samples from the mouse feeding experiment was performed by Andrea Ernert, Institut für Sozialmedizin, Epidemiologie und Gesundheitsökonomie, Charité Berlin, Berlin, Germany.

The data from dual-luciferase reporter gene assay was analyzed using Excel (Microsoft, Redmond, USA) and the GraphPadPrism 4 software (GraphPad Software, LaJolla, USA). Significance was tested with unpaired, two-tailed t-tests for a 95% confidence interval.

2.2.15 Repeat analysis

Using the *RepeatMasker Web Server* tool (http://www.repeatmasker.org/cgi-bin/WEBRepeatMasker) the sequences of the various primates were analyzed for *Alu* incidence.

2.2.16 Transcription factor binding site analysis

The analysis by *TFSEARCH* transcription factor search web tool (http://molsun1.cbrc.aist.go.jp/research/db/TFSEARCH.html) revealed putative transcription factor binding sites in the applied sequences.

3 Results

The POMC locus exhibits two CpG islands (CGIs). The 5' CGI is associated with the promoter region and embeds the exon1 start that coincides with the transcription start site (TSS) of regular POMC transcripts. The intragenic 3' CGI surrounds the exon3 start (Figure 12). The DNA methylation patterns of both CGIs were established by Kuehnen *et al.* (Kuehnen et al., in revision).

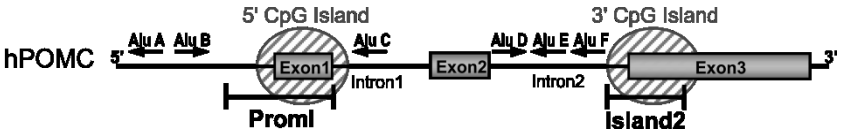

Figure 12: human POMC gene indicating the location of the PromI and Island2 fragments for functional analysis. Grey boxes indicate exons. Hatched ovals mark the location of CGIs. *Alu* element positions are marked by horizontal arrows.

The aim of this thesis was to reveal various core issues of the DNA methylation patterns of the POMC CGIs: their function in gene activity, their tissue distribution and stability, as well as their ontogenetic and phylogenetic development. Therefore, I tested the postulated four hypotheses regarding the DNA methylation patterns of the POMC locus with appropriate methodological approaches as posed in Paragraph 1.7.

3.1 The POMC DNA methylation status influences its gene expression

Generally, DNA methylation interferes with gene expression. In this thesis work, fragments of both CGIs of the POMC locus were tested for promoter activity. The constructs of interest were built using a luciferase-containing CpG-free vector backbone (pCpGL) to prevent unspecific inhibiting influences of vector backbone-CpGs (Klug and Rehli, 2006). Thereby, only effects of functionally important CpG residues within the fragments of interest could be detected.

The so-called pCpGL-PromI construct contains a fragment of the 5' CGI. The second construct, the so-called pCpGL-Island2, contains a fragment of the 3' CGI (Figure 12). Both pCpGL-constructs were methylated using the generic CpG methylase SssI for complete methylation and target specific CpG methylases HhaI (target site = GCGC) and HpaII (target site = CCGG) for partial methylation (Figure 13B and Figure 14B).

Cells of the GT1-7 hypothalamic cell line were transfected with SssI-, HhaI-, HpaII-methylated or unmethylated constructs. A renilla vector was used as a control for transfection efficiency. After 48 h, the cells were lysed and a dual-luciferase assay was performed. The transfection efficiency was determined by putting the luciferase signal in relation to the renilla signal.

3.1.1 Functional analysis of the pCpGL-PromI construct

As shown in Figure 12 and Figure 13B, the PromI fragment spans -493 bp to +98 bp of the 5' CGI in relation to the TSS (= exon1 start). This fragment includes 48 CpG dinucleotides, which were all methylated after incubation with SssI. Methylation with HhaI and HpaII resulted in six and three methylated CpG positions respectively (Figure 13B). *In silico* analysis revealed, that one of the HpaII-methylation sites coincides with a nucleotide sequence that is similar to a binding site of the group of signal transducers and activators of transcription (STAT).

The unmethylated vector construct showed signaling in comparison to the negative control. However, no response was observed when the vector construct pCpGL-PromI was completely methylated (SssI). Partial methylation with HhaI showed no significant effects while methylation with HpaII reduced the response significantly (Figure 13A).

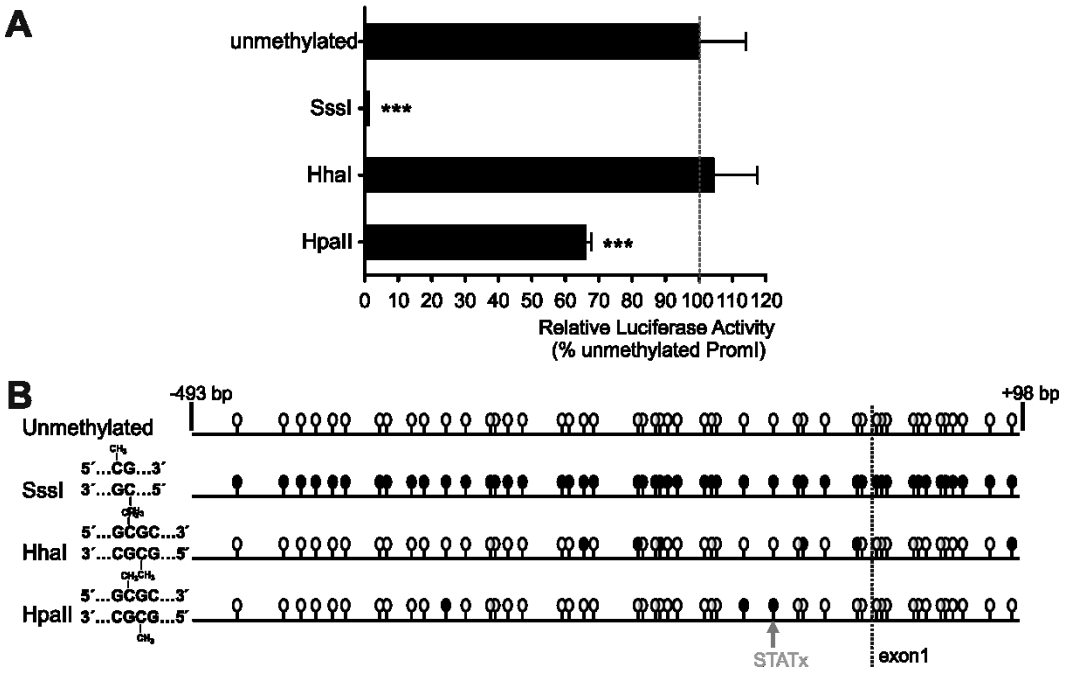

Figure 13: Functional analysis of the hPOMC 5' CGI (pCpGL-PromI construct). (A) Effects of DNA methylation (SssI-, HhaI-, or HpaII-methylation) on signaling activity in dual-luciferase reporter gene assays. Results are shown relative to the activity of the unmethylated pCpGL-PromI construct and are normalized for transfection efficiency by co-transfection of Renilla construct. Values are the mean ± SD from three independent experiments. *** *p*-value < 0.001 (t-test for a 95% confidence interval). (B) Lollipop figures of the differentially methylated PromI fragment (unmethylated, SssI-, HhaI-, or HpaII-methylated). The target sites of respective enzymes are shown. Each lollipop indicates the position of one CpG group within the fragment. white circles = non-methylated, black circles = methylated. The vertical arrow marks the CpG position that coincides with an *in silico* predicted STAT binding site. Illustration of the CpG positions and fragment lengths are in proportion and the vertical dashed line indicates the starting point of exon1.

3.1.2 Functional analysis of the pCpGL-Island2 construct

The 3' CGI of the human POMC was also analyzed as pCpGL vector construct. First GT1-7 hypothalamic cells were transfected with the long construct pCpGL-Island2 long (-256 bp to +294 bp of the exon3 boundary) either unmethylated or SssI-, HhaI- or HpaII-methylated. Next, the pCpGL-Island2 construct was tested in different lengths variations to determine, which regions are important for signaling.

3.1.2.1 Differentially methylated Island2 fragment

The Island2 fragment spans over the intron2-exon3 junction within the 3' CGI of the human POMC (-256 bp to +294 bp of the exon3 boundary, Figure 12) and possesses 53 CpG dinucleotides. All of these 53 CpG dinucleotides were methylated by SssI. The methylases HhaI and HpaII only methylated five and six CpGs respectively in this region (Figure 14B). Also for the Island2 fragment *in silico* analysis revealed a coincidence of one HpaII-methylation site with a hypothetical STATx-binding site. Additionally, the subsequent CpG position of the p300 binding site is also a target site of HpaII.

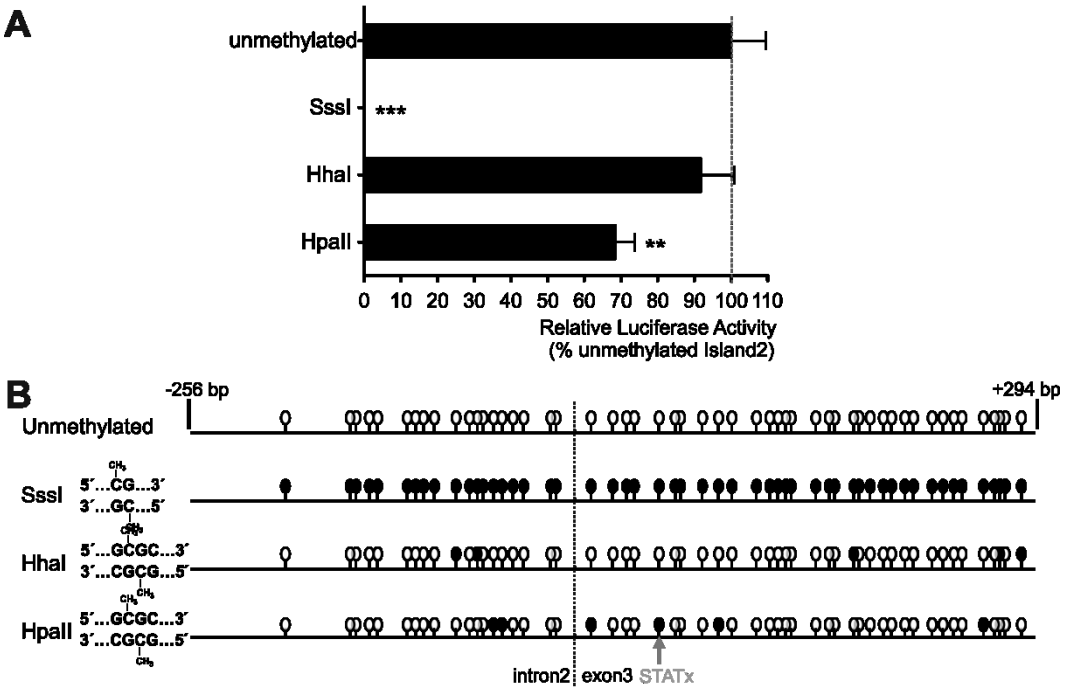

Figure 14: Functional analysis of the hPOMC 3' CGI (pCpGL-Island2 construct). (A) Effects of DNA methylation (SssI-, HhaI-, or HpaII-methylation) on signaling activity in dual-luciferase reporter gene assays. Results are shown relative to the activity of the unmethylated pCpGL-Island2 construct and are normalized for transfection efficiency by co-transfection of Renilla construct. Values are the mean ± SD from three independent experiments. ** p-value = 0.001 – 0.01; *** p-value < 0.001 (t-test for a 95% confidence interval). (B) Lollipop figures of the differentially methylated Island2 fragment (unmethylated, SssI-, HhaI-, or HpaII-methylated). The target sites of respective enzymes are shown. Each lollipop indicates the position of one CpG group within the fragment. white circles = non-methylated, black circles = methylated. The vertical arrow marks the CpG position that coincides with an in silico predicted STAT binding site. Illustration of the CpG positions and fragment lengths are in proportion and the vertical dashed line indicates the starting point of exon3.

Compared to the negative control (empty vector), the unmethylated vector construct showed significant signaling and, therefore, promoter function. However, when the Island2 fragment was completely methylated, the response disappeared. Partial methylation with HpaII resulted in significant but not complete reduction of the activity. HhaI methylation showed no significant effects (Figure 14A).

3.1.2.2 Variations in length of the Island2 fragment

The Island2 fragment showed promoter activity in the previous experiments. To find out about crucial regions for the identified activity, two additional pCpGL constructs of the 3' CGI were created and tested. Assuming that the Island2 construct is the 'long' fragment, also a 'medium' and a 'short' fragment were designed. All three fragments had the same starting position (-256 bp to the exon3 boundary) but the 'long' fragment ended in the middle of the exon3 at position +294 bp relative to the exon3 start. Therefore, it contained the p300 binding site with subsequent CpG residue at the intron-exon junction, as well as the putative STATx binding site surrounding the CpG position at +53 bp. Those two CpG sites were identified in the previous experiment to be target sites of HpaII methylation, which reduced the promoter activity of the fragment significantly. The medium-sized fragment ended downstream of the p300 binding site (+32 bp) and included the succeeding CpG position but not the putative STATx binding site. The 'short' fragment ended before the exon3 start at -10 bp and contained neither the p300 nor the putative STAT binding site (Figure 15B).

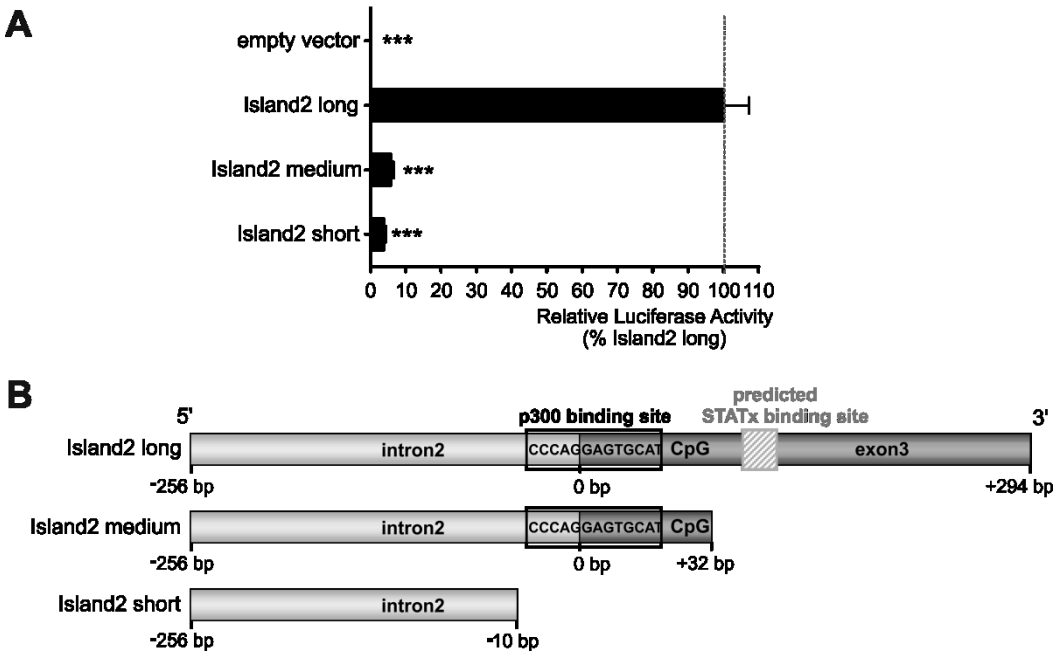

Figure 15: Functional analysis of the 3' CGI (pCpGL-Island2 construct) in various lengths. (A) Effects of length variations (long, medium, and short) on signaling activity in dual-luciferase reporter gene assays. Results are shown relative to the activity of the pCpGL-Island2 long construct and are normalized for transfection efficiency by co-transfection of Renilla construct. Values are the mean ± SD from three independent experiments. *** *p*-value < 0.001 (t-test for a 95% confidence interval). (B) Scheme of the Island2-fragments with the lengths long, medium, and short. Length indications are relative to the exon3 start. The p300 binding site is marked with a black box. The grey hatched box indicates the *in silico* predicted STATx binding site.

Transfection of the long fragment into GT1-7 cells resulted in a proper luciferase signal. However, the medium and the short versions of the pCpGL-Island2 construct were significantly reduced in their activity and showed practically no response in the reporter gene assays (Figure 15A). To examine further a possible involvement of the p300 binding site in the promoter activity of the Island2 fragment, the p300 binding site was modified in different ways and afterwards again tested in dual-luciferase assays.

3.1.2.3 Modifications of the p300 binding site of the Island2 fragment

The long Island2 fragment, which contains the p300 binding site and the *in silico* predicted STATx binding site, was modified in three ways in the region of the p300 binding site (Figure 16B) to elucidate the role of the p300 binding site for the promoter activity of the Island2 fragment:

- → Island2 long-del: the three bases GAG were deleted to make the p300 binding site unrecognizable.
- → Island2 long-mut: a GAG → CTC mutation was introduced to make the p300 binding site unrecognizable.
- → Island2 long-mutCpG: CpG residue +1 downstream of the p300 binding site was mutated to TpG.

Transfection of the long, unmodified Island2 fragment into GT1-7 cells resulted in a proper luciferase signal (Figure 16A). Deletion of the three bases 'GAG' within the p300 binding site (Island2 long-del) lead to unrecognizability of the binding site and resulted in a slight but significant reduction of signaling activity. In the Island2 long-mut construct the p300 binding site was also unrecognizable, but caused a significant increase of promoter activity. However, even though this mutation destroyed the p300 binding site it created a putative GATA-1 binding site at the same time. The CpG → TpG mutation of the CpG residue that is directly downstream of the p300 binding site (Island2 long-mutCpG), showed no effect on the signaling activity of the Island2 fragment. The p300 binding site was unaffected by this mutation.

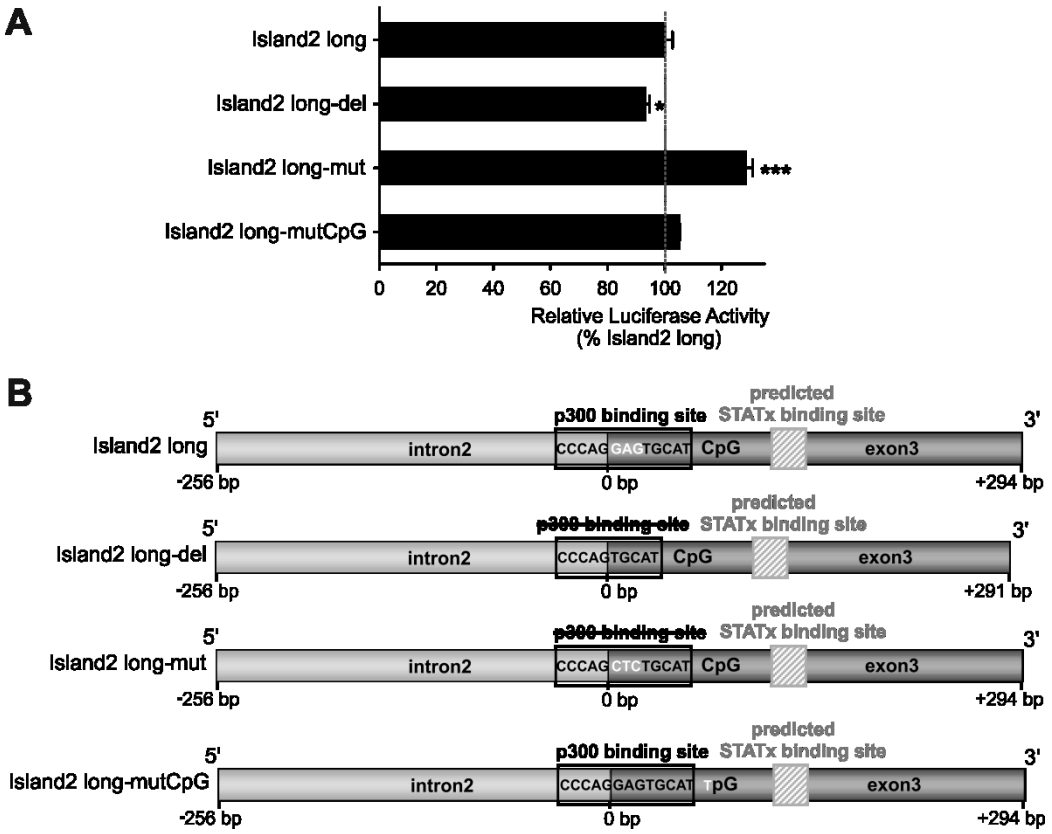

Figure 16: Functional analysis of the 3' CGI (pCpGL-Island2 construct) with p300 binding site modifications. (A) Effects of modifications of the p300 binding site (del, mut, and mutCpG) on signaling activity in dual-luciferase reporter gene assays. Results are shown relative to the activity of the pCpGL-Island2 long construct and are normalized for transfection efficiency by co-transfection of Renilla construct. Values are the mean ± SD from three independent experiments. * *p*-value = 0.01 - 0.05; *** *p*-value < 0.001 (t-test for a 95% confidence interval). (B) Scheme of the Island2-fragments with different modifications. Length indications are relative to the exon3 start. The p300 binding site is marked with a black box. The grey hatched box indicates the putative STATx site. del = deletion of 'GAG'; mut = 'GAG' → 'CTC'-mutation; mutCpG = CpG → TpG-mutation of the moiety +1.

These reporter gene assays showed, that both CGI fragments exert promoter activity *in vitro*, which can be influenced by length or sequence modifications of the fragment, as well as by changes in the methylation state. Hence, it was interesting to establish the methylation states of both CGIs of the POMC *in vivo* and to test their constancy during life.

3.2 The POMC DNA methylation pattern is stably established early during ontogenesis

The *in vitro* reporter gene assays showed, that the promoter activity of both CGIs could be influenced by the methylation status. Since the *in vivo* DNA methylation status of a promoter region can also be associated with its transcriptional activity of the gene, the occurrence and tissue distribution of POMC DNA methylation patterns was analyzed in various murine tissues.

DNA methylation of the genome changes during lifetime. For instance, periconceptional the DNA methylation is reprogrammed. In this phase, the DNA methylation patterns of a genome are established. Hence, it is important to understand the dynamics of the ontogenetic formation and development of DNA methylation pattern. Therefore, the ontogenetic development of DNA methylation patterns of the POMC locus was further elucidated.

3.2.1 POMC DNA methylation in various tissues of adult mice

→ The DNA methylation patterns of the two CGIs within the POMC gene region were determined in peripheral blood cells (PBC).

→ By comparing the patterns of various murine tissues of adult members of two different mouse strains (NMRI and C57BL/6) the intraindividual constancy of POMC methylation was estimated.

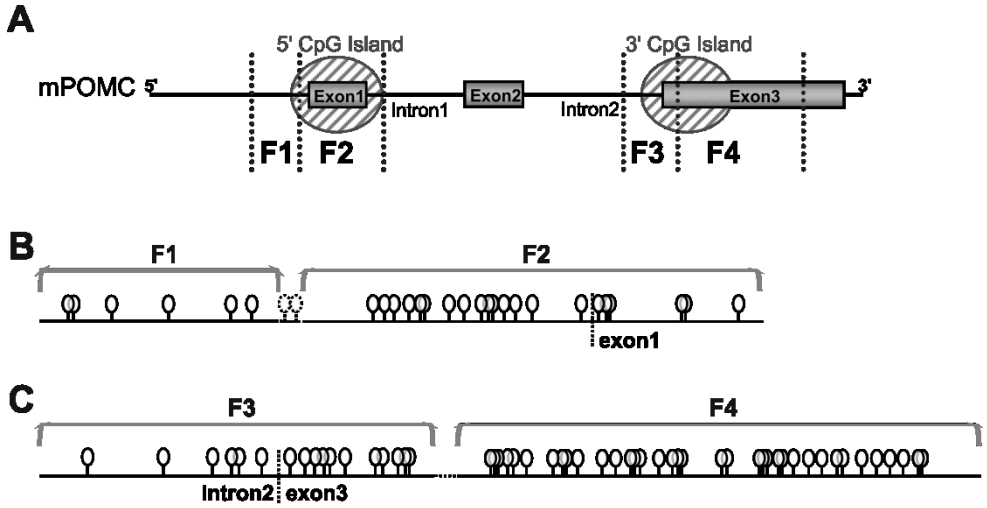

Figure 17: mouse POMC gene denoting the 5' and 3' CGI. (A) Scheme of the mouse POMC gene. Hatched ovals mark the location of the 5' and the 3' CGI. The F1, F2, F3, F4 labeled segments mark the location of the four fragments of interest (mPOMC-F1 = 243 bp, 6 CpGs; mPOMC-F2 = 450 bp, 21 CpGs; mPOMC-F3 = 328 bp, 17 CpGs; mPOMC-F4 = 493 bp, 37 CpGs). (B) Lollipop figures of the two fragments of the 5' CGI (mPOMC-F1and -F2). (C) Lollipop figures of the two fragments of the 3' CGI (mPOMC-F3and -F4). Each lollipop indicates the position of one CpG residue within the fragment. The illustration of the CpG positions is in proportion. Upstream boarders of the exons1 and exon3 are marked by vertically dashed lines.

The samples of genomic DNA from mouse blood and various mouse tissues were bisulfite converted. The four fragments of interest, mPOMC-F1, -F2, -F3 and -F4 (Figure 17), were PCR amplified using the primers listed in Paragraph 2.1.7.1. The resulting fragments from the bisulfite PCRs were directly sequenced. Not all CpG positions within and in between the fragments were accessible because of the primer positions and sequencing reasons.

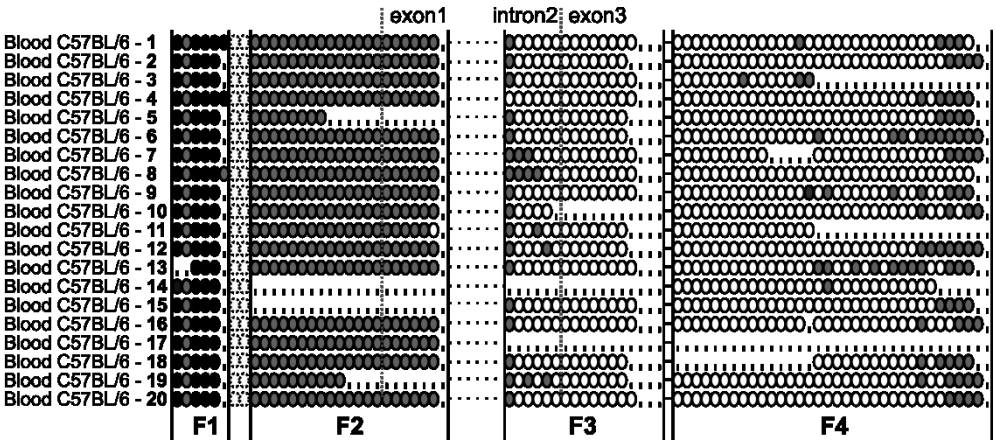

Figure 18: DNA methylation patterns in DNA samples from peripheral blood cells (PBC, n = 20) of adult C57BL/6 mice. Vertical solid lines indicate the margins of the four fragments (mPOMC-F1/-F2/-F3/-F4). Dotted vertical lines mark the upstream boundaries of exon1 and exon3 respectively. Each circle of one row represents one CpG position within the gene region. Vertical dashes indicate CpGs with a non-analyzable methylation status. Black circles represent methylated CpGs; white circles non-methylated CpGs and grey circles represent heterogeneously methylated CpGs.

Bisulfite converted DNA samples from peripheral blood cells (PBC) of 20 different C57BL/6 mice showed the following DNA methylation pattern (Figure 18): The 5' CGI, covered by the fragments mPOMC-F1 and mPOMC-F2, was distinctly methylated with hypermethylation in the mPOMC-F1 region and predominant heterogeneous methylation for the mPOMC-F2 fragment. In the mPOMC-F1 fragment, a methylation dip around CpG position -19 (respective to exon1 start) could be detected. The 3' CGI, covered by mPOMC-F3 and mPOMC-F4, showed sporadic heterogeneous methylation for the intron2 region of the mPOMC-F3 fragment (first to sixth CpG position), and hypomethylation for the exon3 region (posterior part of mPOMC-F3 and mPOMC-F4). This patterning was similar for all mice examined.

The analysis of the DNA samples from different tissue of the C57BL/6 mouse strain and the NMRI mouse strains showed similar patterning for the examined tissues (Figure19). All samples showed the overall hypomethylation for the third and fourth fragment (exon3 region), which increased up to 50% of sporadic methylation in the intron2 region. In addition, the patterns of heterogeneous methylation of the second fragment and hypermethylation of the first fragment were consistent. Even the methylation decrease at CpG position -19 (respective to exon1) in the mPOMC-F1 fragment was reproducible in most samples.

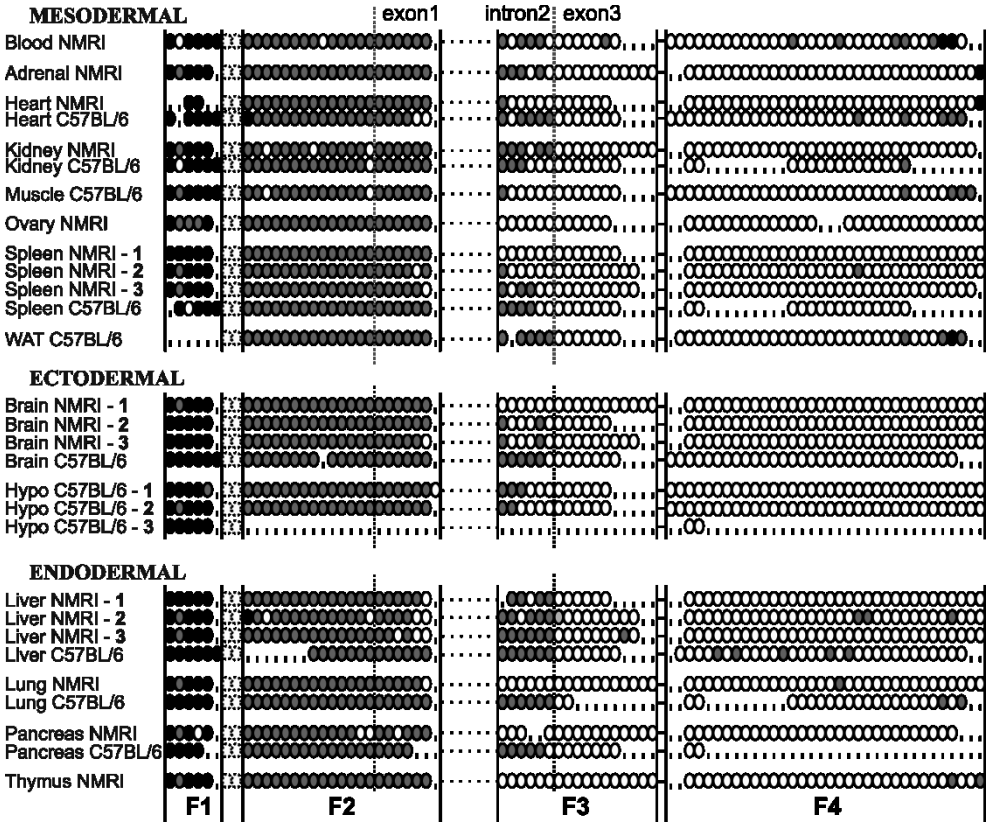

Figure 19: DNA methylation patterns in DNA samples from various tissues of adult NMRI and C57BL/6 mice. The tissues are sorted by germ layer origin (derived from literature). Vertical solid lines indicate the margins of the four fragments (mPOMC-F1/-F2/-F3/-F4). Dotted vertical lines mark the upstream boundaries of exon1 and exon3 respectively. Each circle of one row represents one CpG position within the gene region. Vertical dashes indicate CpGs with a non-analyzable methylation status. Black circles represent methylated CpGs; white circles non-methylated CpGs and grey circles represent heterogeneously methylated CpGs.

Summing up, the DNA methylation patterns were largely the same in all tissue samples examined, independent from the tissue, the mouse strain, or the POMC expression status. Even the germ layer of origin of the tissue did not have an influence on the methylation pattern. Hence, the question aroused when these constant patterns evolve, if they are established before the differentiation of the germ layers, or if they develop independently in the various tissues. To find out about the time point when the DNA

methylation patterns of *POMC* are established, they were analyzed in various embryonic stages of NMRI mice.

3.2.2 POMC DNA methylation in various embryonic stages of NMRI mice

During cell division, the DNA methylation is passed to the daughter cells. However, in the periconceptional phase, DNA methylation is reprogrammed and patterns are established. To find out about the developmental dynamics of the POMC methylation patterns, we aimed to determine, when the consistent patterns, we observed in PBC and different mouse tissues, evolve. Therefore, a comparative analysis of the POMC methylation patterns in mice was performed using samples of various prenatal stages. The results from the embryonic samples were compared to the patterns found in adult mice.

The samples of genomic DNA from mouse embryos of various prenatal stages (E8.0, E8.5, E9.5, E10.5, E11.5, and E14.5) were bisulfite converted. The four fragments of interest, mPOMC-F1, -F2, -F3 and -F4 (Figure 17), were PCR amplified using the primers listed in Paragraph 2.1.7.1. The resulting fragments from the bisulfite PCRs were directly sequenced. Not all CpG positions within and in between the fragments were accessible because of the primer positions and sequencing reasons.

All embryonic samples showed the same patterning (Figure 20): Heterogeneous methylation of intron2 and hypomethylation of exon3 characterized the 3' CGI. Distinct hypermethylation with a heterogeneous methylation dip at CpG -19 in the front part was observable for the 5' CGI. However, the back part of the 5' CGI showed slight pattern variations amongst the different samples but was at large heterogeneously methylated. Comparative analyses revealed that the patterns of both POMC CGIs from whole embryo samples resemble the patterns of PBC and tissue samples received from adult mice.

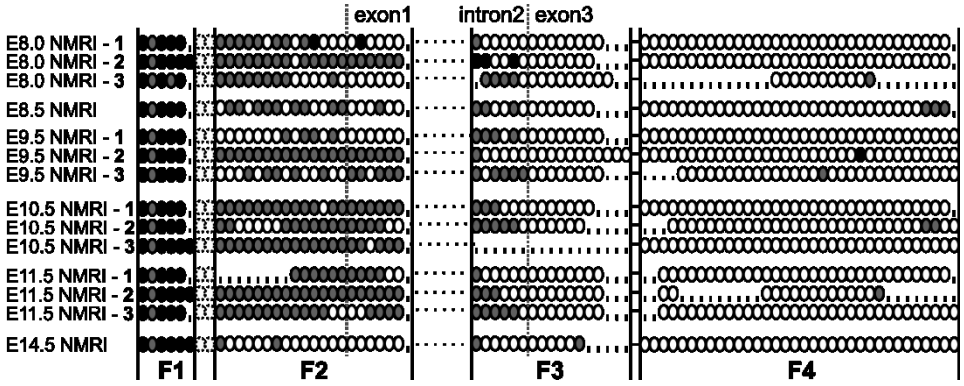

Figure 20: DNA methylation patterns in DNA samples from various embryonic stages (E8.0 to E14.5) of NMRI mice. Vertical solid lines indicate the margins of the four fragments (mPOMC-F1/-F2/-F3/-F4). Dotted vertical lines mark the upstream boundaries of exon1 and exon3 respectively. Each circle of one row represents one CpG position within the gene region. Vertical dashes indicate CpGs with a non-analyzable methylation status. Black circles represent methylated CpGs; white circles non-methylated CpGs and grey circles represent heterogeneously methylated CpGs. E = embryonic day.

3.2.3 POMC DNA methylation in mouse blastocysts

To examine further, if the observed patterns are established before the differentiation of the germ layers, or if they develop independently in the various tissues, samples from an earlier developmental stage, the blastocystal stage (E3.5), were examined. Because of the nature of a blastocyst sample and its small number of cells, a modified version of the bisulfite conversion was applied (Methods 2.2.12.2) to capture the small amount of DNA from a blastocyst within an agarose bead before conversion. The four fragments of interest, mPOMC-F1, -F2, -F3 and -F4 (Figure 17), were amplified using one blastocyst-agarose bead as template per PCR. After amplification, the PCR products were TOPO cloned, as well as directly sequenced. Following the TOPO cloning step, various clones of one blastocyst-sample were sequenced. The sequences

of all clones originating from one blastocyst template represent its methylation pattern. For each fragment (mPOMC-F1/-F2/-F3/-F4) all clones of one blastocyst are shown exemplary for the results of all analyzed blastocysts (Figure 21).

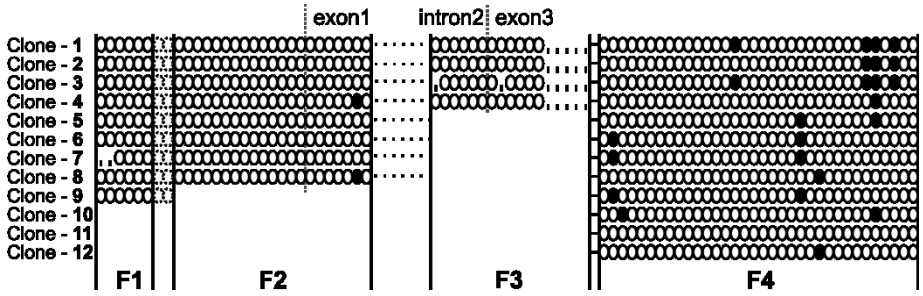

Figure 21: DNA methylation patterns in blastocyst samples of the C57BL/6 mouse strain. Vertical solid lines indicate the margins of the four fragments (mPOMC-F1/-F2/-F3/-F4). Dotted vertical lines mark the upstream boundaries of exon1 and exon3 respectively. Each row represents one analyzed clone. Each circle of one row represents one CpG position within the gene region. Vertical dashes indicate CpGs with a non-analyzable methylation status. Black circles represent methylated CpGs; white circles non-methylated CpGs and grey circles represent heterogeneously methylated CpGs. All shown clones for one fragment originate from the same blastocyst sample. The posed sequences are exemplary for the results obtained from all analyzed blastocysts. In sequences obtained from direct sequencing, analogue results were observed.

All analyzed clones of various blastocysts displayed similar methylation states. The four fragments of interest were uniformly hypomethylated with only a few CpG residues showing methylation with a random distribution. In sequences obtained from direct sequencing, analogue results were observed.

The mPOMC-F1 fragment, which was hypermethylated in all samples from embryos and adult mice, was also non-methylated in blastocysts. The same applied for mPOMC-F2, as well as the intron2 region of mPOMC-F3, which were heterogeneously methylated in all other samples. The exon3 regions were also non-methylated as observed before in adult mice and mouse embryos. These results differed significantly from those of various mouse tissues and embryonic stages later than E8.0, described in the paragraphs above, suggesting reprogramming and establishment of the patterns in early development. For validation if the consistency of the POMC DNA methylation patterns observed in this study also applies for the human POMC locus, samples from newborns were analyzed.

3.2.4 POMC DNA methylation in newborn humans

Parallel to the ontogenetic examinations in mice also the stability of the human POMC DNA methylation pattern was tested. Therefore, the human DNA methylation patterns of newborn PBC DNA samples were analyzed using samples obtained from *Whatman Protein SaverTM 903®* newborn screening cards. Due to obvious ethical reasons, it was not possible to examine the human patterns prenatally in different embryonic stages.

The DNA samples of eight newborn humans were bisulfite converted. The three fragments of interest, hPOMC-F1, -F2, and -F3 (Figure 22) were PCR amplified using primers listed in Paragraph 0. The resulting fragments from the bisulfite PCRs were directly sequenced. Not all CpG positions within and in between the fragments were accessible because of the primer positions and sequencing reasons.

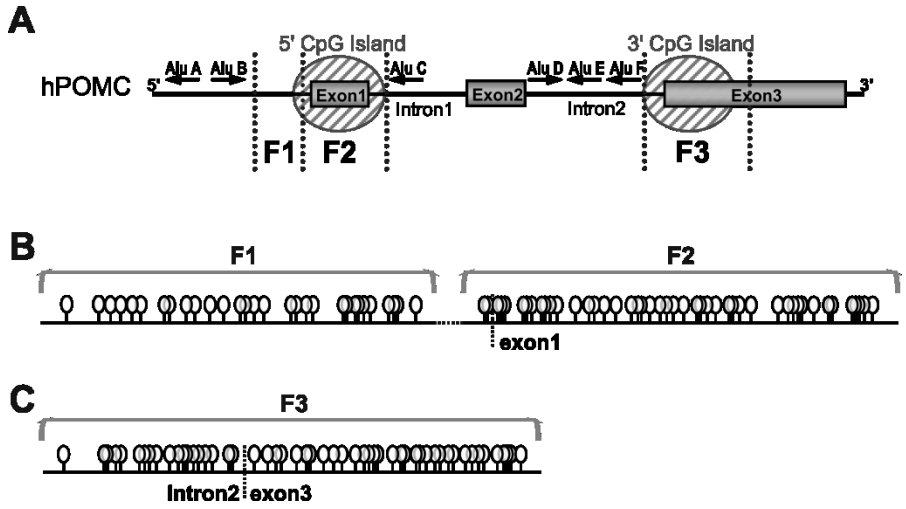

Figure 22: human POMC gene denoting the 5' and 3' CGI. (A) Scheme of the human POMC gene. Hatched ovals mark the location of the 5' and the 3' CGI. The F1, F2, and F3 labeled segments mark the location of the three fragments of interest (hPOMC-F1 = 416 bp, 30 CpGs; hPOMC-F2 = 442 bp, 46 CpGs; hPOMC-F3 = 513 bp, 53 CpG). *Alu* element positions are marked by arrows. (B) Lollipop figures of the two fragments of the 5' CGI (hPOMC-F1 and -F2). (C) Lollipop figure of the fragment of the 3' CGI (hPOMC-F3). Each lollipop indicates the position of one CpG residue within the fragment. The illustration of the CpG positions is in proportion. Upstream boarders of the exons1 and exon3 are marked by vertically dashed lines.

The results of the newborn humans are not depicted as lollipop figures as the mouse samples, but as semi-quantitative descriptive plots that show the CpG methylation intensity over the particular CpG position (Figure 23), as it was done by Kuehnen *et al.* for the DNA methylation patterns from human adolescents and β-MSH positive cells (Figure 7). The patterns, received from PBC samples from newborns, showed heterogeneous DNA methylation for the 5' CGI. The gene region upstream of the exon1 start was irregularly heterogeneously methylated with peaks at CpG positions -23, -27 and -29. The region downstream of the exon1 start was hypomethylated. For the 3' CGI a prominent pattern of hypermethylation in the intron2 region and hypomethylation in exon3 was observed. Within the block of hypermethylation in intron2, a constant reduction of methylation to approximately 50% was detectable. The transition from hypermethylation in the intron2 region to hypomethylation in the exon3 occurred as sudden decline between CpG position -3 and CpG +2, which downright forms a 'drop zone' at the intron2-exon3 junction (Figure 23).

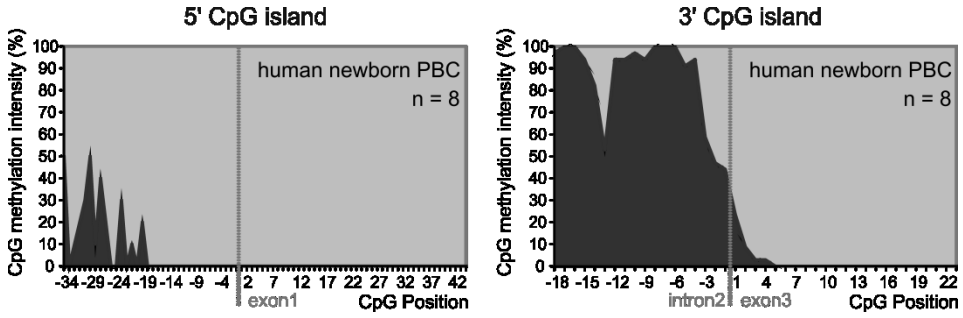

Figure 23: DNA methylation pattern of the human POMC locus in samples from human newborns (n = 8) depicted as methylation intensity plots. The plots are semi-quantitative and descriptive and display CpG methylation intensity (in %) over the particular CpG position within this region. CpG positions are numbered according to their relative position to the next exon start. Vertical dashed lines mark the exon starts. 5' CpG island (CGI) = hPOMC-F1 + hPOMC-F2; 3' CGI = hPOMC-F3.

The detected methylation pattern was compared to the established human patterns from adult PBC DNA (Figure 7*)*. The patterns from newborn PBCs were consistent with the findings of adult PBC and

microdissected ß-MSH positive cells of the human arcuate nucleus. Even the dip to heterogeneous methylation at CpG position -13 of the 3' CGI showed conservation

The methylation dip at CpG -13 and the distinct drop zone at the intron2-exon3 junction are conserved in all three kinds of human samples: newborn PBC, adult PBC and microdissected ß-MSH positive cells. The conservation of those structural features suggests some kind of function. Therefore, we tested both the CpG -13 position and the intron2-exon3 transition for putative transcription factor binding sites *in silico,* to estimate their importance and relevance in this coherence.

The comparative analysis of the human POMC DNA methylation patterns in newborn PBC, adult PBC and ß-MSH positive cells showed high constancy of the patterns in human postnatal life. The methylation pattern of humans differs highly from the murine methylation pattern. A possible influencing factor for this was examined in Paragraph 3.4. However, the findings of the constancy of the POMC methylation in humans are in accordance with the findings from mice made in samples from various tissues of different germ layer origin and in various developmental stages. If these stable patterns can be changed by exposure to long-time application of a high fat diet to mice, was tested in the following part.

3.3 The POMC DNA methylation pattern is stable postnatally

Mice were fed for 29 weeks (starting at week 3 after weaning) with either a high fat diet (HFD) or a standard maintenance diet (SMD). This was tested in two different mouse models, the C57BL/6 and the BFMI860 mouse strain. The C57BL/6 mouse strain is considered a lean wild type strain. The members of the BFMI860 strain are considered predisposed for being obese (Meyer et al., 2009; Wagener et al., 2006). The DNA samples from PBC of 39 mice taken at week 10 (seven weeks of feeding) and week 32 (29 weeks of feeding and end of the test period) were bisulfite converted. The four fragments of interest, mPOMC-F1, -F2, -F3 and, -F4 (Figure 17) were PCR amplified. The resulting fragments were directly sequenced. Not all CpGs within the region were accessible because of the primer positions and sequencing reasons.

All analyzed groups - high fat diet and control diet groups of both mouse strains - showed similar DNA methylation patterns (Figure 24). This was true for the comparison of different groups, as well as for the comparison of both time points within one group. The 5' CGI, covered by the fragments mPOMC-F1 and mPOMC-F2, was hypermethylated in the mPOMC-F1 region, and predominantly heterogeneously methylated for the mPOMC-F2 fragment. In mPOMC-F1, a methylation drop around CpG position -19 was detected. The 3' CGI was heterogeneously methylated in the intron2 region (first to sixth CpG position of mPOMC-F3), whereas the exon3 region (posterior region of mPOMC-F3 + mPOMC-F4) showed hypomethylation. These patterns for the 5' CGI and 3' CGI were observed for all samples analyzed, with mild irregularities, independent of mouse strain, time point, or diet.

Various statistical tests (exploratory data analysis and non-parametric statistics) were applied to the data, whereby all CpGs positions analyzed were tested as one group. Additionally, two subgroups were created and independently tested with the same statistical tests. This was done, because the regions of the subgroups showed prominent extremes of DNA methylation. One subgroup consisted of the first five CpG positions (subgroup CpG 1 - 5), which showed hypermethylation in comparison to the other regions. The other subgroup was formed of the data from the last 20 CpG moieties (subgroup CpG 60 - 80), which showed regions of irregular heterogeneous methylation within the hypomethylated exon3 region.

For the C57BL/6 mice, no statistically significant differences could be detected. In the non-parametric Mann-Whitney-Test a difference in CpG position 63 was detected, which was almost significant showing a *p*-value of 0.054. This difference was only observed in the CpG 60 - 80 subgroup data without correction for binding influences.

The data obtained from the BFMI mice were equally insignificant. Only the subgroup CpG 1 - 5 showed a significant difference in the Mann-Whitney-Test between the normal diet group and the high fat diet group at week 32 (*p*-value = 0.035). This significant difference vanished after correction for binding influences. Altogether, no meaningful alterations of the DNA methylation patterns by postnatal diet were found in mouse PBC in these experiments.

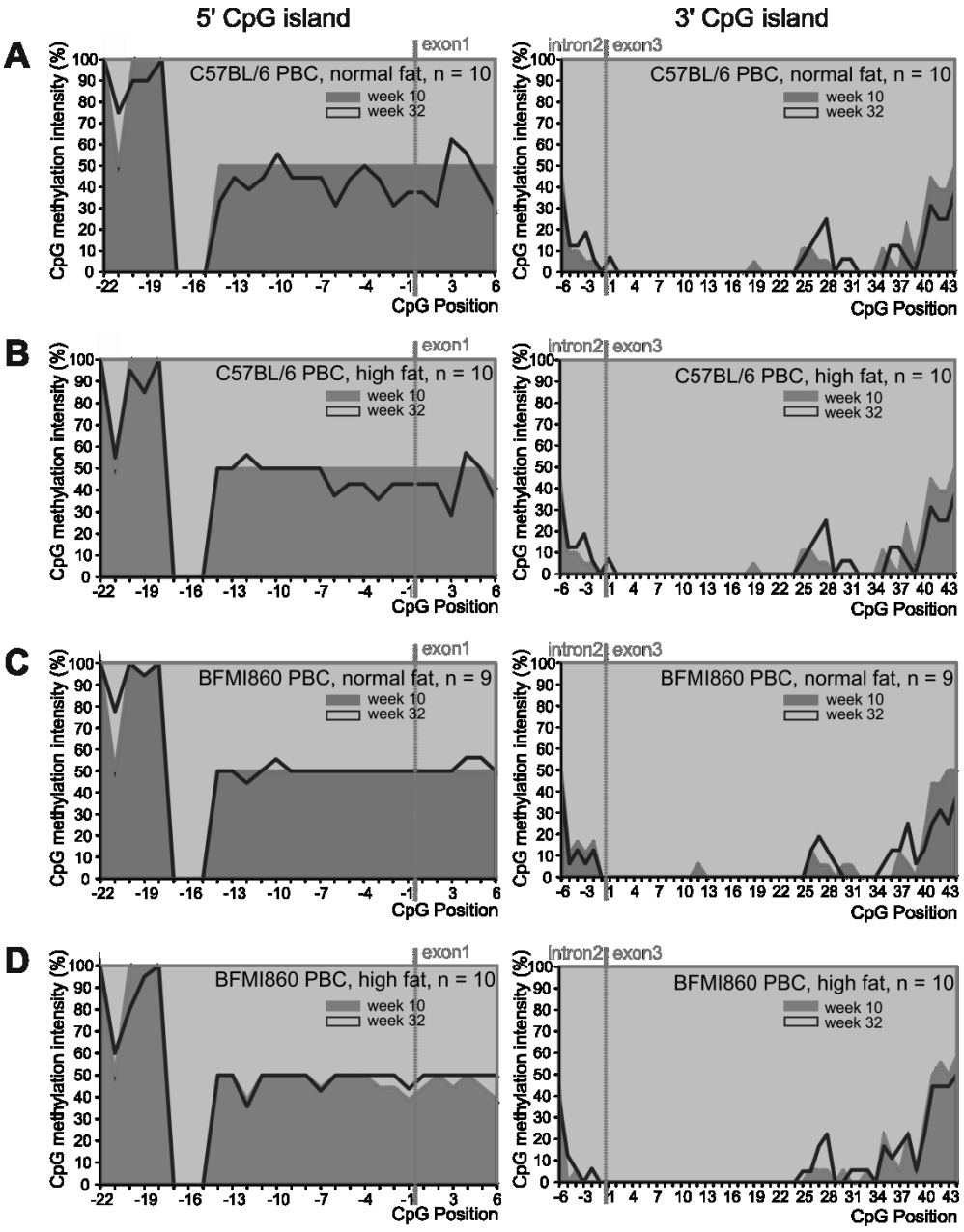

Figure 24: DNA methylation patterns of the mouse POMC locus before and after 29 weeks of high fat or control diet. Two mouse strains were tested: C57BL/6 = wild type and BMFI860 = predisposed for obesity. (A) PBC of C57BL/6 mice on a normal diet (n = 10). (B) PBC of C57BL/6 mice on a high fat diet (n = 10). (C) PBC of BFMI860 mice on a normal diet (n = 9). (D) PBC of BFMI860 mice on a high fat diet (n = 10). The plots are semi-quantitative and display CpG methylation intensity (in %) over the particular CpG position within this region. CpG positions are numbered according to their relative position to the next exon start. Vertical dashed lines mark the exon starts. 5' CpG island (CGI) = mPOMC-F1 + mPOMC-F2; 3' CGI = mPOMC-F3 + mPOMC-F4.

3.4 The phylogenetic development of POMC DNA methylation is associated with *Alu* element incidence within the intron2 region

The comparison of the murine and human POMC DNA methylation patterns is difficult, as long as the the human patterns are depicted as methylation intensity plots (Figure 23) and the mouse patterns as lollipop figures (Figure 18). To make them comparable, the mouse lollipop figures of PBC samples were translated into methylation intensity plots (Figure 25B). Then it gets obvious that the human and murine DNA methylation patterns of POMC are divergent. (Figure 25). The 5' CGIs DNA methylation patterns of both species are heterogeneous. In humans the upstream region of exon1 is heterogeneously methylated and the exon1 region is hypomethylated (Figure 25A). The mouse is also heterogeneously methylated upstream of exon1, but the heterogeneous methylation extends further into exon1 (Figure 25B). However, the 3' CGI showed a more striking divergence. While the hypomethylation of the exon3 region was consistent in both species, the intron2 part differs fundamentally. In human samples, a prominent block of hypermethylation in the intron2 area ends in a distinct drop to hypomethylation exactly at the exon3 boundary (Figure 25A). This effect was not observed in the murine pattern where the intron2 is heterogeneously methylated (Figure 25B).

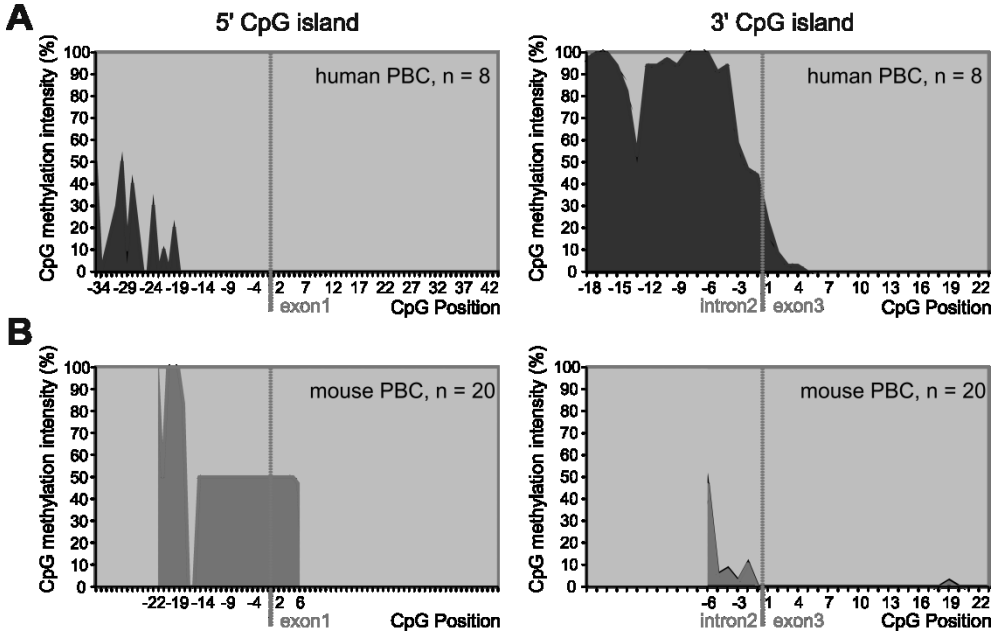

Figure 25: Comparison of POMC DNA methylation patterns in (A) human PBC of newborn (n = 8) and (B) murine PBC (n = 20). The data obtained from mouse blood samples (Figure 18; C57BL/6 strain, week 10, Paragraph 3.2) were converted into the same format as the data from newborn humans. The plots are semi-quantitative and descriptive and display CpG methylation intensity (in %) over the particular CpG position within this region. CpG positions are numbered according to their relative position to the next exon start. Vertical dashed lines mark the exon starts.

To find out about the background, or even cause, of this observed divergence in DNA methylation patterns of mice and humans, a comparative sequence analysis of the human and the murine POMC gene locus was performed. The exon regions showed high sequence homology, while the consensus in non-exon regions is lower. A large difference between the human and murine POMC sequences lies in the presence of six retrotransposable elements of the *Alu* family in the human POMC gene. No equipollents were found for the murine POMC gene (Tsukada et al., 1982) (Figure 17 and Figure 22). Three of those *Alu* elements (*Alu*s) are located in the intron2 region just upstream of the 3' CGI. Viewed from 5' to 3' the first *Alu* is of the most ancient 'J family' and is oriented in 5' → 3'. The middle one is of the most recent 'Y type', oriented backward in 3' → 5', and the third one is an *Alu* of the second oldest 'S family', which is also in the

backwards direction 3' → 5' oriented. They are labeled *Alu* D, *Alu* E and *Alu* F in the following, that also includes the analogy of the type – J, Y or S – and the orientation:

- → *Alu* D = most upstream one of the three; of the J family; 5' → 3' oriented.
- → *Alu* E = middle one of the three; of the Y family; 3' → 5' oriented.
- → *Alu* F = most downstream one of the three; of the S family; 3' → 5' oriented.

These three *Alu* elements lie just upstream of the 3' CGI, which showed the distinct hypermethylation in humans but not in mice (Figure 25). *Alu* elements can influence the methylation of their vicinity. Hence, it is an assumption that the hypermethylation of the intron2 region in the human POMC gene can be caused by the presence of those three *Alu* repeats. To test this hypothesis, genomes of other primates were analyzed: First, the presence and distribution of the primate-specific *Alu* elements were described. Secondly, the methylation status of the 3' CGI of the primate POMC locus was tested. Last, the *Alu* element incidence was correlated to the methylation patterns of the different primates.

3.4.1 Sequence analysis of various primate POMC loci for *Alu* element incidence

Alu elements are a primate-specific family of retrotransposable elements. To test the influence of *Alu*s within the intron2 region of the POMC gene on the methylation pattern of the subsequent 3' CGI, the sequences of various non-human primates were tested for *Alu* element incidence in this region. For some non-human primates like *Pan troglodytes* (chimpanzee, ENSPTRG00000011721), *Gorilla gorilla* (gorilla, ENSGGOG00000003480), *Pongo pygmaeus* (orangutan, ENSPPYG00000012592), *Macaca mulatta* (macaque, ENSMMUG00000016463), *Callithrix jacchus* (marmoset, ENSCJAG00000008148), and *Eulemur macaco* (lemur, ENSMICG00000001616) DNA sequence information was available online. Nevertheless, DNA of gorilla, orangutan, and lemur was resequenced to fill gaps in the available sequences and to elucidate possible convergences between the published sequences and the exact sequence of the available DNA samples. Furthermore, the complete intron2 regions of *Papio hamadryas* (baboon) and *Galago senegalensis* (galago) were sequenced. All newly obtained sequences were submitted to NCBI GeneBank to obtain accession numbers (Figure 26). Using the *RepeatMasker Web Server* tool, the sequences of the various primates were analyzed for *Alu* incidence (Figure 26).

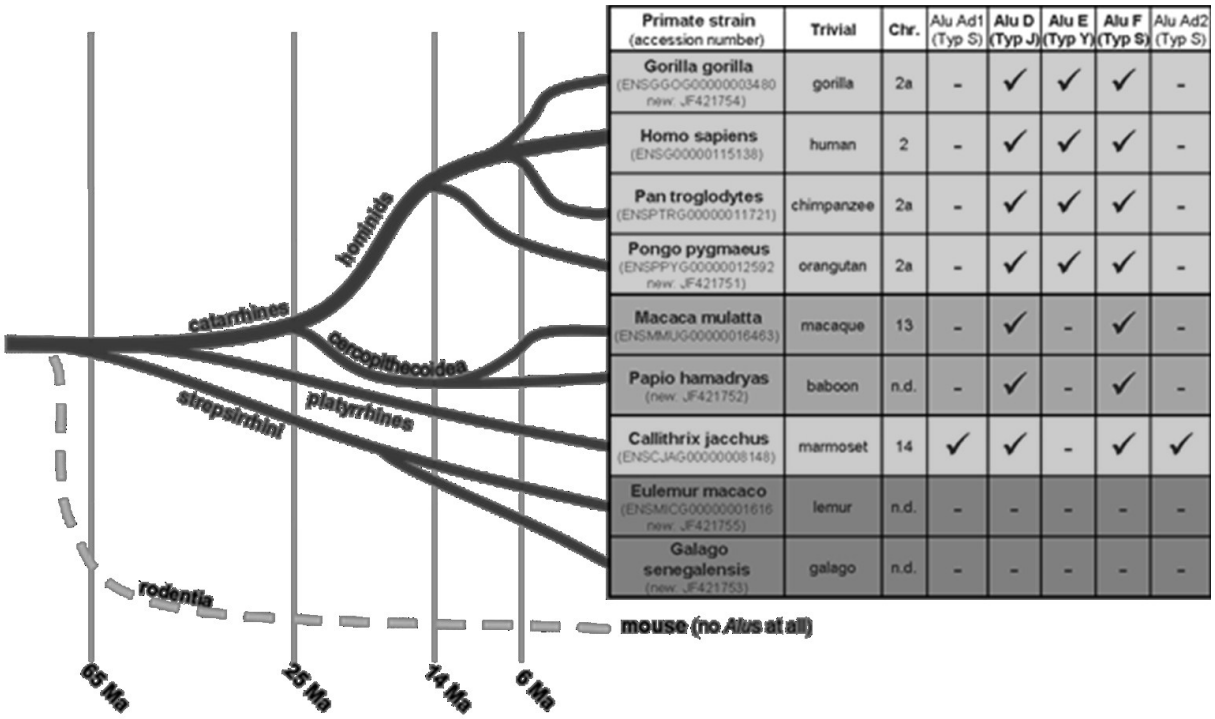

Primate strain (accession number)	Trivial	Chr.	Alu Ad1 (Typ S)	Alu D (Typ J)	Alu E (Typ Y)	Alu F (Typ S)	Alu Ad2 (Typ S)
Gorilla gorilla (ENSGGOG00000003480 new: JF421754)	gorilla	2a	-	✓	✓	✓	-
Homo sapiens (ENSG00000115138)	human	2	-	✓	✓	✓	-
Pan troglodytes (ENSPTRG00000011721)	chimpanzee	2a	-	✓	✓	✓	-
Pongo pygmaeus (ENSPPYG00000012592 new: JF421751)	orangutan	2a	-	✓	✓	✓	-
Macaca mulatta (ENSMMUG00000016463)	macaque	13	-	✓	-	✓	-
Papio hamadryas (new: JF421752)	baboon	n.d.	-	✓	-	✓	-
Callithrix jacchus (ENSCJAG00000008148)	marmoset	14	✓	✓	-	✓	✓
Eulemur macaco (ENSMICG00000001616 new: JF421755)	lemur	n.d.	-	-	-	-	-
Galago senegalensis (new: JF421753)	galago	n.d.	-	-	-	-	-

Figure 26: Overview of the branching of various primates and their *Alu* incidence within the POMC intron2 region. Primate strains with trivial names are designated to primate families. Accession numbers of the POMC loci, *Alu* element incidence within the intron2 region and chromosomal location are listed. *Alu* elements are noted in the order in which they appear within the intron2 region. The time scale is based on (Goodman, 1999; Janecka et al., 2007; Siepel, 2009). n.d. = no data available; - = *Alu* not present; ✓ = *Alu* of this type is present in the DNA sequence; *Alu* Ad1 = additional *Alu*1; *Alu* Ad2 = additional *Alu*2; *Alu*D/E/F = the three *Alu* elements which are present in the intron2 of the human POMC.

3.4.1.1 Hominids sequences

Humans are most closely related to chimpanzees, gorillas, and orangutans. They are all members of the hominids group. Therefore, the sequences of the POMC gene of three hominids, the chimpanzee, the gorilla, and the orangutan, were analyzed for *Alu* incidence.

Pan troglodytes = chimpanzee

The POMC gene of *Pan troglodytes* (ENSPTRG00000011721) is located on chromosome 2a. Sequence analysis revealed that chimpanzees have three *Alu* elements integrated in the intron2 region of the POMC gene that are highly equivalent to the human *Alu* elements D, E and F in this region. Just like in humans, the upstream *Alu* element of the intron2 region is of the most ancient *Alu*J family. This *Alu* element is oriented in the 5' → 3' direction. The next *Alu* element is a member of the most recent discovered *Alu*Y family, while the *Alu* element located downstream in this region belongs to the second oldest *Alu*S family. The latter two *Alu*s are both orientated 'backwards' in the 3' → 5' direction.

Gorilla gorilla = gorilla

The gorilla POMC gene is also located on chromosome 2a. The gaps of ENSGGOG00000003480 were filled by sequencing (JF421754). Analysis for the existence of retrotransposable elements by RepeatMasker showed the same results as obtained for the chimpanzee sequence. All three *Alu*s D, E, and F are present in the intron2 region of the gorilla POMC gene.

Pongo pygmaeus = orangutan

Just as the other two hominids examined, the POMC sequence of the orangutan (ENSPPYG00000012592 and JF421751) contains all three *Alu* elements D, E, and F in its intron2 region, corresponding in type and orientation to the human ones.

To summarize: all three apes of the hominid family analyzed here showed the same number, kind, orientation, and distribution of *Alu* elements within the intron2 region of their POMC genes. The *Alu* elements correspond with the *Alu*s D, E, and F from the human sequence (ENSG00000115138) in type, order, and orientation. The three *Alu* repeats found are of the three different types: the upstream one is of the J family and orientated in sense direction, the middle one is of the Y family and is orientated antisense, just as the *Alu* element downstream, which is of the S family.

3.4.1.2 Cercopithecoidea sequences

Cercopithecoidea and hominids both belong to the catarrhines, which are often referred to as *old world monkeys* in common parlance (Figure 26). Therefore, cercopithecoidea are closely related to hominids and branched approximately 25 million years ago. The genomes of the baboon and the macaque, two members of the cercopithecoidea, were tested for the presence of *Alu* elements in their POMC regions.

Papio hamadryas = baboon

The baboon POMC gene (JF421752) only possesses two *Alus* in its intron2, which are equivalent to the adverse oriented *Alu* D and *Alu* F.

Macaca mulatta = macaque

Analysis of the macaque *POMC* (ENSMMUG00000016463) located on chromosome 13 revealed the presence of only two *Alu*s in the intron2 of the POMC gene. The upstream *Alu* D-equivalent is orientated in the 5' → 3' direction and the downstream *Alu* F-equivalent is orientated the other way around.

The two cercopithecoidea members macaque and baboon have one *Alu* repeat less than the tested hominids. The middle *Alu* E-equivalent, a member of the most modern Y family, is missing.

3.4.1.3 Platyrrhines sequences

Platyrrhines, colloquial named *new world monkeys*, branched off the main strain 40 million years ago (Figure 26). *Callithrix jacchus* is a platyrrhine and its POMC sequence was tested for *Alu* incidence.

Callithrix jacchus = marmoset

The marmoset POMC intron2 sequence (ENSCJAG00000008148) contains four *Alu* elements. The anterior one is not present in the human or any other sequence analyzed. It is of the second oldest *Alu*S family and orientated in antisense direction. I will refer to it as '*Alu* Ad1' (additional1). The second and the third *Alu* elements correspond to the two *Alu* elements identified in catarrhines, *Alu* D- and *Alu* F-equivalents. They occur in opposing directions. The fourth *Alu* element is again a member of the S family, and is orientated in the antisense direction. I will refer to it as '*Alu* Ad2' (additional2). Similar to the cercopithecoidea, the *Alu* element of the most recent Y family is also missing in the platyrrhines.

3.4.1.4 Strepsirrhinis sequences

Strepsirrhinis are the farthermost relatives to humans within the primates. They branched off the hominid strain approximately 65 million years ago (Figure 26). The POMC genes of the two strepsirrhinis members, the *Galago senegalensis* and the *Eulemur macaco*, were sequenced for presence of *Alu* elements.

Galago senegalensis = galago

The POMC intron2 sequence of galagos (JF421753) is *Alu*-free.

Eulemur macaco = lemur

Analysis of the lemur POMC intron2 (JF421755) with RepeatMasker showed that there are no *Alu* elements in the region of interest at all.

The farthermost relatives of humans within the group of non-human primates, the strepsirrhinis, diversed off the main strain almost 65 Ma ago at the time that the *Alu* elements began to proliferate in the genomes of primates (Batzer and Deininger, 2002). The strepsirrhinis have no *Alu* elements in the gene region of interest.

Figure 26 illustrates the *Alu* incidence in the intron2 region of *POMC* of various primates in the context of their relation to each other. However, besides *Alu* elements there are also other relevant structural elements within this gene region, such as binding sites of transcription factors (TF) or regulatory proteins. All primate gene sequences were analyzed for a selection of this sequence features. The results of this analysis are posed in the next paragraph.

3.4.2 *In silico* analysis of POMC sequences of various primates for identification of putative binding sites

The POMC locus of primates exhibits various potential binding sites for transcription factors or regulatory proteins. We chose three of them for further analysis in all primate intron2 sequences, based on their estimated relevance regarding DNA methylation or energy homeostasis regulation. These were: (i) the p300 binding site, (ii) the STATx binding site and (iii) the Sp1 binding site. The intron2-exon3 junction in human *POMC* exhibits a histone acetylase p300 complex binding site. STATx is involved in the POMC activation through leptin signaling. The Sp1 transcription factor is involved in gene expression in the early development of an organism and is said to influence DNA methylation establishment (Graff et al., 1997; Turker, 1999). Binding dynamics of these factors could possibly be influenced by DNA methylation status of respective binding regions. Thus, a putative existence of those three binding site in the intron2 region of the different primate sequences were *in silico* analyzed using the *TFSEARCH* transcription factor search web tool (Table 11).

We found that all primates, except the galago, have a predicted p300 complex binding site. The p300 binding sites have all the exact same sequence and location at the intron2-exon3 junction. For the putative Sp1 and STATx binding sites the results were more diverse. Only lemurs, galagos, and mice exhibit predicted Sp1 binding sites in this region. All recognized target sequences differ and lie in different locations. In lemurs and galagos, Sp1 binding sites lie upstream of the exon3 start, while in mice the Sp1 binding site is located within the exon3. Predicted STATx binding sites in humans and macaques have similar but not equivalent sequences and a similar location within the exon3. In lemurs and mice, putative STATx binding sites differ highly and lie upstream of the exon3 start.

Table 11: Putative binding sites for Sp1, STATx, and histone acetylase p300 complex in the POMC intron2 sequences of various primates and mice. Sp1 binding sites have different locations within the sequences in which they occur. In lemurs [-78 bp (1.) and -507 bp (2.)] and galagos [-241 bp (1.) and -1.871 bp (2.)] they are located upstream of exon3 start. In mice, the Sp1 binding site is +193 bp downstream of the exon3 start. STATx binding sites are downstream of the exon3 start in humans (+57 bp) and macaques (+58 bp) and upstream in lemurs [-1.556 bp (1.) and -1.822 bp (2.)] and mice [-1.129 bp (1.) and -1.445 bp (2.)]. The p300 binding sites, if existent, have always the same location exactly at the intron2-exon3 junction.

Primate strain (accession number)	Trivial	Family	Chr.	Sp1 binding site	STATx binding site	p300 binding site
Homo sapiens (ENSG00000115138)	human	hominids	2	---	TTCCCGGGA	CCCAGGAGTGCATC
Pan troglodytes (ENSPTRG00000011721)	chimpanzee	hominids	2a	---	---	CCCAGGAGTGCATC
Gorilla gorilla (ENSGGOG00000003480 new: JF421754)	gorilla	hominids	2a	---	---	CCCAGGAGTGCATC
Pongo pygmaeus (ENSPPYG00000012592 new: JF421751)	orangutan	hominids	2a	---	---	CCCAGGAGTGCATC
Macaca mulatta (ENSMMUG00000016463)	macaque	cercopithecoidea	13	---	TTCCGGGCA	CCCAGGAGTGCATC
Papio hamadryas (new: JF421752)	baboon	cercopithecoidea	n.d.	---	---	CCCAGGAGTGCATC
Callithrix jacchus (ENSCJAG00000008148)	marmoset	platyrrhines	14	---	---	CCCAGGAGTGCATC
Eulemur macaco (ENSMICG00000001616 new: JF421755)	lemur	strepsirrhinis	n.d.	1. TCCCCGCCGC 2. GAGGCGGGTT	1. TTAGGGGAA 2. TTCAGGGAA	CCCAGGAGTGCATC
Galago senegalensis (new: JF421753)	galago	strepsirrhinis	n.d.	1. GGGTGGGGT 2. TGGGGCTGGGA	---	---
Mus mulucus (ENSMUSG00000020660)	mouse	-	12	GAGGCGGTGT	1. TTCCCCCAA 2. TTCAGGGAAA	---

3.4.3 POMC DNA methylation of the 3' CpG island of various primates

The primates of which the sequences were previously determined and tested for *Alu* element incidence (Paragraph 3.4.1) were also analyzed for their methylation status in the 3' CGI region. Therefore, the sequences of the POMC loci of the primates were first *in silico* converted into bisulfite treated sequences. Based on those sequences, appropriate primers were designed for bisulfite genomic sequencing to amplify fragments that span the intron2-exon3 junction and are similar to the hPOMC-F3 fragment. The location of the primers varies in the different primates due to the sequence reasons. As a result, the amplified fragments vary in length. Moreover, the fragments of interest of different primates show varying numbers and locations of CpG moieties (Figure 27). Figure 27 depicts the different fragments in proportion; hence, comparison of the CpG moiety location relative to the exon3 start is possible. The CpG number and location in the hominid fragments (human, chimpanzee, and gorilla) are similar. In addition, the fragments of the two cercopithecoidea, baboon and macaque, reveal a comparable CpG incidence within this region. The marmoset has another pattern than the hominids and the cercopithecoidea, especially in the intron2 region. The galago sequence shows depletion of CpGs within the intron2 region; 12 CpG moieties instead of 18 CpG moieties in an equivalent stretch of DNA in humans. The other strepsirrhini, the lemur, had more CpG moieties in the intron2 region, than the human, 21 CpG moieties instead of 18 CpG moieties. The exon3 regions of both strepsirrhini look more similar to the human region, with 10 CpGs in the stretch of galago sequence and 11 CpGs in the lemur, where the human possessed 11 CpG moieties. The sequences of the other primates showed high similarity in the exon3 regions, too.

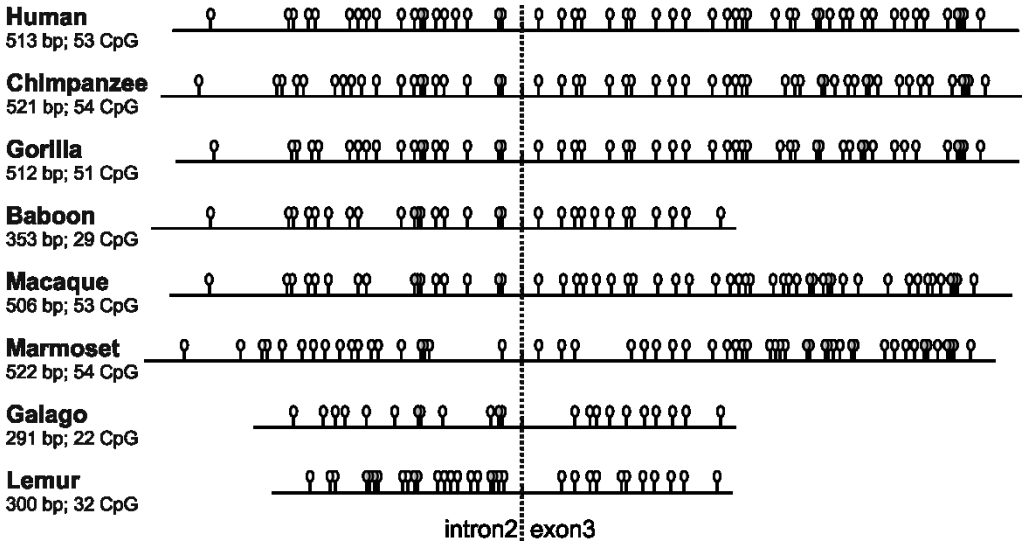

Figure 27: Lollipop figures of the 3' CGI fragments of the POMC locus in different primates. Each lollipop indicates the position of one CpG group within the fragment. Illustration of the CpG positions and fragment lengths are in proportion. The dashed line indicates the intron2-exon3 junction. human = 513bp, 53 CpGs; chimpanzee = 521bp, 54 CpGs; gorilla = 512bp, 51 CpGs; baboon = 353bp, 29 CpGs; macaque = 506bp, 53 CpGs; marmoset = 522bp, 54 CpGs; galago = 291bp, 22 CpGs; lemur = 300bp, 32 CpGs.

The DNA of the primates was analyzed using the genomic bisulfite sequencing strategy by application of primate-specific primers for amplification. The resulting fragments were purified from the agarose gel and TOPO cloned. Single colonies were picked for colony PCR, subsequent Exo/SAP and sequencing reaction. Not all CpG positions within the fragments were accessible because of the primer positions and sequencing reasons. The results were converted in semi-quantitative descriptive methylation intensity plots, comparable to the human and mouse data (Figure 25). The CpG moieties, which were not detectable or readable due to methodological reasons especially in the posterior parts of the fragments, were excluded from the displayed methylation intensity plots (Figure 28, Figure 29, and Figure 30) to prevent from misinterpretation.

3.4.3.1 Hominids DNA methylation

Homo sapiens = human

The hPOMC-F3 fragment, which coincides with the 3' CGI, is 511 bp long with 19 CpG dinucleotides in the intron2 region and 34 CpGs in the exon3 region. The DNA methylation pattern is striking as described above with hypermethylation in the intron2 region and hypomethylation in the exon3 region. The transition from hypermethylation to hypomethylation is sudden at the exon3 boundary and at CpG position -13 a heterogeneous methylation dip is recognizable (Figure 28A). *In silico* analysis revealed, CpG -13 lies within a putative binding area for upstream transcription factors (USF) and transcription factors of the myelocytomatosis viral related oncogene family (N-Myc).

Pan troglodytes = chimpanzee

The amplified chimpanzee DNA fragment (521 bp) contains 19 CpG dinucleotides in the intron2 region and 35 CpG dinucleotides in the exon3 region. The DNA of five different chimpanzees was converted, amplified, and sequenced. The resulting methylation intensity plot (Figure 28B) looked similar to the human pattern with hypermethylation in the intron2 region, hypomethylation in the exon3 region and a clear drop zone in between at the boundary of exon3. Likewise, the dip to heterogeneous methylation at CpG position -13 was noticeable. The sequence around the CpG -13 also codes for equivalent transcription factor binding sites as detected for humans.

Gorilla gorilla = gorilla

The 50 CpG moieties (18 in intron2 plus 32 in exon3) of the gorilla fragment are spread over a fragment size of 512 bp. The DNA methylation pattern from five gorillas was determined and was similar to the human and chimpanzee patterns. It showed a hypermethylated intron2 and a strictly non-methylated exon3 which starts exactly at the junction of exon3. The distinct methylation reduction at CpG -13 was not as pronounced as seen in humans and chimpanzees but also detectable (Figure 28C).

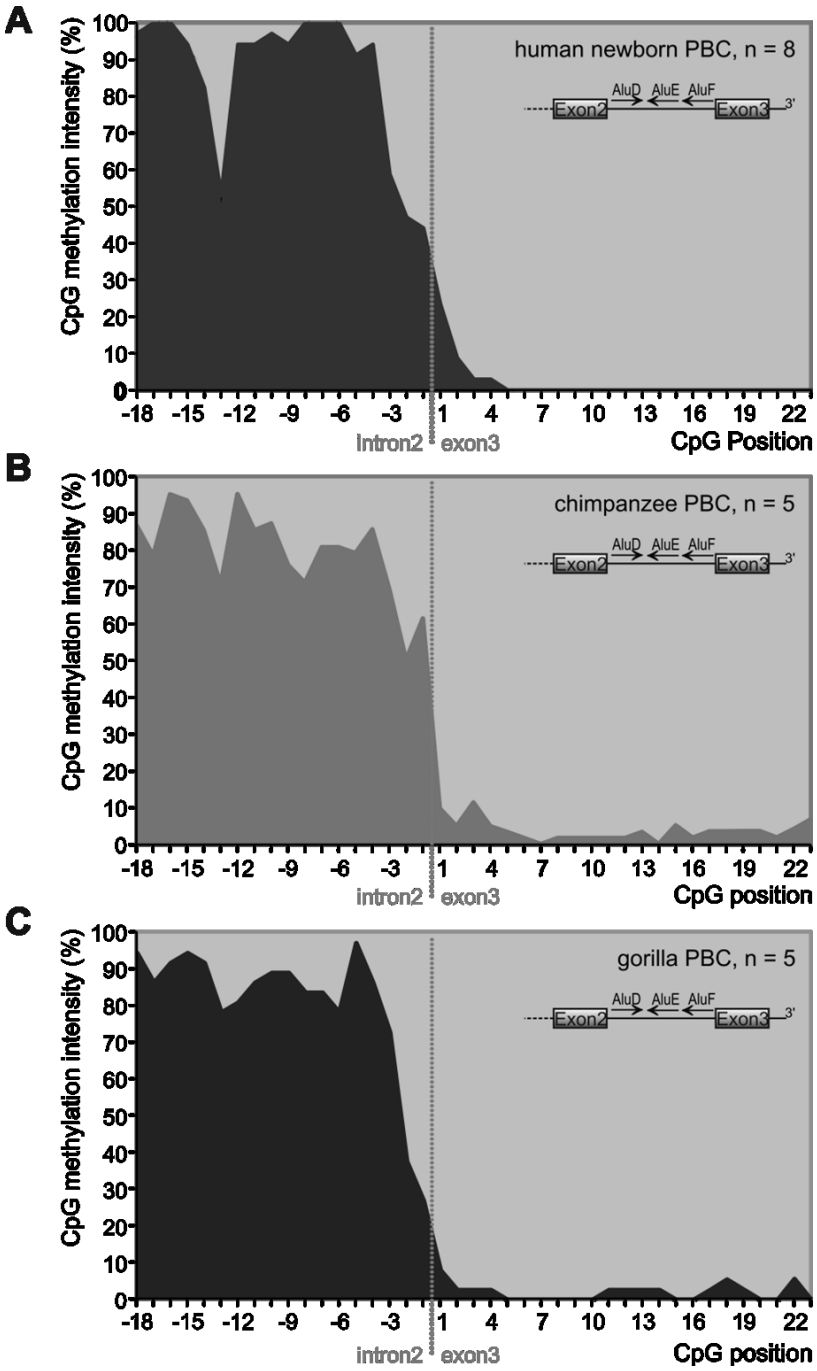

Figure 28: DNA methylation pattern of the 3' CGI of POMC of the hominids humans, chimpanzees, and gorillas. The plots are semi-quantitative and display CpG methylation intensity (in %) over the particular CpG position within this region. CpG positions are numbered according to their relative position to the exon3 start. Vertical dashed lines mark the intron2-exon3 junction. POMC gene schemes indicate number, orientation, and distribution of *Alu* elements in the intron2 region of respective primate. (A = human newborns; B = chimpanzees, C = gorillas).

All members of the hominid family have a similar POMC DNA methylation pattern of the 3' CGI with a clear difference between hypermethylation in the intron, hypomethylation in the exon and an obvious methylation drop zone at exon3 start. The methylation dip at CpG -13 was observed in all three primates. In combination with the sequencing results described above, it can be said that all examined hominids possess equivalent three *Alu* elements upstream of exon3 and showed a block of hypermethylation in the intron2 region.

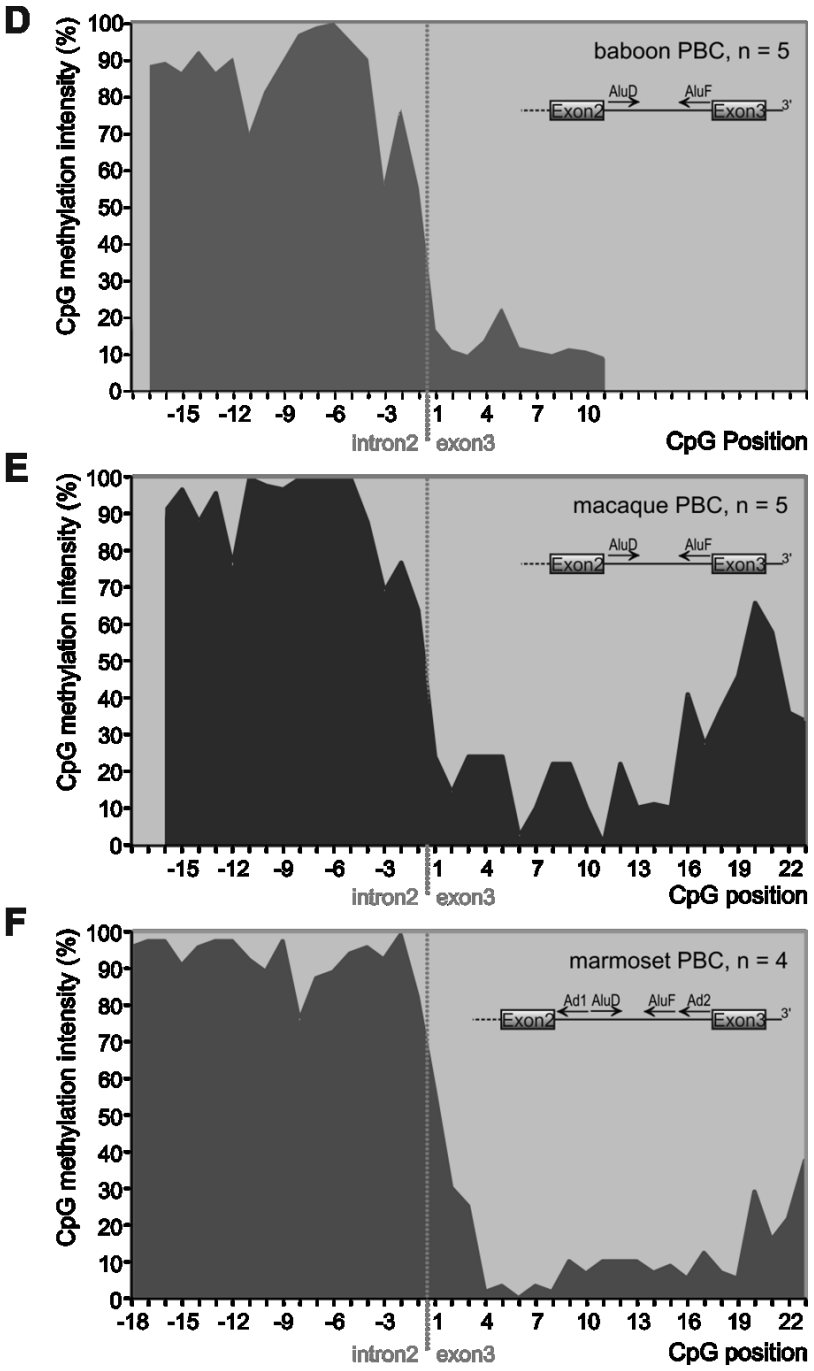

Figure 29: DNA methylation pattern of the 3' CGI of POMC of the caterrhines baboon and macaque and the platerrhine marmoset. The plots are semi-quantitative and display CpG methylation intensity (in %) over the particular CpG position within this region. CpG positions are numbered according to their relative position to the exon3 start. Vertical dashed lines mark the intron2-exon3 junction. POMC gene schemes indicate number, orientation, and distribution of *Alu* elements in the intron2 region of respective primate. (D = baboons; E = macaques; F = marmoset).

3.4.3.2 Cercopithecoidea DNA methylation

The two members of the cercopithecoidea, the baboon and the macaque, both possess only two *Alu* elements within the intron2 region upstream of the 3' CGI. The middle *Alu* E element of the Y-family, which is present in hominids, is missing in both.

Papio hamadryas = baboon

The 3' CGI fragment of the baboon counts 353 bp and 17 CpG positions in the intron region plus 11 CpG positions in the exon region. Five members of the family were analyzed. The summary of all colony sequences is displayed in Figure 29D.In the anterior part of the amplified fragment, the hypermethylation was similar to the plots of the hominids. Towards the boundary of exon3, the methylation intensity decreased stepwise. At CpG residue -3 and -11, heterogeneous methylation dips were detectable. In addition, in the predominantly hypomethylated exon region a small noise peak of 20% methylation at CpG position +5 was observed. *In silico* analysis of the three areas of conspicuous methylation change showed no association to specific putative binding sites.

Macaca mulatta = macaque

The pattern of the macaque 3' CGI fragment, which was observed in the five samples (Figure 29E), was similar to that of the baboons. The 16 CpG moieties lying in the intron2 region of the fragment showed hypermethylation like the hominids and the baboons, with two dips of distinct heterogeneous methylation at CpG position -12 and -3. The methylation decrease to hypomethylation in the exon region was stepwise. Furthermore, the methylation of the exon part (37 CpGs) was low but noisier than in baboons and hominids and showed an irregular slow increase towards the posterior part of the 506 bp long fragment. At positions +20 and +27 distinct peaks of methylation were detectable. As seen for the baboon, the macaque's areas of methylation dips and peaks did also not lie within specific predicted binding sites.

Both cercopithecoidea members only possess the *Alu* D and *Alu* F elements. Nevertheless, they showed similar methylation patterns to the hominids. However, their patterns appeared less strict concerning the extreme conditions of methylation and the transition from hypermethylation to hypomethylation. Moreover, both families had a hypermethylation dip at CpG -3.

3.4.3.3 Platyrrhines DNA methylation

Callithrix jacchus = marmoset

Fragments of 522 bp length were amplified from the marmoset samples. The mean of the results of all four monkeys are shown in Figure 29F. A distinct block of hypermethylation in the intron2 region with a dip at CpG -8 was noticeable. The exon3 region predominantly showed hypomethylation with prominent peaks at CpG +20 and +23. However, the transitional drop zone was shifted downstream, into the exon3 region, in comparison to all previously described patterns. While for the methylation peak-areas not putative binding sites can be detected, the dip at CpG -8 is associated with a predicted binding site area for USF, N-Myc, c-Myc and the aryl hydrocarbon receptor (AHR) nuclear translocator (ARNT). Interestingly, the position of CpG -8 in the marmoset sequence coincided with the human CpG -13, when the fragments were aligned (Figure 27).

The platyrrhine family member *Callithrix jacchus* combines the characteristics of the hominid and cercopithecoidea DNA methylation patterns, but shows a slightly later drop zone and small peaks of

methylation within the exon3 region. If this methylation pattern could be influenced by the two additional *Alu*s of the S-family present in the marmoset POMC locus, will be debated in the discussion paragraph.

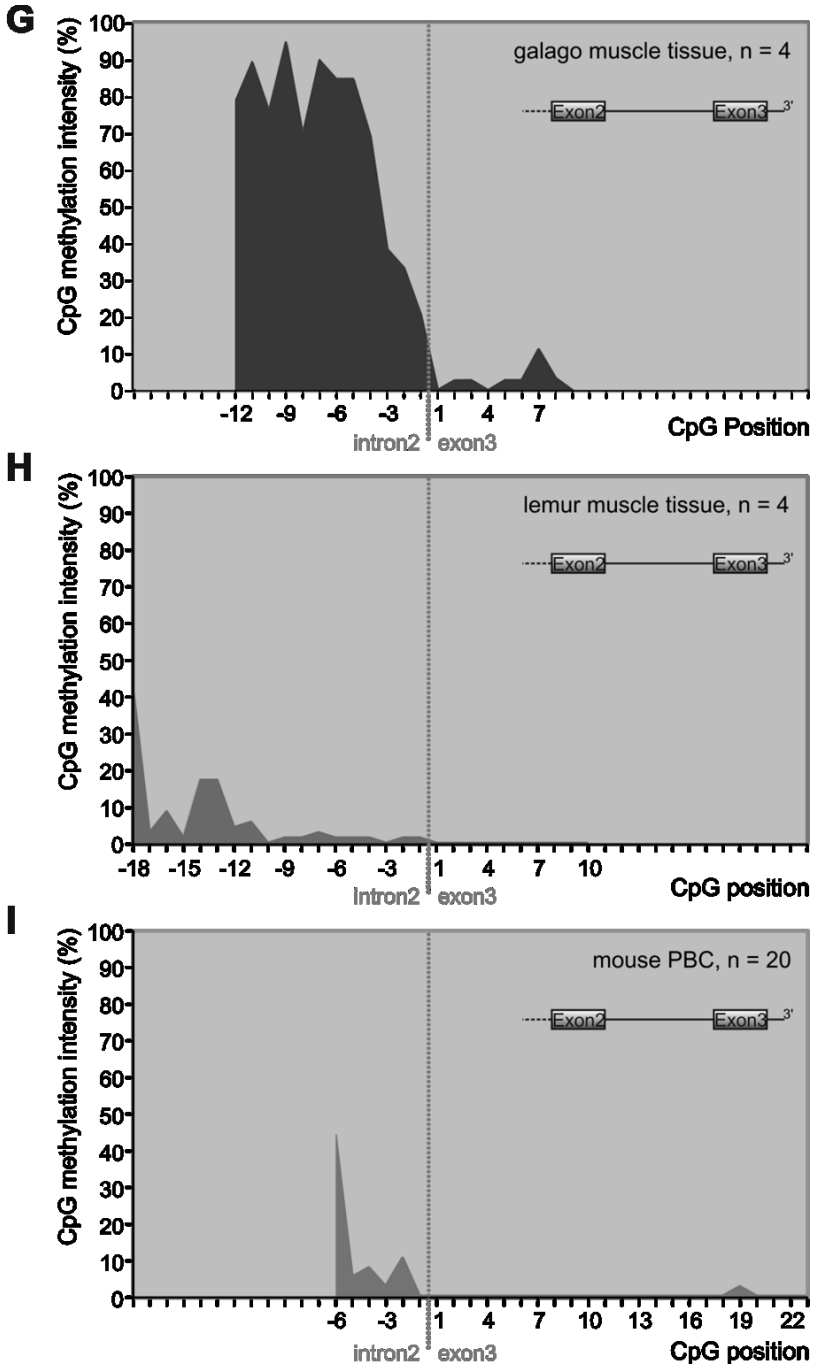

Figure 30: DNA methylation pattern of the 3' CGI of POMC of strepsirrhinis and the mouse. The plots are semi-quantitative and display CpG methylation intensity (in %) over the particular CpG position within this region.CpG positions are numbered according to their relative position to the exon3 start. Vertical dashed lines mark the intron2-exon3 junction. The plots are semi-quantitative and descriptive. POMC gene schemes indicate number, orientation, and distribution of *Alu* elements in the intron2 region of respective organism. (G = galago; H = lemur; I = mouse).

3.4.3.4 Strepsirrhinis DNA methylation

Galago senegalensis = galago

Due to the sequence characteristics of the galago POMC locus, the amplified fragment of the galago DNA is relatively short (291 bp) and contains only 21 CpG positions (12 in the intron plus 9 in the exon region).

Four DNA samples were processed and analyzed. The results are shown in Figure 30G. Hypermethylation was detectable in the intron region with heterogeneous methylation dips at CpG positions -8 and -10, of which the dip at CpG -10 coincides with a putative GATA-1 binding site. The exon region was hypomethylated. However, the descent from hypermethylation to hypomethylation started more upstream, already at CpG position -5, and was softer than and not as abrupt as in the previous samples.

Eulemur macaco = lemur

In the relative of the galago, the lemur, the methylation state was completely different (Figure 30H). Even though the amplified fragment is only 300 bp long, there are more CpG groups in the region, respectively 21 in the intron2 and 10 in the exon3. The determined pattern of the four lemurs is unusual. In contrast to the patterns described above, the lemur POMC gene was not hypermethylated in the intron2 region, but rather heterogeneous hypomethylated with some irregularities in the anterior region, peaking in CpG -18 at a methylation intensity of 45%. The whole remaining fragment, intron region as well as exon region, was throughout hypomethylated. The sequence around the major peak at CpG -18 was inconspicuous concerning predicted TF binding sites. Interestingly, the noise peak at CpG -14 draw our attention on a putative binding site for factors with myeloid zinc finger domains (MZF1) and the human transcription factor specific protein 1 (Sp1).

The galago and the lemur showed divergent methylation patterns for the intron2 region of the POMC locus, although sequence analysis revealed no *Alu* elements within this region for both. There is no occurrence of retrotransposable elements in this gene region of interest in the two primates, exactly as in the murine POMC locus. The lemur pattern was highly similar to the murine pattern (Figure 30I) and showed hypomethylation in the intron and exon region. However, the pattern of the galago, was rather similar to the patterns of all other primates analyzed, including the human pattern.

Interestingly, all primates analyzed had a hypomethylated exon3 region, even though some patterns showed regions of heterogeneous methylation peaks. This was independent of primate family and *Alu* incidence within the intron2 region. Moreover, the hypomethylation of exon3 was also detected for the POMC locus in mice.

4 Discussion

The BMI is estimated to be heritable for 50 to 84% (Allison et al., 1996; Barsh et al., 2000; Stunkard et al., 1986). However, the overall impact of identified mutations and genetic variations that are associated to the weight phenotype variation is minor. Only about 10% of the severe obesity cases with early onset can be explained by diagnosed genetic causes, which mostly constitute insufficiencies within the leptin-melanocortin pathway (Speliotes et al., 2010). Consequently, it is compulsive to elucidate the pathogenesis of obesity further. This may ultimately lead to identification of early markers for obesity enabeling customized prevention, intervention, and treatment strategies. Inherently, this may also lead to the reduction of the related health care costs and to increased quality of life for the individual.

Epigenetic modifications, like DNA methylation, are metastable and capable of changing gene expression without changing the DNA sequence itself. Therefore, it is conceivable that, in the context of body weight regulation, epigenetic changes of involved genes might lead to disruption of the minute control of food intake and the energy expenditure equilibrium. Moreover, stable epigenetic modifications of specific genes may suite as early recognition markers for diseases, such as obesity.

The pre-proopiomelanocortin (POMC) gene is a central pivot in the catabolic leptin-melanocortin-axis of the body weight regulating system. Previous studies detected a CpG-methylation polymorphism (CMP) - a stable change in the DNA methylation pattern - in the 3' CpG island (CGI) in humans that is significantly associated with obesity (Kuehnen et al., in revision). For a better estimation of the role of POMC DNA methylation in the development of obesity, or as early marker for the disease, it is important to gain insight in the function and origin of the DNA methylation of the POMC locus.

Therefore, it was the aim of this thesis to examine the ontogenetic development of the POMC methylation patterns and possible influencing factors, as well as the phylogenetic origin of the POMC DNA methylation. In *in vitro* reporter gene assays, I analyzed the promoter function of both CGI regions of the human POMC gene, and tested the influence of DNA methylation on the promoter activity, to estimate a potential functional relevance of the obesity-associated CMP in the 3' CGI.

4.1 DNA methylation influence on the promoter activity of the POMC CGIs

Ten years ago, Newell-Price *et al.* revealed that the promoter region and transcription start site (TSS) of the regular long POMC transcripts of the human POMC gene is located within the 5' CGI, which surrounds the exon1 start site. This 5' CGI promoter shows differentially methylation in concordance with the POMC expression status of the respective tissue examined. Predominant methylation of the 5' CGI promoter was detected in somatic and tumor cells with repressed POMC gene expression. In contrast, the 5' CGI promoter was specifically unmethylated in expressing cells and cell lines (Newell-Price, 2003; Newell-Price et al., 2001). However, CGIs that are not located in 5' regions of annotated genes, but lie within their gene body, can also exert characteristics of functional promoters and are referred to as alternative promoters (Illingworth et al., 2010). For the POMC gene, it is conceivable that such an intragenic alternative promoter region is associated with the 3' CGI that surrounds the exon3 start.

Hence, I tested the promoter activity of both CGIs of the human *POMC* in this thesis work. As proof-of-concept for the assay with the CpG-free vector backbone and the hypothalamic mouse cell line (GT1-7), I used the defined 5' CGI fragment (PromI) of the human *POMC* (-493 bp to +98 bp relative to exon1, 48 CpG residues), which was also used by Newell-Price *et al.* (2001), to analyze the promoter activity of this region *in vitro*. In contrast to our approach, the construct of Newell-Price *et al.* was based on a CpG-containing vector backbone (Newell-Price et al., 2001). As expected, the CpG-free backbone construct of the 5' CGI also exhibited transcriptional activity in the performed promoter gene assays, and its activity

was abolished by complete methylation of the fragment, as shown before (Newell-Price et al., 2001). These data outline the functional role of the 5' CGI fragment as promoter of POMC and confirm the impact of hypermethylation on promoter activity for the POMC gene, which was also detected *in vivo*.

In addition, a novel fragment from the intragenic 3' CGI region of the human POMC gene was analyzed (Island2; -256 bp to +294 bp relative to exon3 start, 53 CpG residues). This fragment significantly activated transcription of the downstream-located luciferase gene in an unmethylated state, too. This result suggests a separate activity of an intragenic alternative promoter within the 3' CGI, which was never described before for *POMC*, but for other genes (Illingworth et al., 2010; Kleinjan et al., 2004; Macleod et al., 1998).

After SssI-induced complete methylation of the alternative promoter (Island2) construct, the luciferase expression vanished completely. That is analogous to the effect shown for the 5' CGI promoter of *POMC* and in concordance with the findings that gene body methylation can interfere with gene transcription and is involved in the regulation of alternative promoters (Ball et al., 2009; Flanagan and Wild, 2007). For alternative promoters it was shown that their activity depends in a larger extend on their methylation state than the activity of 5' promoter regions (Illingworth et al., 2010; Maunakea et al., 2010). This methylation state-dependent activity of alternative promoters may regulate the expression of associated transcripts in a cell context-specific manner (Maunakea et al., 2010). In the case of *POMC*, short POMC-related transcripts were detected in peripheral tissues such as testis (Gardiner-Garden and Frommer, 1994), encoding for truncated peptides including the functional relevant MSH peptides, but lacking the signal peptide that seems to be essential for processing and secretion (Clark et al., 1990). However, to date no peptides derived from the alternative short POMC transcripts were observed *in vivo*. Nevertheless, it is tempting to speculate that the alternative POMC transcripts originate from the alternative promoter in the 3' CGI and that their transcription is controlled by DNA methylation. However, due to methodical reasons the expression of short POMC transcripts cannot be quantified directly. Therefore, a correlation of the 3' CGI methylation state with the transcription of the short transcripts is not possible. Moreover, the identified 3' CGI-associated alternative promoter of *POMC* might also influence the expression of genes, which lie in the downstream vicinity of the POMC locus. These include several non-characterized loci and pseudogenes, but also the adenylate cyclase 3 (ADCY3) gene. The ADCY3 is part of the cAMP-dependent pathway and shall be involved in a number of physiological and pathophysiological metabolic processes (Haber et al., 1994). If the 3' alternative POMC promoter influences the expression of the 150,000 bp downstream located ADCY3 gene, and if this expression is associated to the methylation state of the 3' POMC promoter should be subject of future research. Nevertheless, this work reveals that the DNA methylation statuses of both CGI regions of the human POMC influence the gene activity in general. Hence, further analyses of the regular 5' promoter and the novel alternative 3' promoter were performed to find out about methylation sites and structural motifs that are important for POMC gene regulation.

The application of methyltransferases HhaI and HpaII stimulated methylation of isolated specific CpG moieties. Thereby, it was possible to elucidate the importance of specific DNA methylation for gene regulation in contrast to random methylation changes. For instance, no significant reduction of the promoter activity of both CGI fragments was observed after partial methylation with HhaI. In contrast, partial methylation of both CGI fragment catalyzed by HpaII resulted in significant reduction of luciferase expression. For both fragments, always one of the HpaII target sites was situated within a putative STATx binding site. Members of the STAT family (STAT1, STAT3, and STAT5) are known to be involved in leptin induced hypothalamic POMC expression (Munzberg et al., 2003). However, those STATx binding sites were only predicted based on sequence homology and not empirical tested. Nevertheless, this may suggests a possible influence of the predicted STATx binding site methylation on the reduced transcriptional activity of both fragments. To investigate the hypothetical relevance of unmethylated

STATx binding sites for POMC expression further, it would be reasonable to verify STAT-binding to the putative binding sites first, for instance by chromatin immunoprecipitation (ChIP) and electrophoretic mobility shift assays (EMSA).

In the 3' CGI fragment, the first CpG position downstream of the exon3 start (CpG +1) was also identified to belong to the HpaII targets, which in their entirety caused significant reduction of the 3' promoter activity upon methylation. CpG +1 is adjacent to the p300 binding site, which spans the intron2-exon3 junction. Interestingly, this CpG residue also shows significant hypermethylation in obese patients in comparison to normal weight humans, and the p300 binding site at the intron2-exon3 junction of the POMC was identified by ChIP assays to be a probable biological transcription factor binding site (Kuehnen et al., in revision). The p300 protein, which acts as a coactivator of transcription and is involved in the formation of open euchromatin by its integrated histone acetyltransferase (HAT) activity (Liu et al., 2008; Ogryzko et al., 1996; Spiegelman and Heinrich, 2004), is expressed moderately in GT1-7 cells, as I detected by RT-PCR. Therefore, it seems reasonable that the transcriptional activity of the 3' CGI fragment is diminished by HpaII methylation due to methylation of the CpG +1 residue, which may change the binding dynamics of the p300 complex to its binding site and, therefore, transcription activity of *POMC* and subsequent signaling. This would be in concordance with the findings that the p300 binding is significantly decreased in obese patients with the POMC hypermethylation variant in this region (Kuehnen et al., in revision).

Altogether, these data support the theory that rather the specific location (Newell-Price et al., 2001) than the quantity of methylated CpG dinucleotides seems to be critical to exert effects on expression activity (Boyes and Bird, 1992; Harris et al., 1994). Hence, drastic methylation changes of individual CpG moieties, as described for the CMP associated with obesity (Kuehnen et al., in revision), could have a relevant effect for gene expression depending on the location of the CpG residue. Therefore, they should be considered as potentially functional relevant. For further estimation of the relevance of the CpG +1 residue methylation status in particular, the application of the CpG +1-mutation variant in reporter gene assays after HpaII methylation would be a possibility. This mutant construct showed no activity difference to the non-mutated original construct in an unmethylated state. After HpaII methylation, which would exclude the mutated CpG +1 (since it is a TpG), the specific influence of the CpG +1 methylation on the 3' promoter might be elucidated.

To narrow down, which sequence elements of the 3' CGI are crucial for the activity of the alternative 3' promoter, further transfection experiments were performed, applying various modification and length variations of the 3' CGI fragment constructs. Partial deletion of the p300 binding site significantly decreased the promoter function of the fragment, underlining the theory that adequate p300 binding is required for normal transcription activity. However, destruction of the p300 recognition sequence due to mutation of this region, introduced a putative GATA-1 binding site instead. Although GATA-1 is considered to be an erythroid development regulating transcription factor (Ohneda and Yamamoto, 2002), a slight GATA-1 expression in the used GT1-7 cell line was detectable. Nevertheless, it was surprising that the GATA-1 variant of the 3' CGI construct increased the transcription activity of the fragment. The performed experiments did not resolve which structural elements of the 3' CGI region are crucial for the *in vitro* observed activity of the alternative promoter. However, it is reasonable that sequence and structural elements that occur in the exon3 region could be important. Which sites or elements that are, should be analyzed in future research.

As observed for the 5' CGI promoter, also the methylation state of the alternative 3' CGI promoter is associated with its transcription activity *in vitro*. Hence, the analysis of the POMC DNA methylation patterns of both regions *in vivo* could be informative regarding their role for the gene expression not only of the POMC gene. While the 5' CGI promoter was already described to have a methylation-correlated

expression state (Newell-Price et al., 2001), the information about the 3' CGI promoter methylation are rather rare to date. It is known that human peripheral blood cells (PBC) and *arcuate nucleus* cells, which originate from different germ layers and both express POMC, although in different functional contexts, show identical methylation patterns for the 3' CGI promoter region (Kuehnen et al., in revision). That implies stable methylation states of this region, independent of the physiological function of the cells and contrasts with the expressing-matched methylation state of the 5' promoter. To test this hypothesis, comparative analysis of the POMC DNA methylation patterns of different tissues and sundry developmental stages were performed to determine the occurrence and stability of POMC DNA methylation during the ontogenetic development.

4.2 Ontogenesis and stability of the POMC DNA methylation patterns

CGIs are regions of interest for analysis of the DNA methylation status of genes since (i) CGIs are frequently located in promoter regions and (ii) changes in their methylation status can affect promoter activity. As shown in this thesis work *in vitro*, this also accounts for both promoter regions of the human POMC gene: the regular 5' CGI promoter and the alternative 3' CGI promoter. To get insight in the stability of the DNA methylation patterns of both regions *in vivo*, the methylation statuses of both CGIs were determined in various POMC-expressing and non-expressing tissues of different mice strains. In DNA samples from peripheral blood cells (PBC) of 20 different C57BL/6 mice (wild type), distinct patterns for the 5' CGI and 3' CGI region were observed. This high resemblance of DNA methylation patterns in different mice suggests that the patterns are predestined and not established by chance.

The observed CGI methylation patterns from C57BL/6 PBC were also found in DNA from ten different other tissues of C57BL/6 mice. Also in NMRI mice, identical patterns were detected in blood, as well as in ten additional tissues. Despite the high concordance of DNA methylation patterns in diverse tissues from different mouse strains, minute differences in methylation patterns were observed for a few stray CpG positions in some samples, independent of strain, germ layer of origin, or tissue. However, in terms of *methylation patterns* and in the scope of a basic overview of the pattern development it seems reasonable to neglect the differences in single CpGs as random variations and to assume the patterns of the various tissues of different mouse strains as similar, independent of the germ layer of origin and the physiological function.

It is known that the methylation status of a gene is metastable, meaning it is passed to the daughter cells during cell division (Bestor, 2000; Bird, 2002). Regarding the observed congruence of the POMC methylation patterns in various tissues from different mouse strains some questions arise: (i) Do the observed methylation patterns develop independently in the different tissues or do they have a common origin? (ii) If the patterns have a common origin, do they develop during embryogenesis before the deviation of the germ layers, or do they resist global demethylation after fertilization and are directly transmitted from the parental germ cells as it has been observed recently for several other genes (Borgel et al., 2010)?

To tackle those questions, embryonic mouse samples from various prenatal stages were examined. Analysis of these samples showed similar patterns as observed before in the various tissues of adult mice, except for slight heterogeneous methylation variances in the posterior part of the 5' CGI (mPOMC-F2 fragment). Apart from that the methylation pattern of the samples from embryonic stages E8.0 until E14.5 were exactly the same as the patterns observed in adult mice with distinct hypermethylation of the anterior part of the 5' CGI, heterogeneous methylation of intron2, and the strict hypomethylation in exon3. In conclusion, it can be stated that the distinct methylation patterns of the mouse POMC locus are already present in embryonic stage E8.0 and remain stable during further development throughout tissues.

Therefore, these methylation patterns are most likely established during embryogenesis before the deviation of the germ layer cell fates or are directly transmitted and preserved from the parental germ cells.

Besides its maintenance during cell division, the DNA methylation of the genome changes during lifetime in a well-staged way. A substantial part of the genome is demethylated after fertilization followed by a phase where new DNA methylation patterns are established (Dean et al., 2003; Reik et al., 2001). However, recent studies showed that several non-imprinted germline and somatic genes resist the post-fertilization DNA methylation reprogramming and inherit their promoter DNA methylation from parental gametes (Borgel et al., 2010). To test the fate of the POMC methylation patterns in the post-fertilization phase, I determined the DNA methylation of early mouse blastocysts. In this early stage of embryogenesis, the CGI regions were completely hypomethylated, and only a few stray methylated CpGs were detectable. The interval of minimal methylation is really narrow, since the demethylation event has its nadir at the morula stage and *de novo* methylation occurs between the morula and blastocystal stage of the germ just before implantation (Santos et al., 2002). Therefore, it is possible that the observed stray CpGs were still or already *de novo* methylated. That the stray methylated CpG in the predominantly non-methylated blastocysts samples showed hypermethylation in positions which were heterogeneously methylated at the most in embryo or adult samples has a methodical background: To treat the blastocysts samples reasonable, sequencing was performed after sub cloning. Sub cloned constructs contain only a single strand of target DNA and not a variegation as PCR products. As a result, no C/T-double peaks appear in sequencing readouts, suggesting heterogeneous methylation, but only C or T peaks. If sufficient numbers of sub-cloned constructs of one sample are sequenced, the prediction of heterogeneously methylated areas should match the results that would be obtained from the same samples when directly sequenced.

It can be concluded that the overall hypomethylation of *POMC* in blastocysts differs significantly from all POMC DNA methylation patterns described for later developmental stages. This shows that the methylation patterns of the POMC locus are not directly transgenerational transmitted from the parental germ cells. The mechanism of direct transgenerational transmission of DNA methylation patterns was already suggested for the A^{vy} and $Axin^{Fu}$ loci ten years ago, to explain the transgenerational heritability of epigenetic states and related phenotypes (Morgan et al., 1999; Rakyan et al., 2003), but was never specifically proved for these loci, but for IAPs in general (Lane et al., 2003). However, recently transgenerational transmission of DNA methylation patterns from parental germ cells was genuinely observed for specific genes. For instance, the somatic expressed genes *Rrh* (retina) or *Cd4* and *Fyb* (hematopoietic cells) were shown to escape the post-fertilization DNA methylation reprogramming process (Borgel et al., 2010).

Yet, my data indicates that the DNA methylation patterns of the POMC gene are not directly transgenerational transmitted, but arise during early embryogenesis. That means that existing patterns of POMC DNA methylation of the germ cells are erased after fertilization. Subsequent *de novo* methylation leads then to the establishment of the methylation patterns that were detectable after the blastocystal stage. However, I could not show when these new methylation events take place, and if the methylation patterns are already fully established before germ layer division. Since the *de novo* methylation wave is usually observed before implantation (Santos et al., 2002) it is likely that the POMC gene is also newly methylated before division of germ layers. Consequently, the distinct methylation patterns observed in this study did not develop independently in the different tissues but originate from the newly established pattern of the blastocystal stage.

How the development of the specific DNA methylation patterns is determined and signaled in numerous different individuals remains unclear. A case of transgenerational epigenetic inheritance of the patterns, as described for the imprinted IGF2/H19 locus, is thinkable. Thereby, the methylation profile is somehow

genetically transmitted from the parental generation, possibly through *cis* or *trans* regulation, even though the methylation is dynamic in the periconceptional phase (Tost et al., 2006). That the DNA methylation patterns of the POMC locus are erased and newly established during the periconceptional period and maintained stably throughout intrauterine and postnatal life, I revealed for the POMC locus in mice. If this also accounts for the human POMC locus was tested within the possible scope.

Due to obvious ethical reasons, it was not possible to examine the human POMC methylation patterns prenatally. An alternative for that would have been the analyses of non-human primate samples of prenatal stages. The implementation of primate embryonic stem cells (ESC) as model for the early embryogenesis state is not possible, since ESC show abnormal methylation states. It is indicated that cultured ESC bear the DNA signature resembling the postimplantation embryo, possibly due to culture conditions (Borgel et al., 2010). However, I studied human newborn PBC samples from the earliest possible time point after birth and found DNA methylation patterns that were highly similar to the patterns determined for adult humans from PBC and *arcuate nucleus* cells for the 5' and 3' CGI promoter (Kuehnen et al., in revision). Beyond the distinct shift of hypermethylation to hypomethylation at the intron2-exon3 junction, the DNA methylation pattern from newborn PBC also showed the heterogeneous methylation dip at CpG -13 in the intron2 region that was already detected in adult PBC and *arcuate nucleus* cells.

The high conservation of the block of hypermethylation in intron2, the distinct shift to hypomethylation in exon3 and the heterogeneous methylation dip at CpG -13 suggest some kind of function of those features. It is known that DNA methylation influences the accessibility of DNA regions to proteins that modulate chromatin formation and gene transcription and, hence, interfere with gene expression (Bird, 2007; Cedar, 1988; Lorincz et al., 2004). DNA methylation of promoters can influence a genes transcription via two possible mechanisms: (i) Direct inhibition by inaccessibility of TF binding sites or (ii) indirect repression by recruitment of inhibiting proteins, such as methyl-CpG binding proteins (MeCP-1), induction of inactive chromatin states, or expression regulation of repressing antisenseRNAs or microRNAs (Bartel, 2004; Boyes and Bird, 1992; Tate and Bird, 1993). Accordingly, the hypermethylation of the intron2 region could exert repressing function via both mechanisms. As opposed to this, the hypomethylated state of exon3, which is highly conserved among species, suggests importance of an associated open chromatin state of this POMC region, for instance for adequate gene expression. The 3' CGI region has never been described as alternative promoter of *POMC* before, not to mention being involved in the expression of the functional full-length transcripts. The 3' CGI region was just suggested to serve as TSS for the short alternative POMC transcripts (Gardiner-Garden and Frommer, 1994). Thereby, it is argumentative that the regulation of the short transcripts may be a direct mechanism, while the influence on full-length transcript expression might be indirect. However, the function of the short POMC transcripts has not been resolved yet and is even doubted, since the lack of the signal sequence probably renders the molecule to be nonfunctional (Clark et al., 1990; Rees et al., 2002), even though it is moderately expressed (Ehrlich et al., 2010). Maunakea *et al.* detected recently that intragenic located alternative promoters are common, and can induce the expression of alternative transcripts *in vivo*, regulated by DNA methylation in a cell-context specific manner (Maunakea et al., 2010). Furthermore, it is suggested that alternative intragenic CGI promoters play a functional role during development (Illingworth et al., 2010). Since the POMC locus retains its methylation patterns once they are established a cell- or developmental-context specific expression due to the 3' CGI promoter does not seem probable, but a regulatory role of the short transcripts, maybe in the line of regulating antisense-RNAs, could be considered. Further investigation is needed to get insight into the role of the alternative 3' CGI promoter with its stable DNA methylation pattern and the alternative short POMC transcripts *in vivo*.

To summarize: the DNA methylation patterns of the 5' CGI and the 3' CGI region of the murine POMC locus are not directly transgenerational transmitted as shown for other genes, but are established by *de novo* methylation in early embryogenesis and are perinatal stable. Furthermore, the DNA methylation patterns of the murine, as well as the human POMC loci are stable in postnatal life throughout tissues. These results match the available information about DNA methylation stability and constancy, which state that the constancy of methylation in various somatic tissues is high (Eckhardt et al., 2006) despite a high interindividual variability of the methylation of specific loci (Feinberg et al., 2010; Heijmans et al., 2007). While the global methylation has been reported to change over time (Bjornsson et al., 2008; Fraga et al., 2005), the DNA methylation of some specific loci was detected to be more stable (Feinberg et al., 2010; Heijmans et al., 2007; Talens et al., 2010). According to our findings, the POMC locus is one of the specific loci with stable methylation throughout life and tissues. Therefore, it seems reasonable to see the POMC methylation pattern of PBC as representative for the pattern of different tissues and cells.

Despite the high stability of the POMC methylation patterns over time and tissues, one should not forget that the DNA methylation of specific loci could differ significantly between individuals. For instance, Feinberg *et al.* identified more than 200 genomic regions in humans that showed extreme interindividual variability and called them *variably methylated regions* (VMR). Approximately half of them are stable within individuals and can represent a *personalized epigenetic signature*, which could have marker function regarding disease risks (Feinberg et al., 2010). One VMR-analogue for the POMC locus is the CMP, whose hypermethylation variant is associated with obesity (Kuehnen et al., in revision). This demonstrates clearly that methylation of the POMC locus can also vary interindividual. How and when the variations in the POMC VMR arise has not been resolved yet. However, I tried to determine if intraindividual changes could emerge due to life characteristics of the individual or environmental effects, as it was shown for global DNA methylation (Zhu et al., 2010).

For several years it is communicated that interindividual differences in disease susceptibility, such as predisposition for obesity, is not only depend on genetic circumstances but also on epigenetic factors. Epigenetic factors are capable of influencing the phenotype through changing gene expression without altering the nucleotide sequence of the DNA. Dietary components have the potency to influence epigenetic events such as DNA methylation (Singh et al., 2003; Walsh et al., 1998; Waterland and Jirtle, 2003), altering gene expression and potentially modify disease risk. This phenomenon was often discussed. Already 35 years ago, Ravelli *et al.* detected in a cohort from the Dutch famine an association of nutrition deprivation *in utero* with obesity in later life (Barker, 2004; Gluckman et al., 2007; Ravelli et al., 1976)). Further studies about the role of prenatal nutrition also detected various correlation of exposure to nutritional extremes with increased risk for disease states in adulthood, such as coronary heart disease, raised lipids, obstructive airways disease, decreased glucose tolerance, and schizophrenia (Painter et al., 2005; St Clair et al., 2005). Thereby, the timing of the exposure seems to be relevant for the outcome. All these data is only strong on epidemiological basis, but not proven molecularly. Nevertheless, also molecular alterations, such as changes in DNA methylation patterns, could be correlated with early nutritional exposures like the Dutch famine or seasonal changes. However, the persistent epigenetic changes detected in humans could not be matched to specific phenotypes so far (Heijmans et al., 2008; Steegers-Theunissen et al., 2009; Tobi et al., 2009; Waterland et al., 2011).

In animal models, also nutritional effects on epigenetic marks of specific loci are detectable. Since animal experiments are better to regulate and easier to survey, also associations of altered epigenetic states with (pathophysiological) phenotypes can be made. For example, the *in utero* methyl donor supplementation of $A^{vy/a}$ mice can determine the epigenetic state of the A^{vy} locus of the offspring and the associated weight and fur phenotype (Wolff et al., 1998). For the studies showing molecular associations to prenatal

nutritional exposures, also a relevance of timing was observed (Tobi et al., 2009; Waterland, 2009a; Waterland, 2009b).

The role of postnatal nutrition in the modification of epigenetic patterns and the potential transmission of changed patterns through gametes is a subject of debate (Cobiac, 2007). Although some specific loci were studied, human data about epigenetic changes arising after birth are rare and focus largely on the global methylation of the genome. However, in general, the postnatal environment can be associated with changes in the epigenome (Campion et al., 2009; Fraga et al., 2005; Wong et al., 2005). Some animal studies claim that postnatal nutritional exposure, for example to overfeeding or high fat diet, is capable of changing the DNA methylation of specific body weight related loci (Plagemann et al., 2009; Widiker et al., 2010). Even though, the observed effects are significant in numbers, it should be critical estimated if the observed changes are relevant.

In this thesis work, the influence of 29 weeks high fat diet after weaning on the DNA methylation of the murine POMC locus was tested. Since longitudinal comparative tissue analyses suggest good correlation of pattern-development between tissues, the DNA methylation of PBC appears to be representative for other tissues (Talens et al., 2010). Moreover, the usage of PBC samples enables the analysis of the patterns before and after the feeding period in the same animals. Two different mouse strains, a lean wild type strain (C57BL/6) and members of the obesity-predisposed strain BFMI860, were analyzed. No significant alterations of the methylation patterns by postnatal diet were observed. In conclusion, it can be stated that neither the diet nor the different mouse strain origins had influence on the DNA methylation patterns of the murine POMC locus, at least not in this study design. It would have been more reasonable to implement a different study design, for example with enlarged group sizes and the first blood sampling parallel to the beginning of the 29 week long feeding period. Moreover, a study exposing periconceotional germs to a high fat diet *in utero* might have been more promising regarding the observation of DNA methylation changes, as already stated above. Nevertheless, the results of the samples from this feeding experiment are analogue to the observation of the ontogenetic analyses. The DNA methylation patterns of the POMC locus are highly stable longitudinal, as well as throughout different mouse strains.

This suggests that DNA methylation pattern-formation at the POMC locus can rather be attributed to genetics with stochastic components, than environmental factors. The stochastic component of DNA methylation was underscored for other specific loci by the observation of substantial discordances of DNA methylation patterns in monozygotic twins (Kaminsky et al., 2009; Ollikainen et al., 2010; Waterland et al., 2011), while a strong locus specific genetic component was detected for the imprinted IGF2/H19 locus. The substantial variation of the IGF2/H19 methylation of the imprinted allele is mainly accounted to single nucleotide polymorphisms (SNPs) in humans (Heijmans et al., 2007), hence to genetic control. In addition, DNA methylation maintenance relies on genetic components. This was indicated in a family-based cohort from Utah, showing familial clustering of methylation changes over time (Bjornsson et al., 2008). In the scope of genetic factors, not only genetic variations like SNPs seem to play a role, but also *cis*-acting genetic factors were described to participate in DNA methylation pattern manifestation fundamentally. DNA binding proteins with respective binding sites, such as Sp1 and VEZF1, are suggested to determine the methylation, but also sequence motifs like retrotransposable elements were identified to contribute to pattern establishment (Dickson et al., 2010; Han et al., 2001; Li et al., 2010c). Beyond that, transgenerational parental effects on the manifestation of DNA methylation patterns are observable, in imprinted and in non-imprinted loci. For instance, the epigenetic state at the $Axin^{fu}$ locus can be inherited after maternal and paternal transmission, while the inheritance of the A^{vy} epigenetic state occurs through the female line only (Rakyan et al., 2003). That militates for a system that is under strong genetic influence, rather than facilitating easy dynamical changes through environmental factors, and, therefore, capable of establishing stable predetermined epigenetic signatures. Hence, it virtually obtrudes to

investigate the origin of the distinct 3' CGI DNA methylation pattern of POMC on a genetic basis. Thereby, I considered the sequence of the locus as indicatory and chose a comparative phylogenetic approach to investigate the manifestation of the 3' CGI DNA methylation pattern of *POMC* in association with the presence of *Alu* elements within the gene region.

4.3 Potential phylogenetic origin of the 3' CGI DNA methylation pattern

The 3' CGI methylation pattern of the human *POMC* shows a prominent hypermethylation in the intron2 region and a distinct shift to hypomethylation at the intron2-exon3 junction. In accordance the mouse exon3 is also hypomethylated, indicating a phylogenetically conservation of this non-methylated state. Hence, the hypomethylation of exon3 might be important for POMC expression, for example to enable binding of proteins which are crucial for the activity of the gene (Choy et al., 2010). However, the murine methylation pattern of the intron2 region differs fundamentally from the human one with heterogeneous methylation. Comparison of the underlying sequences of the POMC locus in mice and humans revealed high sequence homology in the exon regions, while the consensus in non-exon regions was, as expected, significantly lower (Eberwine and Roberts, 1983; Notake et al., 1983). A large difference in the locus structures is represented by the presence of six retrotransposable elements of the primate-specific *Alu* family in the human POMC gene that have no equipollents in the murine POMC gene (Tsukada et al., 1982) (Figure 17 and Figure 22). Three of those six *Alu* elements of the human POMC locus are located in the intron2 region just upstream of the distinctly methylated 3' CGI. In general, retrotransposable elements like *Alu* elements are methylated to prevent them from retroposition (Liu and Schmid, 1993; Yoder et al., 1997b). This methylation is established for silencing reasons and can spread on the surrounding regions, resulting in modification of the DNA methylation near an *Alu* element (Batzer and Deininger, 2002; Turker and Bestor, 1997; Xie et al., 2010). Hence, the hypothesis arose that the hypermethylated region of the 3' CGI detected in humans is caused by the presence of those three *Alu* repeats within the intron2. To test this hypothesis, initially genomes of other primates were analyzed for *Alu* incidence, since *Alu* elements are only present in primate genomes but to a different extend (Xing et al., 2007). Afterwards, it was evaluated if the methylation status of the 3' CGI of the other primates is associated with the *Alu* incidence in their genomes.

All analyzed non-human primates of the hominid strain (chimpanzee, gorilla, and orangutan) exhibited the same *Alu* element incidence in the intron2 region as humans. The three *Alu* elements detected in all four sequences were congruous for type and orientation, indicating integration of the three *Alu*s before the branching of the different families of the hominids. The two cercopithecoidea macaque and baboon have one *Alu* repeat less in their intron2 region compared to the hominids tested. Types and orientations of the two remaining *Alu*s are congruent to the *Alu* D and *Alu* F of the hominid genomes, suggesting a common origin, since the distribution of *Alu* elements is free from homoplasy (Batzer and Deininger, 1991). Interestingly, the middle *Alu* E, which is not present in the baboon and the macaque genome, is of the youngest *Alu* family, the Y-family that still shows transposition activity (Batzer et al., 1996; Bennett et al., 2008; Liu and Schmid, 1993). Most likely, this *Alu* element was integrated into the genome after the catarrhines split into hominids and cercopithecoidea 25 Ma ago. In the marmoset, the primate family with the greatest density of *Alu* elements (Liu et al., 2009), again only the *Alu* D- and *Alu* F-equivalents of the human genome can be detected. However, there are also two additional (Ad) repeats present, which were not found in one of the other primate genomes examined. *Alu* Ad1 and *Alu* Ad2 are of the S type, which is considered the second oldest *Alu* family. Either these repeats were located in their positions already before the off splitting of the new-world strains 40 Ma ago and were subsequently eliminated in the catarrhine branch, or they were integrated into the POMC gene in platyrrhines just after branching 50 Ma ago.

Lemurs and galagos belong to the group of the strepsirrhinis and are the farthermost relatives of humans within the group of primates. For lemurs and galagos, no *Alu* elements in the gene region of interest were detected. The separation of strepsirrhinis from the main branch took place almost 65 Ma ago. Around the same time *Alu* elements began to proliferate in the genomes of primates (Batzer and Deininger, 2002). Global assessment of the distributions, phylogenies, and consensus sequences for *Alu* elements in primates revealed a steady rate of *Alu* retrotransposition activity in lemurs (Liu et al., 2009). Hence, not a general *Alu* deprivation but rather the early branching is likely the reason why there are no *Alu* elements located within the strepsirrhinis intron2 region of the POMC locus, which are present in all other analyzed primates.

In conclusion, it can be stated that closely related primates share the same *Alu* elements in the POMC intron2 region. Further, several strain-specific *Alu* elements were established after the branching of strains and are, therefore, only present in one of the branches where they form an individual signature. In general the differences in *Alu* incidence and distribution in various primate genomes have played an important role in shaping the primary structure of the genome, but the secondary and tertiary structure, as well, and make functional consequences of these changes among the diverse primate lineages rather likely (Liu et al., 2009). Of which type and to which extend these functional consequences of the *Alu* incidence within the POMC intron2 region are was not examined in detail here, but at the level of DNA methylation pattern-manifestation in the adjacent 3' CGI region.

The DNA methylation status of the 3' CGI regions of most primates was determined in PBC. Only the DNA of the strepsirrhinis was obtained from muscle tissue due to sampling reasons. Since this work revealed high conservation of the POMC DNA methylation patterns in fourteen different mouse tissues, including PBC and muscle tissue, the difference of samples should be negligible. To determine the DNA methylation status of the 3' CGI regions of the various primates, species-specific primer pairs were designed. As a result, the fragments of different primates not only vary in length, but also in CpG number and location. The latter is not only result of the different lengths but more importantly of the dynamics of DNA. CpG positions are prone to mutate by conversion of methylated cytosine to thymine *in vivo* (Bird, 1980). Therefore, CpG dinucleotides are underrepresented in the human genome (Duret and Galtier, 2000) and lead to differences in the sequences of different primates. Nevertheless, there is a high consensus of CpG positions within the exon3 regions of the different primates. This is in accordance with the high level of conservation of the translated regions due to the common ancestor of the POMC locus (Dores and Baron, 2011). In contrast, the CpG occurrence in the intron2 region has a higher variability, especially between primate families, which are not so closely related, such as strepsirrhini and hominids. Interestingly, also a high variability in the CpG moiety distribution in the galago and the lemur can be observed, although both species belong to the group of strepsirrhinis and their intron2 region sequences align well. Thus, the mutation rate of CpGs → TpGs must be higher in galagos than in lemurs. A quarter century ago, it was proposed that the clustering and spacing of CpG residue contribute to the *de novo* methylation process (Bolden et al., 1985; Bolden et al., 1986). However, Yates *et al.* found the CpG density for methylation of the Aprt gene in mice as negligible, and instead demonstrated the importance of a tandem B1 repetitive element-motif upstream of the gene instead (Yates et al., 1999). In addition to acting as strong signals for *de novo* methylation, the tandem B1 element also acted synergistically in the scope of spreading methylation. This function was also indicated for *Alu* elements before (Turker and Bestor, 1997), which are the primate equivalents to the murine B1 elements. Therefore, I focused on a presumable association of the final methylation pattern of the 3' CGI region with the incidence of *Alu* elements in the upstream region.

In all primates examined, the POMC exon3 region was hypomethylated as also observed in mice and humans before. This high degree of conservation of the hypomethylated state of the exon3 region in

different species underscores the hypothesis of a related functional relevance, since the methylation state of a gene region can be correlated with the gene activity by interrelating with TF binding and the chromatin formation (Choy et al., 2010; Martinowich et al., 2003).

Alu elements are strongly methylated, presumably to reduce transcriptional activity of the retrotransposomal DNA. Mummaneni *et al.* coined the term *methylation center* for *cis*-acting genomic regions that provide significant *de novo* methylation signals (Mummaneni et al., 1993; Turker, 2002; Yates et al., 1999). By acting as methylation center, *Alu* elements trigger methylation in their genomic vicinity (Graff et al., 1997; Li et al., 2010c). Therefore, I expected primates with the same *Alu* incidence as humans to share a similar methylation pattern in this region. The hypothesis was confirmed by the results of the chimpanzees and gorillas, which also have the three 'human' *Alu* elements in their intron2 sequence. For chimpanzees and gorillas, the same distinct methylation patterns as in humans could be observed and matched in details, such as the sharp junction from hypermethylation to hypomethylation at the intron-exon junction and the heterogeneous methylation dip in the anterior intron2 region. This correlation between the occurrence of *Alu* elements in the intron2 region and the establishment of the methylation state in this region indicates that those *Alu* elements function as a trigger for methylation. However, this methylation force seems to be restricted in areas that are presumably relevant for expression, such as CpG -13 and the exon3 region.

Similar methylation patterns were also found for primate families like baboons, macaques, and marmosets that share only two *Alu*s of this region with humans. Even the methylation dip of hominids was conserved and occurred in marmosets at CpG -8 instead of CpG -13 due to CpG depletion reasons. However, a minor dose-effect of *Alu* number could be observed. In baboons and macaques with the two *Alu* elements, the drop zone at the intron-exon junction is flatter and step wise. Marmosets have additional *Alu*s and show a slightly shift of the drop zone into the exon region. This dose-effect has never been described before and is strengthened by the methylation pattern observed in lemurs.

The lemur pattern is highly similar to the murine pattern and showed predominant hypomethylation throughout the whole fragment. Both, mice and lemurs, do not possess *Alu* elements or equipollents in the gene region of interest. This supports the hypothesis that the distinct hypermethylation in the intron2 region of the human, hominids, cercopithecoidea, and platyrrhine POMC is correlated to – or even caused by – the upstream-located *Alu* elements. Therefore, it is tempting to pose that (i) the methylation of this region is induced by the upstream-located *Alu* acting as methylation center during early development and is stably transmitted to daughter cells during further development. (ii) The methylation force that emanates from the methylation center has a dose-effect depending on the number of *Alu* elements that are present in the methylation center region. (iii) The *Alu*-triggered methylation is restricted to the intron2 region to keep the exon3 region non-methylated.

Of course, the variance of the DNA methylation pattern of lemurs in comparison to the human-like methylation pattern might also have other causes apart from the missing *Alu* elements. For example, DNA binding proteins, such as the Sp1 protein, were frequently suggested to be *cis*-acting factors, which prevent DNA methylation of promoter regions and CGIs (Graff et al., 1997; Holler et al., 1988; Straussman et al., 2009; Tate and Bird, 1993; Turker and Bestor, 1997). The two *in silico* predicted Sp1 binding sites within the lemur intron2 sequence could inhibit the methylation of this region. However, these binding sites were not empirical proved by ChIP analysis. In addition, further weakening this possibility, in mice no Sp1 binding sites within the intron2 region are predicted that could exert an equivalent effect. That would imply that the analogue hypomethylation of the intron2 region in lemurs and mice would be due to different causes. Since this seems unlikely, it abates the hypothesis that the hypomethylation of the lemur intron2 region of POMC may result from the Sp1 binding sites in the intron2 regions. By implication, the hypothesis of the *Alu*-dependency of the intron2 methylation is strengthened.

For galagos like lemurs, Sp1 binding sites are predicted to be located in the intron2 region of the POMC gene. Nevertheless, galagos show no predominant hypomethylation of the 3' CGI region as lemurs, weakening the possible influence of Sp1 on the specific methylation deprivation of intron2 even further. Instead, the galago pattern is more similar to the human pattern, than to the lemur and mouse, with hypermethylated regions within the intron2, although the start of the transition to hypomethylation is shifted upstream.

Resembling the sequences of lemurs and mice, the galago also does not possess *Alu*s in the POMC intron2 region. Given the human-like DNA methylation pattern of the galago the observation of an *Alu*-free intron2 raises assumptions about additional involved factors besides the direct influence of intron2 *Alu* elements on the hypermethylation of the subsequent region. It is known that chromatin is a complex system. Within this three-dimensional assembly of DNA and proteins, not only directly adjacent regions of the genome influence each other. Also further afar regions are capable of cross acting in a regulatory way (Gondor and Ohlsson, 2009; Lanctot et al., 2007). Moreover, it was observed that the epigenetic regulation of gene expression can be controlled in *trans* by long-range chromatin interactions, and that those long-range chromatin interactions can coordinate epigenetic changes (Gondor and Ohlsson, 2009; Kurukuti et al., 2006; Lanctot et al., 2007). Presumably, there are further 5' sequence-motifs involved in DNA methylation establishment of the POMC locus. For instance, three more *Alu* elements are present in more upstream regions of the human POMC gene aside from the three *Alu*s located in the intron2. They might act in *trans* on the methylation drive. For both investigated strepsirrhinis, not the complete POMC locus has been sequenced to date. Therefore, it is possible, that galagos and lemurs differ from each other in the upstream region of the POMC gene. It is conceivable that the galago possesses *Alu* elements in the intron1 or further upstream that exert DNA methylation force, which the lemur lacks. Therefore, it should be a goal of future research to further sequence and analyze the unexploited gene regions of less familiar primates, such as the strepsirrhinis. Then investigation of chromatin interactions of the POMC locus in various primates would be possible, such as the application of new techniques for comprehensive three-dimensional analyses (Fullwood et al., 2010; Fullwood and Ruan, 2009; Li et al., 2010a). That could bear further insights in the triggering mechanisms of the POMC methylation patterns.

In parallel, the elucidation of the role of the intron2 *Alu* elements as methylation center could be promoted by research focusing on other species. It would be useful to determine the POMC DNA methylation patterns of species, (i) which do not possess *Alu*s or equivalent retrotransposable elements in this region as the mouse (for example horses or dogs), (ii) that exhibit retrotransposable elements in the locus, but different from *Alu* elements (for example dolphins and cows).

In conclusion, I can state that the comparative sequence and methylation analyses of the intron2 and 3' CGI region of the POMC locus of various primates and mice provide strong evidence that the *Alu* elements in the intron2 region act as methylation center that triggers the DNA methylation pattern of the subsequent 3' CGI. This concept of *Alu*-triggered DNA methylation of the 3' CGI region is applicable to mice and all analyzed primates with exception of the galago. The galago data necessitate considering of further *trans*-acting factors and mechanisms determining the POMC DNA methylation pattern, which should be investigated in future research. However, the methylation force exerted by the intron2 *Alu* elements is apparently restricted to the intron2 region, preserving the exon3 region hypomethylated. The molecular mechanism that regulates the exact border restriction of the CpG-methylation in the case of POMC 3' CGI is unknown. However, there are some theories about the limitations of DNA methylation to specific regions. Certain DNA binding proteins are thought to protect gene regions from *de novo* methylation (Han et al., 2001). The Sp1 protein was detected to segregate highly methylated *Alu* element containing flanks from unmethylated CGI sites, a mechanism that is overridden in pathological states (Graff et al., 1997). In the

region of interest of the human POMC locus, Sp1 binding sites are only predicted to be located within the exon3 region, approximately 600 bp downstream of the exon start. If DNA binding proteins have a far-distance effect, this might explain the methylation restriction to the POMC intron2 region, but this has not been described to date. However, analogous methylation restricting effects have also been described for other DNA binding proteins (Dickson et al., 2010). Therefore, it is possible that other binding proteins, which are located in the methylation junction region, can exert the observed effect.

In addition to DNA binding proteins, also sequence motifs, such as an A-rich repeat sequence in the human GSTP1, have been shown to form a boundary between methylated and unmethylated DNA (Millar et al., 2000). Turker proposed in 1999 a model of the *dynamic equilibrium* between forces that support and inhibit the spread of DNA methylation (Turker, 1999). Respective *methylation-counteracting* forces could be *Alu* elements exerting methylation force and active promoter regions promoting an open chromatin state. Thereby, the methylation boundary might be shifted slightly back or forth, depending on the strength of both forces (Turker, 2002). For the POMC intron2-exon3 boundary the following scenario is thinkable: The intron2 *Alu* elements form an upstream methylation center, which counteracts to the methylation blocking force of the POMC 3' CGI promoter, whose functional relevant sites are probably located in the exon3 region. That could determine the intron2-exon3 methylation border of the POMC locus, with possible stochastically defects leading to epigenetic variants like the obesity-associated CMP described by Kuehnen *et al*. This theory would also fit the observation of a dose-dependent methylation force depending on the number of *Alu* elements present in the intron2 region.

Differences in the distribution and rates of *Alu* transposition have played an important role in shaping the structure of primate genomes and defining the activity of certain gene regions by various mechanisms, including epigenetic regulation (Batzer and Deininger, 2002; Liu et al., 2009). They are described to have a close relation to DNA methylation in the genome. Hence, they contribute to genome organization, gene expression, and related phenotypes in various ways. Transposon-induced methylation spreading can be observed in the melon plant where it determinates the sex of the flowers (Martin et al., 2009). This phenotype-determining transposon-induced alteration of the DNA methylation is stably forwarded to the next generation. Therefore, it not only has a marker function for the sex of the flower, but also contributes to the evolution of the species. Similar to the DNA methylation mechanism in melon, I detected that the DNA methylation pattern of the POMC locus may have evolved upon *Alu* insertion into the gene region. Events like this can lead to pathological consequences, as observed in the X-linked dystonia-parkinsonism. The X-linked dystonia-parkinsonism is a movement disorder in humans, in which a newly retroposed element induces abnormal DNA methylation. The changed DNA methylation is assumed responsible for decreased TAF1 gene expression and, therefore, involved in the disease genesis (Makino et al., 2007). In the case of the human POMC gene, the *Alu* presence and position is manifested in the genome. Therefore, it is possible that these *Alu* elements induce the conserved regular DNA methylation pattern of the 3' CGI of the *POMC*. If the *Alu*-induced methylation pattern changed the expression of the whole gene per se, remains unclear. However, it was shown, that in individuals with the hypermethylation variant of the weight phenotype-associated CMP of *POMC*, the POMC expression is decreased (Kuehnen et al., in revision). Therefore, an altered methylation of only a few CpG residues might be causally linked to the weight phenotype via a changed gene dose effect. That abnormal CpG methylation of only a few CpG moieties can be associated with disease was also observed in ependymomas. In the pediatric intracranial ependymomas, the aberrant DNA methylation is correlated with progression of the tumorigenesis. The aberrantly hypermethylated CpG sites are found in the vicinity of *Alu* elements (Xie et al., 2010), comparable to the hypermethylated CMP site in obese children. However, in contrast to ependymomas only one specific gene site near *Alu* elements is affected in the POMC CMP. Application of the hypothesis of

methylation-counteracting forces for the DNA methylation border restriction makes it seem possible that the abnormal methylation of individual CpG residues – in the ependymoma-genome and in the POMC CMP – could be exerted by an excessive *Alu* methylation force. As result, an *Alu* element-triggered methylation defect might emerge.

In general, it is debated, how and when anomalous methylation states arise, and how stable they are. Data imply that genetic and stochastic factors, as well as environmental factors may contribute to the establishment of the epigenome (Bjornsson et al., 2008; Boks et al., 2009; Campion et al., 2009; Fuke et al., 2004; Heijmans et al., 2007). Studies examining the influence of concrete environmental exposures on disease states in humans tend to have difficulties to filtrate explicit outcomes on molecular level that are associated with a certain phenotype. There are various studies showing an association of (i) environmental influences with increased disease risk in later life (Gluckman et al., 2007; Painter et al., 2005; St Clair et al., 2005) and (ii) altered DNA methylation – genome wide or of specific loci – with disease (Heijmans et al., 2008; Steegers-Theunissen et al., 2009; Tobi et al., 2009; Waterland et al., 2011). Nevertheless, the linkage of environmental exposure with changes in DNA methylation that are associated with an increased disease risk seems to be challenging. This could be due to various reasons: In a normal environment, exposing events are manifold and can cross-act. The same applies for compensating mechanisms. Therefore, the outcome – on molecular and phenotype level – may be disguised. However, it is also possible that environmental-based alterations are minute and are superposed by stochastic and genetic factors.

How the POMC CMP develops in particular in humans can be estimated based on the results of this thesis work, which demonstrate that the methylation patterns of the POMC locus are established in early embryogenesis, most likely due to *Alu*-triggered methylation spreading. After being passed through all germ layers, the POMC methylation patterns are highly stable in various tissues throughout life. In contrast to studies focusing on global DNA methylation (Zhu et al., 2010), my experiments revealed no effects of individual life characteristics (mouse strain) or environmental influence (long-term exposure to high fat diet) on the POMC methylation patterns in mice. That indicates resistance against environmental factors, at least postnatal, and independence of life characteristics of the POMC DNA methylation. Environmental factors cannot be excluded to have an influence on the specific DNA methylation pattern. Based on my results it is likely that the POMC CMP arises during the reprogramming phase in early embryogenesis on a stochastically basis. Since the CMP is not associated with genomic rearrangements of any kind, it may be connected to stochastically occurring termination failure of the *Alu*-triggered methylation.

In individuals with the obesity-associated hypermethylated POMC CMP variant, reduced p300 binding and reduced POMC expression were detected. Regarding the observed 3' CGI promoter activity, which is diminishable *in vitro* by methylation, the CMP might have functional relevance for POMC expression. This could be either by influencing TF binding or elongation efficiency through DNA methylation directly (Choy et al., 2010; Lorincz et al., 2004) or indirectly by participating in chromatin formation (Pennings et al., 2005; Tanaka et al., 2010; Vaissiere et al., 2008). Hence, the 3' CGI promoter could be involved in the transcription of full-length transcripts by inducing an open and active chromatin structure long-range, in addition to the direct regulation of short alternative transcripts. In this line of thought, the CMP might affect total POMC expression and reduce the gene dosage effect. Consequently, this could increase the risk of developing obesity. Insufficient gene expression due to transposable element-induced methylation alteration has been described before (Makino et al., 2007; Martin et al., 2009; Morgan et al., 1999), as well as aberrant DNA methylation being directly involved in the genesis of diseases, such as obesity (Bjornsson et al., 2004). Thus, it should be an issue of future investigation to find out about the role of variegating *Alu*-

triggered DNA methylation on POMC expression, to determine if the POMC CMP has direct functional relevance or if it could serve indirectly as a marker for an increased obesity risk.

Stable interindividual differences in DNA methylation of specific loci, such as the *Alu* element-triggered POMC CMP, are common. It is becoming more evident that this kind of epigenetic variation might be connected to obesity susceptibility. The VMR identified by Feinberg *et al.* included a handful of stable VMR that were found near, or within, body weight- or diabetes-regulating genes. They were significantly associated with the BMI (Feinberg et al., 2010), just like the VMR-analogue POMC CMP. In the meanwhile, more and more obesity-associated epigenetic changes are detected (Campion et al., 2009). For most of them, it is not clear if the BMI-associated epigenetic aberrations have functional relevance or not. Either way, they represent a *personalized epigenetic signature* and may serve as risk markers for obesity susceptibility. The identification of individuals possessing these changes in their epigenetic profile could help to predict their risk to develop obesity. That might allow the implementation of sufficient prevention or therapy interventions to impede the progress of obesity development.

Besides their involvement in the pathogenesis of obesity, epigenetic factors are also discussed to be involved in the genesis of diseases in general (Bjornsson et al., 2004). Various studies identified global epigenetic changes in disease states, such as cancer, and postulated their contribution to aberrant gene regulation and genomic instability (Robertson, 2005; Wilson et al., 2007). Global epigenetic changes are hardly assignable to one concrete disease state. Moreover, it is difficult to distinguish between cause and effect (Laird and Jaenisch, 1996), which makes global epigenetic changes useless as early-recognition markers. Gene-specific epigenetic changes are easier to correlate with diseases and could be used as early-recognition markers for screening (Jiang et al., 2004; Karouzakis et al., 2009; Urdinguio et al., 2009). Developmental and exposure analysis may help to find out about the stability of specific epigenetic changes to estimate their sense as marker-aberration, as shown in this work. Thereby, it might be useful to pay attention to changes near *Alu* elements, since *Alu*s trigger the DNA methylation and can induce changes on a stochastic basis.

This kind of epigenetic approaches to diseases opens new chances for their comprehension, early detection, and handling, as genetic analyses have done before. Since genetic analyses met their limitations in various respects, it is a promising opportunity to deepen the knowledge of epigenetic factors that mark or influence the risk of disease susceptibility. Even if the genesis of diseases cannot be elucidated, early-recognition markers could be identified. By establishing appropriate biomarkers for diseases, such as the *Alu*-triggered POMC CMP for obesity, customized intervention strategies could be designed and applied as early as possible, to prevent the development or progression of diseases. This eventually may lead to an increase of health and quality of life of the individual.

5 Summary

Obesity is a chronic disease with an increasing prevalence worldwide. Besides environmental, socio-cultural, and genetic determinants, also epigenetic factors are discussed to contribute to the manifestation of the weight phenotype. The pre-proopiomelanocortin (POMC) gene is a pivotal element of the central anorexigenic leptin-melanocortin signaling pathway. Mutations within this gene can cause severe monogenic early onset obesity in humans and mice. In addition to these *POMC* mutations, recently a single nucleotide polymorphism (SNP) in the POMC vicinity and a POMC CpG methylation variant in the intragenic 3' CpG island (CGI) were identified to be associated with obesity. The latter indicates a possible role of epigenetic modifications in body weight regulation. To gain further insight into the functional relevance, stability, and origin of the POMC DNA methylation, both CGIs of the POMC gene - the promoter-associated 5' CGI and the intragenic 3' CGI - were analyzed with regard to the functionality, ontogenesis, and phylogenesis of their DNA methylation status.

Via *in vitro* analyses, DNA methylation-dependent promoter activity for both CGIs was revealed. Thereby, the intragenic 3' CGI was identified as a potential alternative promoter of *POMC*, which has not been described before. Because of the known impact of DNA methylation on gene expression activity, we analyzed the *in vivo* situation of POMC DNA methylation, starting with the ontogenetic aspects. Therefore, we applied bisulfite genomic sequencing (BGS) to (I) murine samples from various tissues, different developmental stages, and from mice receiving distinct diets, and (II) blood samples from newborn humans. Postnatally, stable POMC DNA methylation patterns with interindividual conservation were detected for both CGIs in humans and mice. In addition, it was observed in mouse samples that the POMC DNA methylation patterns are non-tissue-specific, stable upon long time administration of a high fat diet, and already present prenatally at the stage of early organogenesis. However, mouse blastocysts were found to be completely hypomethylated, indicating the establishment of the DNA methylation patterns after this stage.

Comparative analysis of the 3' CGI DNA methylation of humans and mice revealed distinct pattern differences upstream of exon3. These pattern differences could be linked to the presence of *Alu* elements within the intron2 of the human POMC gene, which might trigger methylation spreading in humans, but have no equipollents in the mouse genome. This hypothesis was tested by analyzing primate families for the respective *Alu* elements and their 3' CGI DNA methylation pattern. An association of these particular *Alu* elements with the establishment of the DNA methylation pattern upstream of exon3 was indicated. However, the results also suggest an influence of additional factors on the DNA methylation pattern, such as further *Alu* elements within the POMC gene region.

This work contributes to the field of epigenetics by demonstrating that the DNA methylation patterns of the POMC locus are species-specific highly conserved, and that they are stably established during early embryogenesis possibly triggered by the presence of *Alu* elements within the intron2. Stochastic variances in the manifestation of POMC DNA methylation patterns might alter the POMC gene expression, as indicated by *in vitro* analyses. Consequently, epigenetic variants may increase the risk of developing obesity. Future research will show whether DNA methylation changes might play a role in the development of common diseases, such as obesity.

6 Zusammenfassung

Adipositas ist eine chronische Erkrankung mit weltweit ansteigender Prävalenz. Man geht davon aus, dass neben umfeldbedingten, soziokulturellen und genetischen Determinanten auch epigenetische Faktoren zur Ausbildung des Gewichtsphänotyps beitragen. Das Proopiomelanocortin Gen (*POMC*) ist ein zentrales Element des anorexigenen Leptin-Melanocortin-Signalwegs, und Mutationen im POMC können zu frühmanifester Adipositas führen. Kürzlich konnten ein Single- Nukleotid-Polymorphismus (SNP) in der umgebenden Sequenz des *POMC* sowie eine CpG-Methylierungsvariante in der intragenischen 3' CpG-Insel (CGI) identifiziert werden, die mit Adipositas assoziiert sind. Die CpG-Methylierungsvariante weist auf einen möglichen Einfluß von epigenetischen Modifikationen auf die Gewichtsregulation hin. Zur Aufklärung der Relevanz, der Stabilität und des phylogenetischen Ursprungs der POMC-DNA-Methylierung, wurden beide CGIs (die Promoter-assoziierte 5' CGI und die intragenische 3' CGI) in Hinsicht auf ihre Funktionalität, Ontogenese und Phylogenese untersucht.

In *in vitro* Analysen konnte ich für beide CGIs DNA-Methylierungsabhängige Promoteraktivität feststellen. Die Transkriptionsaktivität der 3' CGI konnte somit erstmals beschrieben werden und weist auf einen separaten alternative Promoter des *POMCs* hin. Wegen des bekannten Effekts von DNA-Methylierung auf die Genexpressionsaktivität habe ich die *in vivo* Situation der POMC-DNA-Methylierung untersucht, begonnen mit den ontogenetischen Aspekten. Hierzu wurde Bisulfit-genomische-Sequenzierung auf (I) murine Proben von verschiedenen Geweben und Entwicklungsstadien sowie nach bestimmter Diät, und (II) humane Proben von Neugeborenen angewandt. Postnatal wurden stabile DNA-Methylierungsmuster mit interindividueller Konservierung für beide CGIs im Mensch und in der Maus festgestellt. Des Weiteren zeigte sich eine Gewebeunabhängigkeit der DNA-Methylierung in der Maus mit bereits prenatal im Stadium der frühen Organogenese ausgebildeten Mustern. Die Analyse von murine Blastocysten hingegen deutete auf eine Entstehung dieser Muster in einem späteren Entwicklungsstadium hin.

Der Vergleich des DNA-Methylierungsmusters der 3' CGI in Mensch und Maus zeigte klare Unterschiede upstream des Exon3, was auf das Vorkommen von *Alu*-Elementen im Intron2 des humanen *POMCs* zurückzuführen sein könnte, die einen Einfluss auf die DNA-Methylierung ihrer Umgebung haben können. Da es für die *Alu*-Elemente keine Äquivalente in der murinen POMC Region gibt, wurde diese Hypothese überprüft, indem verschiedene Primatenfamilien auf das Vorkommen entsprechender *Alu*-Elemente, sowie ihr DNA-Methylierungsmuster der 3' CGI untersucht wurden. Wir konnten eine bedingte Assoziation dieser *Alu*-Elemente mit der Ausprägung der DNA-Methylierung upstream des Exon3 feststellen. Jedoch lassen die Ergebnisse noch weitere Einflussfaktoren auf das DNA-Methylierungsmuster vermuten (zum Beispiel weitere *Alu*-Elemente).

Diese Arbeit ist ein wichtiger Beitrag zur epigenetischen Forschung. Es konnte gezeigt werden, dass die DNA-Methylierungsmuster des *POMC* Spezies-spezifisch konserviert sind und in der frühen Embryogenese ausgebildet werden, vermutlich ausgelöst durch das Vorhandensein von *Alu*-Elementen im Intron2. *In vitro* Ergebnisse weisen darauf hin, dass stochastische Variationen dieser Muster die POMC-Expression beeinflussen und somit das Risiko für Adipositas erhöhen könnten. Zukünftige Untersuchungen werden zeigen, ob spezifische Änderungen der DNA-Methylierung eine Rolle in der Entwicklung von häufigen Erkrankungen, wie zum Beispiel der Adipositas, spielen.

7 References

(!!! INVALID CITATION !!!).

Aaij, C. and Borst, P. (1972): The gel electrophoresis of DNA, Biochim Biophys Acta 269 [2], pp. 192-200.

Adan, R. A. and Gispen, W. H. (2000): Melanocortins and the brain: from effects via receptors to drug targets, Eur J Pharmacol 405 [1-3], pp. 13-24.

Allison, D. B.; Kaprio, J.; Korkeila, M.; Koskenvuo, M.; Neale, M. C. and Hayakawa, K. (1996): The heritability of body mass index among an international sample of monozygotic twins reared apart, Int J Obes Relat Metab Disord 20 [6], pp. 501-6.

Anand, B. K. and Brobeck, J. R. (1951): Hypothalamic control of food intake in rats and cats, Yale J Biol Med 24 [2], pp. 123-40.

Antequera, F. and Bird, A. P. (1988): Unmethylated CpG islands associated with genes in higher plant DNA, EMBO J 7 [8], pp. 2295-9.

Arcot, S. S.; Wang, Z.; Weber, J. L.; Deininger, P. L. and Batzer, M. A. (1995): Alu repeats: a source for the genesis of primate microsatellites, Genomics 29 [1], pp. 136-44.

Babich, V.; Aksenov, N.; Alexeenko, V.; Oei, S. L.; Buchlow, G. and Tomilin, N. (1999): Association of some potential hormone response elements in human genes with the Alu family repeats, Gene 239 [2], pp. 341-9.

Bagnol, D. (2004): G protein-coupled receptors in hypothalamic circuits involved in metabolic diseases, Curr Opin Drug Discov Devel 7 [5], pp. 665-82.

Baker, J. L.; Olsen, L. W. and Sorensen, T. I. (2007): Childhood body-mass index and the risk of coronary heart disease in adulthood, N Engl J Med 357 [23], pp. 2329-37.

Ball, M. P.; Li, J. B.; Gao, Y.; Lee, J. H.; LeProust, E. M.; Park, I. H.; Xie, B.; Daley, G. Q. and Church, G. M. (2009): Targeted and genome-scale strategies reveal gene-body methylation signatures in human cells, Nat Biotechnol 27 [4], pp. 361-8.

Barker, D. J. (2004): The developmental origins of adult disease, J Am Coll Nutr 23 [6 Suppl], pp. 588S-595S.

Barsh, G. S.; Farooqi, I. S. and O'Rahilly, S. (2000): Genetics of body-weight regulation, Nature 404 [6778], pp. 644-51.

Bartel, D. P. (2004): MicroRNAs: genomics, biogenesis, mechanism, and function, Cell 116 [2], pp. 281-97.

Batzer, M. A. and Deininger, P. L. (1991): A human-specific subfamily of Alu sequences, Genomics 9 [3], pp. 481-7.

Batzer, M. A. and Deininger, P. L. (2002): Alu repeats and human genomic diversity, Nat Rev Genet 3 [5], pp. 370-9.

Batzer, M. A.; Deininger, P. L.; Hellmann-Blumberg, U.; Jurka, J.; Labuda, D.; Rubin, C. M.; Schmid, C. W.; Zietkiewicz, E. and Zuckerkandl, E. (1996): Standardized nomenclature for Alu repeats, J Mol Evol 42 [1], pp. 3-6.

Beales, P. L. (2010): Obesity in single gene disorders, Prog Mol Biol Transl Sci 94, pp. 125-57.

Belancio, V. P.; Hedges, D. J. and Deininger, P. (2008): Mammalian non-LTR retrotransposons: for better or worse, in sickness and in health, Genome Res 18 [3], pp. 343-58.

Bennett, E. A.; Coleman, L. E.; Tsui, C.; Pittard, W. S. and Devine, S. E. (2004): Natural genetic variation caused by transposable elements in humans, Genetics 168 [2], pp. 933-51.

Bennett, E. A.; Keller, H.; Mills, R. E.; Schmidt, S.; Moran, J. V.; Weichenrieder, O. and Devine, S. E. (2008): Active Alu retrotransposons in the human genome, Genome Res 18 [12], pp. 1875-83.

Berdasco, M. and Esteller, M. (2010): Aberrant epigenetic landscape in cancer: how cellular identity goes awry, Dev Cell 19 [5], pp. 698-711.

Bertagna, X. (1994): Proopiomelanocortin-derived peptides, Endocrinol Metab Clin North Am 23 [3], pp. 467-85.

Bestor, T. H. (2000): The DNA methyltransferases of mammals, Hum Mol Genet 9 [16], pp. 2395-402.

Bestor, T.; Laudano, A.; Mattaliano, R. and Ingram, V. (1988): Cloning and sequencing of a cDNA encoding DNA methyltransferase of mouse cells. The carboxyl-terminal domain of the mammalian enzymes is related to bacterial restriction methyltransferases, J Mol Biol 203 [4], pp. 971-83.

Betz, N. and Strader, T. (2002): Wizard® SV Gel and PCR Clean-Up System, Promega Notes 82, pp. 2 - 5.

Biemont, C. and Vieira, C. (2006): Genetics: junk DNA as an evolutionary force, Nature 443 [7111], pp. 521-4.

Bird, A. (2002): DNA methylation patterns and epigenetic memory, Genes Dev 16 [1], pp. 6-21.

Bird, A. (2007): Perceptions of epigenetics, Nature 447 [7143], pp. 396-8.

Bird, A. P. (1980): DNA methylation and the frequency of CpG in animal DNA, Nucleic Acids Res 8 [7], pp. 1499-504.

Biro, F. M. and Wien, M. (2010): Childhood obesity and adult morbidities, Am J Clin Nutr 91 [5], pp. 1499S-1505S.

Bjornsson, H. T.; Sigurdsson, M. I.; Fallin, M. D.; Irizarry, R. A.; Aspelund, T.; Cui, H.; Yu, W.; Rongione, M. A.; Ekstrom, T. J.; Harris, T. B.; Launer, L. J.; Eiriksdottir, G.; Leppert, M. F.; Sapienza, C.; Gudnason, V. and Feinberg, A. P. (2008): Intra-individual change over time in DNA methylation with familial clustering, JAMA 299 [24], pp. 2877-83.

Bjornsson, Hans T.; Daniele Fallin, M. and Feinberg, Andrew P. (2004): An integrated epigenetic and genetic approach to common human disease, Trends in Genetics 20 [8], pp. 350-358. URL: http://www.sciencedirect.com/science/article/B6TCY-4CP6B5F-3/2/6636d9039fff18517a007b29d9e5a014

Boks, M. P.; Derks, E. M.; Weisenberger, D. J.; Strengman, E.; Janson, E.; Sommer, I. E.; Kahn, R. S. and Ophoff, R. A. (2009): The relationship of DNA methylation with age, gender and genotype in twins and healthy controls, PLoS One 4 [8], p. e6767.

Bolden, A. H.; Nalin, C. M.; Ward, C. A.; Poonian, M. S.; McComas, W. W. and Weissbach, A. (1985): DNA methylation: sequences flanking C-G pairs modulate the specificity of the human DNA methylase, Nucleic Acids Res 13 [10], pp. 3479-94.

Bolden, A. H.; Nalin, C. M.; Ward, C. A.; Poonian, M. S. and Weissbach, A. (1986): Primary DNA sequence determines sites of maintenance and de novo methylation by mammalian DNA methyltransferases, Mol Cell Biol 6 [4], pp. 1135-40.

Bollati, V.; Schwartz, J.; Wright, R.; Litonjua, A.; Tarantini, L.; Suh, H.; Sparrow, D.; Vokonas, P. and Baccarelli, A. (2009): Decline in genomic DNA methylation through aging in a cohort of elderly subjects, Mech Ageing Dev 130 [4], pp. 234-9.

Borchert, G. M.; Lanier, W. and Davidson, B. L. (2006): RNA polymerase III transcribes human microRNAs, Nat Struct Mol Biol 13 [12], pp. 1097-101.

Borgel, J.; Guibert, S.; Li, Y.; Chiba, H.; Schubeler, D.; Sasaki, H.; Forne, T. and Weber, M. (2010): Targets and dynamics of promoter DNA methylation during early mouse development, Nat Genet 42 [12], pp. 1093-100.

Boston, B. A.; Blaydon, K. M.; Varnerin, J. and Cone, R. D. (1997): Independent and additive effects of central POMC and leptin pathways on murine obesity, Science 278 [5343], pp. 1641-4.

Bouchard, C. (2009): Childhood obesity: are genetic differences involved?, Am J Clin Nutr 89 [5], pp. 1494S-1501S.

Boyes, J. and Bird, A. (1992): Repression of genes by DNA methylation depends on CpG density and promoter strength: evidence for involvement of a methyl-CpG binding protein, EMBO J 11 [1], pp. 327-33.

Braman, J.; Papworth, C. and Greener, A. (1996): Site-directed mutagenesis using double-stranded plasmid DNA templates, Methods Mol Biol 57, pp. 31-44.

Britten, R. J. (1996): DNA sequence insertion and evolutionary variation in gene regulation, Proc Natl Acad Sci U S A 93 [18], pp. 9374-7.

Buttinelli, M.; Negri, R.; Di Marcotullio, L. and Di Mauro, E. (1995): Changing nucleosome positions through modification of the DNA rotational information, Proc Natl Acad Sci U S A 92 [23], pp. 10747-51.

Campion, J.; Milagro, F. I. and Martinez, J. A. (2009): Individuality and epigenetics in obesity, Obes Rev 10 [4], pp. 383-92.

Cedar, H. (1988): DNA methylation and gene activity, Cell 53 [1], pp. 3-4.

Chae, J. J.; Park, Y. B.; Kim, S. H.; Hong, S. S.; Song, G. J.; Han, K. H.; Namkoong, Y.; Kim, H. S. and Lee, C. C. (1997): Two partial deletion mutations involving the same Alu sequence within intron 8 of the LDL receptor gene in Korean patients with familial hypercholesterolemia, Hum Genet 99 [2], pp. 155-63.

Challis, B. G.; Pritchard, L. E.; Creemers, J. W.; Delplanque, J.; Keogh, J. M.; Luan, J.; Wareham, N. J.; Yeo, G. S.; Bhattacharyya, S.; Froguel, P.; White, A.; Farooqi, I. S. and O'Rahilly, S. (2002): A missense mutation disrupting a dibasic prohormone processing site in pro-opiomelanocortin (POMC) increases susceptibility to early-onset obesity through a novel molecular mechanism, Hum Mol Genet 11 [17], pp. 1997-2004.

Chan, R. S. and Woo, J. (2010): Prevention of overweight and obesity: how effective is the current public health approach, Int J Environ Res Public Health 7 [3], pp. 765-83.

Chang, A. C.; Cochet, M. and Cohen, S. N. (1980): Structural organization of human genomic DNA encoding the pro-opiomelanocortin peptide, Proc Natl Acad Sci U S A 77 [8], pp. 4890-4. URL: http://www.ncbi.nlm.nih.gov/entrez/query.fcgi?cmd=Retrieve&db=PubMed&dopt=Citation&list_uids=6254047

Chen, L. L.; DeCerbo, J. N. and Carmichael, G. G. (2008): Alu element-mediated gene silencing, EMBO J 27 [12], pp. 1694-705.

Chimpanzee-Sequencing-and-Analysis-Consortium (2005): Initial sequence of the chimpanzee genome and comparison with the human genome, Nature 437 [7055], pp. 69-87.

Choy, M. K.; Movassagh, M.; Goh, H. G.; Bennett, M. R.; Down, T. A. and Foo, R. S. (2010): Genome-wide conserved consensus transcription factor binding motifs are hyper-methylated, BMC Genomics 11, p. 519.

Christensen, B. C.; Houseman, E. A.; Marsit, C. J.; Zheng, S.; Wrensch, M. R.; Wiemels, J. L.; Nelson, H. H.; Karagas, M. R.; Padbury, J. F.; Bueno, R.; Sugarbaker, D. J.; Yeh, R. F.; Wiencke, J. K. and Kelsey, K. T. (2009): Aging and environmental exposures alter tissue-specific DNA methylation dependent upon CpG island context, PLoS Genet 5 [8], p. e1000602.

Clark, A. J.; Lavender, P. M.; Coates, P.; Johnson, M. R. and Rees, L. H. (1990): In vitro and in vivo analysis of the processing and fate of the peptide products of the short proopiomelanocortin mRNA, Mol Endocrinol 4 [11], pp. 1737-43.

Clark, S. J.; Statham, A.; Stirzaker, C.; Molloy, P. L. and Frommer, M. (2006): DNA methylation: bisulphite modification and analysis, Nat Protoc 1 [5], pp. 2353-64.

Cobiac, L. (2007): Epigenomics and nutrition, Forum Nutr 60, pp. 31-41.

Cohen, S. N.; Chang, A. C. and Hsu, L. (1972): Nonchromosomal antibiotic resistance in bacteria: genetic transformation of Escherichia coli by R-factor DNA, Proc Natl Acad Sci U S A 69 [8], pp. 2110-4.

Coll, A. P.; Farooqi, I. S.; Challis, B. G.; Yeo, G. S. and O'Rahilly, S. (2004): Proopiomelanocortin and energy balance: insights from human and murine genetics, J Clin Endocrinol Metab 89 [6], pp. 2557-62.

Coll, A. P.; Farooqi, I. S. and O'Rahilly, S. (2007): The hormonal control of food intake, Cell 129 [2], pp. 251-62.

Cone, R. D. (2005): Anatomy and regulation of the central melanocortin system, Nat Neurosci 8 [5], pp. 571-8.

Cone, R. D.; Lu, D.; Koppula, S.; Vage, D. I.; Klungland, H.; Boston, B.; Chen, W.; Orth, D. N.; Pouton, C. and Kesterson, R. A. (1996): The melanocortin receptors: agonists, antagonists, and the hormonal control of pigmentation, Recent Prog Horm Res 51, pp. 287-317; discussion 318.

Considine, R. V.; Sinha, M. K.; Heiman, M. L.; Kriauciunas, A.; Stephens, T. W.; Nyce, M. R.; Ohannesian, J. P.; Marco, C. C.; McKee, L. J.; Bauer, T. L. and et al. (1996): Serum immunoreactive-leptin concentrations in normal-weight and obese humans, N Engl J Med 334 [5], pp. 292-5.

Cordaux, R. and Batzer, M. A. (2009): The impact of retrotransposons on human genome evolution, Nat Rev Genet 10 [10], pp. 691-703.

Cordaux, R.; Hedges, D. J.; Herke, S. W. and Batzer, M. A. (2006): Estimating the retrotransposition rate of human Alu elements, Gene 373, pp. 134-7.

Costello, J. F. and Plass, C. (2001): Methylation matters, J Med Genet 38 [5], pp. 285-303.

Cummings, D. E. and Schwartz, M. W. (2003): Genetics and pathophysiology of human obesity, Annu Rev Med 54, pp. 453-71. URL: http://www.ncbi.nlm.nih.gov/entrez/query.fcgi?cmd=Retrieve&db=PubMed&dopt=Citation&list_uids=12414915

de Souza, F. S.; Santangelo, A. M.; Bumaschny, V.; Avale, M. E.; Smart, J. L.; Low, M. J. and Rubinstein, M. (2005): Identification of neuronal enhancers of the proopiomelanocortin gene by transgenic mouse analysis and phylogenetic footprinting, Mol Cell Biol 25 [8], pp. 3076-86.

Dean, W.; Santos, F. and Reik, W. (2003): Epigenetic reprogramming in early mammalian development and following somatic nuclear transfer, Semin Cell Dev Biol 14 [1], pp. 93-100.

Deininger, P. L. and Batzer, M. A. (1999): Alu repeats and human disease, Mol Genet Metab 67 [3], pp. 183-93.

Deininger, P. L.; Moran, J. V.; Batzer, M. A. and Kazazian, H. H., Jr. (2003): Mobile elements and mammalian genome evolution, Curr Opin Genet Dev 13 [6], pp. 651-8.

Dewannieux, M.; Esnault, C. and Heidmann, T. (2003): LINE-mediated retrotransposition of marked Alu sequences, Nat Genet 35 [1], pp. 41-8.

Dickson, J.; Gowher, H.; Strogantsev, R.; Gaszner, M.; Hair, A.; Felsenfeld, G. and West, A. G. (2010): VEZF1 elements mediate protection from DNA methylation, PLoS Genet 6 [1], p. e1000804.

Dolinoy, D. C.; Weidman, J. R.; Waterland, R. A. and Jirtle, R. L. (2006): Maternal genistein alters coat color and protects Avy mouse offspring from obesity by modifying the fetal epigenome, Environ Health Perspect 114 [4], pp. 567-72.

Dores, R. M. and Baron, A. J. (2011): Evolution of POMC: origin, phylogeny, posttranslational processing, and the melanocortins, Ann N Y Acad Sci 1220 [1], pp. 34-48.

Drewnowski, A. (2009): Obesity, diets, and social inequalities, Nutr Rev 67 Suppl 1, pp. S36-9.

Duhl, D. M.; Vrieling, H.; Miller, K. A.; Wolff, G. L. and Barsh, G. S. (1994): Neomorphic agouti mutations in obese yellow mice, Nat Genet 8 [1], pp. 59-65.

Duret, L. and Galtier, N. (2000): The covariation between TpA deficiency, CpG deficiency, and G+C content of human isochores is due to a mathematical artifact, Mol Biol Evol 17 [11], pp. 1620-5.

Ebbeling, C. B.; Pawlak, D. B. and Ludwig, D. S. (2002): Childhood obesity: public-health crisis, common sense cure, Lancet 360 [9331], pp. 473-82.

Eberwine, J. H. and Roberts, J. L. (1983): Analysis of pro-opiomelancortin gene structure and function, DNA 2 [1], pp. 1-8.

Eckhardt, F.; Lewin, J.; Cortese, R.; Rakyan, V. K.; Attwood, J.; Burger, M.; Burton, J.; Cox, T. V.; Davies, R.; Down, T. A.; Haefliger, C.; Horton, R.; Howe, K.; Jackson, D. K.; Kunde, J.; Koenig, C.; Liddle, J.; Niblett, D.; Otto, T.; Pettett, R.; Seemann, S.; Thompson, C.; West, T.; Rogers, J.; Olek, A.; Berlin, K. and Beck, S. (2006): DNA methylation profiling of human chromosomes 6, 20 and 22, Nat Genet 38 [12], pp. 1378-85. URL: http://www.ncbi.nlm.nih.gov/entrez/query.fcgi?cmd=Retrieve&db=PubMed&dopt=Citation&list_uids=17072317

Ehrlich, S.; Weiss, D.; Burghardt, R.; Infante-Duarte, C.; Brockhaus, S.; Muschler, M. A.; Bleich, S.; Lehmkuhl, U. and Frieling, H. (2010): Promoter specific DNA methylation and gene expression of POMC in acutely underweight and recovered patients with anorexia nervosa, J Psychiatr Res 44 [13], pp. 827-33.

Elkabes, S.; Loh, Y. P.; Nieburgs, A. and Wray, S. (1989): Prenatal ontogenesis of pro-opiomelanocortin in the mouse central nervous system and pituitary gland: an in situ hybridization and immunocytochemical study, Brain Res Dev Brain Res 46 [1], pp. 85-95.

Englander, E. W. and Howard, B. H. (1995): Nucleosome positioning by human Alu elements in chromatin, J Biol Chem 270 [17], pp. 10091-6.

Englander, E. W.; Wolffe, A. P. and Howard, B. H. (1993): Nucleosome interactions with a human Alu element. Transcriptional repression and effects of template methylation, J Biol Chem 268 [26], pp. 19565-73.

Erlich, H. A. (1989): Polymerase chain reaction, J Clin Immunol 9 [6], pp. 437-47.

Esteller, M. (2005): Aberrant DNA methylation as a cancer-inducing mechanism, Annu Rev Pharmacol Toxicol 45, pp. 629-56.

Farias, M. M.; Cuevas, A. M. and Rodriguez, F. (2010): Set-Point Theory and Obesity, Metab Syndr Relat Disord.

Farooqi, I. S.; Drop, S.; Clements, A.; Keogh, J. M.; Biernacka, J.; Lowenbein, S.; Challis, B. G. and O'Rahilly, S. (2006): Heterozygosity for a POMC-null mutation and increased obesity risk in humans, Diabetes 55 [9], pp. 2549-53.

Farooqi, I. S.; Keogh, J. M.; Yeo, G. S.; Lank, E. J.; Cheetham, T. and O'Rahilly, S. (2003): Clinical spectrum of obesity and mutations in the melanocortin 4 receptor gene, N Engl J Med 348 [12], pp. 1085-95.

Faulkner, G. J.; Kimura, Y.; Daub, C. O.; Wani, S.; Plessy, C.; Irvine, K. M.; Schroder, K.; Cloonan, N.; Steptoe, A. L.; Lassmann, T.; Waki, K.; Hornig, N.; Arakawa, T.; Takahashi, H.; Kawai, J.; Forrest, A. R.; Suzuki, H.; Hayashizaki, Y.; Hume, D. A.; Orlando, V.; Grimmond, S. M. and Carninci, P. (2009): The regulated retrotransposon transcriptome of mammalian cells, Nat Genet 41 [5], pp. 563-71.

Feinberg, A. P.; Irizarry, R. A.; Fradin, D.; Aryee, M. J.; Murakami, P.; Aspelund, T.; Eiriksdottir, G.; Harris, T. B.; Launer, L.; Gudnason, V. and Fallin, M. D. (2010): Personalized epigenomic signatures that are stable over time and covary with body mass index, Sci Transl Med 2 [49], p. 49ra67.

Feinberg, A. P. and Tycko, B. (2004): The history of cancer epigenetics, Nat Rev Cancer 4 [2], pp. 143-53.

Feng, S.; Cokus, S. J.; Zhang, X.; Chen, P. Y.; Bostick, M.; Goll, M. G.; Hetzel, J.; Jain, J.; Strauss, S. H.; Halpern, M. E.; Ukomadu, C.; Sadler, K. C.; Pradhan, S.; Pellegrini, M. and Jacobsen, S. E. (2010): Conservation and divergence of methylation patterning in plants and animals, Proc Natl Acad Sci U S A 107 [19], pp. 8689-94.

Flanagan, J. M. and Wild, L. (2007): An epigenetic role for noncoding RNAs and intragenic DNA methylation, Genome Biol 8 [6], p. 307.

Fraga, Mario F.; Ballestar, Esteban; Paz, Maria F.; Ropero, Santiago; Setien, Fernando; Ballestar, Maria L.; Heine-SuÃ±er, Damia; Cigudosa, Juan C.; Urioste, Miguel; Benitez, Javier; Boix-Chornet, Manuel; Sanchez-Aguilera, Abel; Ling, Charlotte; Carlsson, Emma; Poulsen, Pernille; Vaag, Allan; Stephan, Zarko; Spector, Tim D.; Wu, Yue-Zhong; Plass, Christoph and Esteller, Manel (2005): Epigenetic differences arise during the lifetime of monozygotic twins, Proceedings of the National Academy of Sciences of the United States of America 102 [30], pp. 10604-10609. URL: http://www.pnas.org/content/102/30/10604.abstract

Frommer, M.; McDonald, L. E.; Millar, D. S.; Collis, C. M.; Watt, F.; Grigg, G. W.; Molloy, P. L. and Paul, C. L. (1992): A genomic sequencing protocol that yields a positive display of 5-methylcytosine residues in individual DNA strands, Proc Natl Acad Sci U S A 89 [5], pp. 1827-31.

Fuke, C.; Shimabukuro, M.; Petronis, A.; Sugimoto, J.; Oda, T.; Miura, K.; Miyazaki, T.; Ogura, C.; Okazaki, Y. and Jinno, Y. (2004): Age related changes in 5-methylcytosine content in human peripheral leukocytes and placentas: an HPLC-based study, Ann Hum Genet 68 [Pt 3], pp. 196-204.

Fullwood, M. J.; Han, Y.; Wei, C. L.; Ruan, X. and Ruan, Y. (2010): Chromatin interaction analysis using paired-end tag sequencing, Curr Protoc Mol Biol Chapter 21, pp. Unit 21 15 1-25.

Fullwood, M. J. and Ruan, Y. (2009): ChIP-based methods for the identification of long-range chromatin interactions, J Cell Biochem 107 [1], pp. 30-9.

Gal-Mark, N.; Schwartz, S. and Ast, G. (2008): Alternative splicing of Alu exons--two arms are better than one, Nucleic Acids Res 36 [6], pp. 2012-23.

Gardiner-Garden, M. and Frommer, M. (1987): CpG islands in vertebrate genomes, J Mol Biol 196 [2], pp. 261-82.

Gardiner-Garden, M. and Frommer, M. (1994): Transcripts and CpG islands associated with the pro-opiomelanocortin gene and other neurally expressed genes, J Mol Endocrinol 12 [3], pp. 365-82. URL: http://www.ncbi.nlm.nih.gov/entrez/query.fcgi?cmd=Retrieve&db=PubMed&dopt=Citation&list_uids=7916974

Gluckman, P. D.; Hanson, M. A. and Beedle, A. S. (2007): Early life events and their consequences for later disease: a life history and evolutionary perspective, Am J Hum Biol 19 [1], pp. 1-19.

Godfrey, K. M.; Lillycrop, K. A.; Burdge, G. C.; Gluckman, P. D. and Hanson, M. A. (2007): Epigenetic mechanisms and the mismatch concept of the developmental origins of health and disease, Pediatr Res 61 [5 Pt 2], pp. 5R-10R.

Goll, M. G. and Bestor, T. H. (2005): Eukaryotic cytosine methyltransferases, Annu Rev Biochem 74, pp. 481-514.

Goll, M. G.; Kirpekar, F.; Maggert, K. A.; Yoder, J. A.; Hsieh, C. L.; Zhang, X.; Golic, K. G.; Jacobsen, S. E. and Bestor, T. H. (2006): Methylation of tRNAAsp by the DNA methyltransferase homolog Dnmt2, Science 311 [5759], pp. 395-8.

Gondor, A. and Ohlsson, R. (2009): Chromosome crosstalk in three dimensions, Nature 461 [7261], pp. 212-7.

Goodman, M. (1999): The genomic record of Humankind's evolutionary roots, Am J Hum Genet 64 [1], pp. 31-9.

Goyal, R.; Reinhardt, R. and Jeltsch, A. (2006): Accuracy of DNA methylation pattern preservation by the Dnmt1 methyltransferase, Nucleic Acids Res 34 [4], pp. 1182-8.

Graff, J. R.; Herman, J. G.; Myohanen, S.; Baylin, S. B. and Vertino, P. M. (1997): Mapping patterns of CpG island methylation in normal and neoplastic cells implicates both upstream and downstream regions in de novo methylation, J Biol Chem 272 [35], pp. 22322-9.

Greally, J. M. (2002): Short interspersed transposable elements (SINEs) are excluded from imprinted regions in the human genome, Proc Natl Acad Sci U S A 99 [1], pp. 327-32.

Haber, N.; Stengel, D.; Defer, N.; Roeckel, N.; Mattei, M. G. and Hanoune, J. (1994): Chromosomal mapping of human adenylyl cyclase genes type III, type V and type VI, Hum Genet 94 [1], pp. 69-73.

Hadley, M. E.; Hruby, V. J.; Blanchard, J.; Dorr, R. T.; Levine, N.; Dawson, B. V.; al-Obeidi, F. and Sawyer, T. K. (1998): Discovery and development of novel melanogenic drugs. Melanotan-I and -II, Pharm Biotechnol 11, pp. 575-95.

Hajkova, P.; Erhardt, S.; Lane, N.; Haaf, T.; El-Maarri, O.; Reik, W.; Walter, J. and Surani, M. A. (2002): Epigenetic reprogramming in mouse primordial germ cells, Mech Dev 117 [1-2], pp. 15-23.

Han, L.; Lin, I. G. and Hsieh, C. L. (2001): Protein binding protects sites on stable episomes and in the chromosome from de novo methylation, Mol Cell Biol 21 [10], pp. 3416-24.

Hansen, R. S. and Gartler, S. M. (1990): 5-Azacytidine-induced reactivation of the human X chromosome-linked PGK1 gene is associated with a large region of cytosine demethylation in the 5' CpG island, Proc Natl Acad Sci U S A 87 [11], pp. 4174-8.

Harris, L. C.; Remack, J. S. and Brent, T. P. (1994): In vitro methylation of the human O6-methylguanine-DNA methyltransferase promoter reduces transcription, Biochim Biophys Acta 1217 [2], pp. 141-6.

Harris, R. B. and Martin, R. J. (1984): Recovery of body weight from below "set point" in mature female rats, J Nutr 114 [6], pp. 1143-50.

Hasler, J. and Strub, K. (2006): Alu elements as regulators of gene expression, Nucleic Acids Res 34 [19], pp. 5491-7.

Hedges, D. J.; Callinan, P. A.; Cordaux, R.; Xing, J.; Barnes, E. and Batzer, M. A. (2004): Differential alu mobilization and polymorphism among the human and chimpanzee lineages, Genome Res 14 [6], pp. 1068-75.

Heijmans, B. T.; Kremer, D.; Tobi, E. W.; Boomsma, D. I. and Slagboom, P. E. (2007): Heritable rather than age-related environmental and stochastic factors dominate variation in DNA methylation of the human IGF2/H19 locus, Hum Mol Genet 16 [5], pp. 547-54.

Heijmans, B. T.; Tobi, E. W.; Stein, A. D.; Putter, H.; Blauw, G. J.; Susser, E. S.; Slagboom, P. E. and Lumey, L. H. (2008): Persistent epigenetic differences associated with prenatal exposure to famine in humans, Proc Natl Acad Sci U S A 105 [44], pp. 17046-9.

Hellmann-Blumberg, U.; Hintz, M. F.; Gatewood, J. M. and Schmid, C. W. (1993): Developmental differences in methylation of human Alu repeats, Mol Cell Biol 13 [8], pp. 4523-30.

Henry, J.B (2001): Clinical Diagnosis and Management by Laboratory Methods, 20th. ed., W.B. Saunders Company, ISBN: 978-0721688640.

Hetherington, A. W. and Ranson, S. W. (1940): Hypothalamic lesions and adiposity in the rat, The Anatomical Record 78 [2], pp. 149-172. URL: http://dx.doi.org/10.1002/ar.1090780203

Holler, M.; Westin, G.; Jiricny, J. and Schaffner, W. (1988): Sp1 transcription factor binds DNA and activates transcription even when the binding site is CpG methylated, Genes Dev 2 [9], pp. 1127-35.

Holliday, R. and Pugh, J. E. (1975): DNA modification mechanisms and gene activity during development, Science 187 [4173], pp. 226-32.

l'Allemand, D.; Wiegand, S.; Reinehr, T.; Muller, J.; Wabitsch, M.; Widhalm, K. and Holl, R. (2008): Cardiovascular risk in 26,008 European overweight children as established by a multicenter database, Obesity (Silver Spring) 16 [7], pp. 1672-9.

Illingworth, R. S.; Gruenewald-Schneider, U.; Webb, S.; Kerr, A. R.; James, K. D.; Turner, D. J.; Smith, C.; Harrison, D. J.; Andrews, R. and Bird, A. P. (2010): Orphan CpG islands identify numerous conserved promoters in the mammalian genome, PLoS Genet 6 [9].

Invitrogen (2004): One Shot® PIR1 and PIR2 Competent E. coli.

Invitrogen (2006): TOPO TA Cloning® User Manual.

Invitrogen (2010): TRIzol® Reagent Manual.

Jaenisch, R. and Bird, A. (2003): Epigenetic regulation of gene expression: how the genome integrates intrinsic and environmental signals, Nat Genet 33 Suppl, pp. 245-54.

Janecka, J. E.; Miller, W.; Pringle, T. H.; Wiens, F.; Zitzmann, A.; Helgen, K. M.; Springer, M. S. and Murphy, W. J. (2007): Molecular and genomic data identify the closest living relative of primates, Science 318 [5851], pp. 792-4.

Jeannotte, L.; Burbach, J. P. and Drouin, J. (1987): Unusual proopiomelanocortin ribonucleic acids in extrapituitary tissues: intronless transcripts in testes and long poly(A) tails in hypothalamus, Mol Endocrinol 1 [10], pp. 749-57.

Jelinic, P. and Shaw, P. (2007): Loss of imprinting and cancer, J Pathol 211 [3], pp. 261-8.

Jiang, Y. H.; Bressler, J. and Beaudet, A. L. (2004): Epigenetics and human disease, Annu Rev Genomics Hum Genet 5, pp. 479-510.

Jintaridth, P. and Mutirangura, A. (2010): Distinctive patterns of age-dependent hypomethylation in interspersed repetitive sequences, Physiol Genomics.

Jirtle, R. L. and Skinner, M. K. (2007): Environmental epigenomics and disease susceptibility, Nat Rev Genet 8 [4], pp. 253-62.

John, J. (2010): Economic perspectives on pediatric obesity: impact on health care expenditures and cost-effectiveness of preventive interventions, Nestle Nutr Workshop Ser Pediatr Program 66, pp. 111-24.

Jones, P. A. (2002): DNA methylation and cancer, Oncogene 21 [35], pp. 5358-60.

Kaminsky, Z. A.; Tang, T.; Wang, S. C.; Ptak, C.; Oh, G. H.; Wong, A. H.; Feldcamp, L. A.; Virtanen, C.; Halfvarson, J.; Tysk, C.; McRae, A. F.; Visscher, P. M.; Montgomery, G. W.; Gottesman, II; Martin, N. G. and Petronis, A. (2009): DNA methylation profiles in monozygotic and dizygotic twins, Nat Genet 41 [2], pp. 240-5.

Karouzakis, E.; Gay, R. E.; Gay, S. and Neidhart, M. (2009): Epigenetic control in rheumatoid arthritis synovial fibroblasts, Nat Rev Rheumatol 5 [5], pp. 266-72.

Keesey, R. E. and Hirvonen, M. D. (1997): Body weight set-points: determination and adjustment, J Nutr 127 [9], pp. 1875S-1883S.

Kelkar, Y. D.; Tyekucheva, S.; Chiaromonte, F. and Makova, K. D. (2008): The genome-wide determinants of human and chimpanzee microsatellite evolution, Genome Res 18 [1], pp. 30-8.

Khatib, H.; Zaitoun, I. and Kim, E. S. (2007): Comparative analysis of sequence characteristics of imprinted genes in human, mouse, and cattle, Mamm Genome 18 [6-7], pp. 538-47.

Kleinjan, D. A.; Seawright, A.; Childs, A. J. and van Heyningen, V. (2004): Conserved elements in Pax6 intron 7 involved in (auto)regulation and alternative transcription, Dev Biol 265 [2], pp. 462-77.

Klug, M. and Rehli, M. (2006): Functional analysis of promoter CpG methylation using a CpG-free luciferase reporter vector, Epigenetics 1 [3], pp. 127-30.

Knoll, J. H.; Nicholls, R. D.; Magenis, R. E.; Graham, J. M., Jr.; Lalande, M. and Latt, S. A. (1989): Angelman and Prader-Willi syndromes share a common chromosome 15 deletion but differ in parental origin of the deletion, Am J Med Genet 32 [2], pp. 285-90.

Kochanek, S.; Renz, D. and Doerfler, W. (1993): DNA methylation in the Alu sequences of diploid and haploid primary human cells, EMBO J 12 [3], pp. 1141-51.

Kopelman, P. G. (2000): Obesity as a medical problem, Nature 404 [6778], pp. 635-43.

Kramerov, D. A. and Vassetzky, N. S. (2005): Short retroposons in eukaryotic genomes, Int Rev Cytol 247, pp. 165-221.

Krayev, A. S.; Kramerov, D. A.; Skryabin, K. G.; Ryskov, A. P.; Bayev, A. A. and Georgiev, G. P. (1980): The nucleotide sequence of the ubiquitous repetitive DNA sequence B1

complementary to the most abundant class of mouse fold-back RNA, Nucleic Acids Res 8 [6], pp. 1201-15.

Kriegs, J. O.; Churakov, G.; Jurka, J.; Brosius, J. and Schmitz, J. (2007): Evolutionary history of 7SL RNA-derived SINEs in Supraprimates, Trends Genet 23 [4], pp. 158-61.

Kromeyer-Hauschild, K., Wabitsch, M., Kunze, D., Geller, F., Geiß, H.C., Hesse, V., von Hippel, A., Jaeger, U., Johnsen, D., Korte, W., Menner, K., Müller, G., Müller, J.M., Niemann-Pilatus, A., Remer, T., Schaefer, F., Wittchen, H.-U., Zabransky, S., Zellner, K., Ziegler, A., Hebebrand, J. (2001): Perzentile für den Body-mass-Index für das Kindes- und Jugendalter unter Heranziehung verschiedener deutscher Stichproben., Monatsschrift für Kinderheilkunde [149], pp. 807–818.

Krude, H.; Biebermann, H.; Luck, W.; Horn, R.; Brabant, G. and Gruters, A. (1998): Severe early-onset obesity, adrenal insufficiency and red hair pigmentation caused by POMC mutations in humans, Nat Genet 19 [2], pp. 155-7.

Krude, H.; Biebermann, H.; Schnabel, D.; Tansek, M. Z.; Theunissen, P.; Mullis, P. E. and Gruters, A. (2003): Obesity due to proopiomelanocortin deficiency: three new cases and treatment trials with thyroid hormone and ACTH4-10, J Clin Endocrinol Metab 88 [10], pp. 4633-40.

Kuehnen, P; Mischke, M; Wiegand, S; Sers, C; Horsthemke, B; Lau, S; Keil, T ; Grueters, A and Krude, H (in revision): An Alu element-triggered CpG methylation polymorphism of the POMC gene is associated with childhood obesity, PLoS Genetics.

Kurth, B.M. and Schaffrath Rosario, A. (2007): The prevalence of overweight and obese children and adolescents living in Germany. Results of the German Health Interview and Examination Survey for Children and Adolescents (KiGGS). , Bundesgesundheitsblatt Gesundheitsforschung Gesundheitsschutz. (5-6) [50], pp. 736-43.

Kurukuti, S.; Tiwari, V. K.; Tavoosidana, G.; Pugacheva, E.; Murrell, A.; Zhao, Z.; Lobanenkov, V.; Reik, W. and Ohlsson, R. (2006): CTCF binding at the H19 imprinting control region mediates maternally inherited higher-order chromatin conformation to restrict enhancer access to Igf2, Proc Natl Acad Sci U S A 103 [28], pp. 10684-9.

Lacaze-Masmonteil, T.; de Keyzer, Y.; Luton, J. P.; Kahn, A. and Bertagna, X. (1987): Characterization of proopiomelanocortin transcripts in human nonpituitary tissues, Proc Natl Acad Sci U S A 84 [20], pp. 7261-5.

Laird, P. W. and Jaenisch, R. (1996): The role of DNA methylation in cancer genetic and epigenetics, Annu Rev Genet 30, pp. 441-64.

Lanctot, C.; Cheutin, T.; Cremer, M.; Cavalli, G. and Cremer, T. (2007): Dynamic genome architecture in the nuclear space: regulation of gene expression in three dimensions, Nat Rev Genet 8 [2], pp. 104-15.

Lander, E. S.; Linton, L. M.; Birren, B.; Nusbaum, C.; Zody, M. C.; Baldwin, J.; Devon, K.; Dewar, K.; Doyle, M.; FitzHugh, W.; Funke, R.; Gage, D.; Harris, K.; Heaford, A.; Howland, J.; Kann, L.; Lehoczky, J.; LeVine, R.; McEwan, P.; McKernan, K.; Meldrim, J.; Mesirov, J. P.; Miranda, C.; Morris, W.; Naylor, J.; Raymond, C.; Rosetti, M.; Santos, R.; Sheridan, A.; Sougnez, C.; Stange-Thomann, N.; Stojanovic, N.; Subramanian, A.; Wyman, D.; Rogers, J.; Sulston, J.; Ainscough, R.; Beck, S.; Bentley, D.; Burton, J.; Clee, C.; Carter, N.; Coulson, A.; Deadman, R.; Deloukas, P.; Dunham, A.; Dunham, I.; Durbin, R.; French, L.; Grafham, D.; Gregory, S.; Hubbard, T.; Humphray, S.; Hunt, A.; Jones, M.; Lloyd, C.; McMurray, A.; Matthews, L.; Mercer, S.; Milne, S.; Mullikin, J. C.; Mungall, A.; Plumb, R.; Ross, M.; Shownkeen, R.; Sims, S.; Waterston, R. H.; Wilson, R. K.; Hillier, L. W.; McPherson, J. D.; Marra, M. A.; Mardis, E. R.; Fulton, L. A.; Chinwalla, A. T.; Pepin, K. H.; Gish, W. R.; Chissoe, S. L.; Wendl, M. C.; Delehaunty, K. D.; Miner, T. L.; Delehaunty, A.; Kramer, J. B.; Cook, L. L.; Fulton, R. S.; Johnson, D. L.; Minx, P. J.; Clifton, S. W.; Hawkins, T.; Branscomb, E.; Predki, P.; Richardson, P.; Wenning, S.; Slezak, T.; Doggett, N.; Cheng, J. F.; Olsen, A.; Lucas, S.; Elkin, C.; Uberbacher, E.; Frazier, M.; Gibbs, R. A.; Muzny, D. M.; Scherer, S. E.; Bouck, J. B.;

Sodergren, E. J.; Worley, K. C.; Rives, C. M.; Gorrell, J. H.; Metzker, M. L.; Naylor, S. L.; Kucherlapati, R. S.; Nelson, D. L.; Weinstock, G. M.; Sakaki, Y.; Fujiyama, A.; Hattori, M.; Yada, T.; Toyoda, A.; Itoh, T.; Kawagoe, C.; Watanabe, H.; Totoki, Y.; Taylor, T.; Weissenbach, J.; Heilig, R.; Saurin, W.; Artiguenave, F.; Brottier, P.; Bruls, T.; Pelletier, E.; Robert, C.; Wincker, P.; Smith, D. R.; Doucette-Stamm, L.; Rubenfield, M.; Weinstock, K.; Lee, H. M.; Dubois, J.; Rosenthal, A.; Platzer, M.; Nyakatura, G.; Taudien, S.; Rump, A.; Yang, H.; Yu, J.; Wang, J.; Huang, G.; Gu, J.; Hood, L.; Rowen, L.; Madan, A.; Qin, S.; Davis, R. W.; Federspiel, N. A.; Abola, A. P.; Proctor, M. J.; Myers, R. M.; Schmutz, J.; Dickson, M.; Grimwood, J.; Cox, D. R.; Olson, M. V.; Kaul, R.; Shimizu, N.; Kawasaki, K.; Minoshima, S.; Evans, G. A.; Athanasiou, M.; Schultz, R.; Roe, B. A.; Chen, F.; Pan, H.; Ramser, J.; Lehrach, H.; Reinhardt, R.; McCombie, W. R.; de la Bastide, M.; Dedhia, N.; Blocker, H.; Hornischer, K.; Nordsiek, G.; Agarwala, R.; Aravind, L.; Bailey, J. A.; Bateman, A.; Batzoglou, S.; Birney, E.; Bork, P.; Brown, D. G.; Burge, C. B.; Cerutti, L.; Chen, H. C.; Church, D.; Clamp, M.; Copley, R. R.; Doerks, T.; Eddy, S. R.; Eichler, E. E.; Furey, T. S.; Galagan, J.; Gilbert, J. G.; Harmon, C.; Hayashizaki, Y.; Haussler, D.; Hermjakob, H.; Hokamp, K.; Jang, W.; Johnson, L. S.; Jones, T. A.; Kasif, S.; Kaspryzk, A.; Kennedy, S.; Kent, W. J.; Kitts, P.; Koonin, E. V.; Korf, I.; Kulp, D.; Lancet, D.; Lowe, T. M.; McLysaght, A.; Mikkelsen, T.; Moran, J. V.; Mulder, N.; Pollara, V. J.; Ponting, C. P.; Schuler, G.; Schultz, J.; Slater, G.; Smit, A. F.; Stupka, E.; Szustakowski, J.; Thierry-Mieg, D.; Thierry-Mieg, J.; Wagner, L.; Wallis, J.; Wheeler, R.; Williams, A.; Wolf, Y. I.; Wolfe, K. H.; Yang, S. P.; Yeh, R. F.; Collins, F.; Guyer, M. S.; Peterson, J.; Felsenfeld, A.; Wetterstrand, K. A.; Patrinos, A.; Morgan, M. J.; de Jong, P.; Catanese, J. J.; Osoegawa, K.; Shizuya, H.; Choi, S. and Chen, Y. J. (2001): Initial sequencing and analysis of the human genome, Nature 409 [6822], pp. 860-921.

Lane, N.; Dean, W.; Erhardt, S.; Hajkova, P.; Surani, A.; Walter, J. and Reik, W. (2003): Resistance of IAPs to methylation reprogramming may provide a mechanism for epigenetic inheritance in the mouse, Genesis 35 [2], pp. 88-93.

Lee, J.; Inoue, K.; Ono, R.; Ogonuki, N.; Kohda, T.; Kaneko-Ishino, T.; Ogura, A. and Ishino, F. (2002): Erasing genomic imprinting memory in mouse clone embryos produced from day 11.5 primordial germ cells, Development 129 [8], pp. 1807-17.

Lee, J. Y.; Ji, Z. and Tian, B. (2008): Phylogenetic analysis of mRNA polyadenylation sites reveals a role of transposable elements in evolution of the 3'-end of genes, Nucleic Acids Res 36 [17], pp. 5581-90.

Lee, T. F.; Zhai, J. and Meyers, B. C. (2010): Conservation and divergence in eukaryotic DNA methylation, Proc Natl Acad Sci U S A 107 [20], pp. 9027-8.

Lee, Y. S.; Challis, B. G.; Thompson, D. A.; Yeo, G. S.; Keogh, J. M.; Madonna, M. E.; Wraight, V.; Sims, M.; Vatin, V.; Meyre, D.; Shield, J.; Burren, C.; Ibrahim, Z.; Cheetham, T.; Swift, P.; Blackwood, A.; Hung, C. C.; Wareham, N. J.; Froguel, P.; Millhauser, G. L.; O'Rahilly, S. and Farooqi, I. S. (2006): A POMC variant implicates beta-melanocyte-stimulating hormone in the control of human energy balance, Cell Metab 3 [2], pp. 135-40.

Li, E.; Bestor, T. H. and Jaenisch, R. (1992): Targeted mutation of the DNA methyltransferase gene results in embryonic lethality, Cell 69 [6], pp. 915-26.

Li, G.; Fullwood, M. J.; Xu, H.; Mulawadi, F. H.; Velkov, S.; Vega, V.; Ariyaratne, P. N.; Mohamed, Y. B.; Ooi, H. S.; Tennakoon, C.; Wei, C. L.; Ruan, Y. and Sung, W. K. (2010a): ChIA-PET tool for comprehensive chromatin interaction analysis with paired-end tag sequencing, Genome Biol 11 [2], p. R22.

Li, S.; Zhao, J. H.; Luan, J.; Luben, R. N.; Rodwell, S. A.; Khaw, K. T.; Ong, K. K.; Wareham, N. J. and Loos, R. J. (2010b): Cumulative effects and predictive value of common obesity-susceptibility variants identified by genome-wide association studies, Am J Clin Nutr 91 [1], pp. 184-90.

Li, Y.; Zhu, J.; Tian, G.; Li, N.; Li, Q.; Ye, M.; Zheng, H.; Yu, J.; Wu, H.; Sun, J.; Zhang, H.; Chen, Q.; Luo, R.; Chen, M.; He, Y.; Jin, X.; Zhang, Q.; Yu, C.; Zhou, G.; Huang, Y.; Cao, H.; Zhou, X.; Guo, S.; Hu, X.; Li, X.; Kristiansen, K.; Bolund, L.; Xu, J.; Wang, W.; Yang, H.; Wang, J.; Li,

R.; Beck, S. and Zhang, X. (2010c): The DNA methylome of human peripheral blood mononuclear cells, PLoS Biol 8 [11], p. e1000533.

Liu, G. E.; Alkan, C.; Jiang, L.; Zhao, S. and Eichler, E. E. (2009): Comparative analysis of Alu repeats in primate genomes, Genome Res 19 [5], pp. 876-85.

Liu, W. M.; Maraia, R. J.; Rubin, C. M. and Schmid, C. W. (1994): Alu transcripts: cytoplasmic localisation and regulation by DNA methylation, Nucleic Acids Res 22 [6], pp. 1087-95.

Liu, W. M. and Schmid, C. W. (1993): Proposed roles for DNA methylation in Alu transcriptional repression and mutational inactivation, Nucleic Acids Res 21 [6], pp. 1351-9.

Liu, X.; Wang, L.; Zhao, K.; Thompson, P. R.; Hwang, Y.; Marmorstein, R. and Cole, P. A. (2008): The structural basis of protein acetylation by the p300/CBP transcriptional coactivator, Nature 451 [7180], pp. 846-50.

Loos, R. J.; Lindgren, C. M.; Li, S.; Wheeler, E.; Zhao, J. H.; Prokopenko, I.; Inouye, M.; Freathy, R. M.; Attwood, A. P.; Beckmann, J. S.; Berndt, S. I.; Jacobs, K. B.; Chanock, S. J.; Hayes, R. B.; Bergmann, S.; Bennett, A. J.; Bingham, S. A.; Bochud, M.; Brown, M.; Cauchi, S.; Connell, J. M.; Cooper, C.; Smith, G. D.; Day, I.; Dina, C.; De, S.; Dermitzakis, E. T.; Doney, A. S.; Elliott, K. S.; Elliott, P.; Evans, D. M.; Sadaf Farooqi, I.; Froguel, P.; Ghori, J.; Groves, C. J.; Gwilliam, R.; Hadley, D.; Hall, A. S.; Hattersley, A. T.; Hebebrand, J.; Heid, I. M.; Lamina, C.; Gieger, C.; Illig, T.; Meitinger, T.; Wichmann, H. E.; Herrera, B.; Hinney, A.; Hunt, S. E.; Jarvelin, M. R.; Johnson, T.; Jolley, J. D.; Karpe, F.; Keniry, A.; Khaw, K. T.; Luben, R. N.; Mangino, M.; Marchini, J.; McArdle, W. L.; McGinnis, R.; Meyre, D.; Munroe, P. B.; Morris, A. D.; Ness, A. R.; Neville, M. J.; Nica, A. C.; Ong, K. K.; O'Rahilly, S.; Owen, K. R.; Palmer, C. N.; Papadakis, K.; Potter, S.; Pouta, A.; Qi, L.; Randall, J. C.; Rayner, N. W.; Ring, S. M.; Sandhu, M. S.; Scherag, A.; Sims, M. A.; Song, K.; Soranzo, N.; Speliotes, E. K.; Syddall, H. E.; Teichmann, S. A.; Timpson, N. J.; Tobias, J. H.; Uda, M.; Vogel, C. I.; Wallace, C.; Waterworth, D. M.; Weedon, M. N.; Willer, C. J.; Wraight; Yuan, X.; Zeggini, E.; Hirschhorn, J. N.; Strachan, D. P.; Ouwehand, W. H.; Caulfield, M. J.; Samani, N. J.; Frayling, T. M.; Vollenweider, P.; Waeber, G.; Mooser, V.; Deloukas, P.; McCarthy, M. I.; Wareham, N. J.; Barroso, I.; Jacobs, K. B.; Chanock, S. J.; Hayes, R. B.; Lamina, C.; Gieger, C.; Illig, T.; Meitinger, T.; Wichmann, H. E.; Kraft, P.; Hankinson, S. E.; Hunter, D. J.; Hu, F. B.; Lyon, H. N.; Voight, B. F.; Ridderstrale, M.; Groop, L.; Scheet, P.; Sanna, S.; Abecasis, G. R.; Albai, G.; Nagaraja, R.; Schlessinger, D.; Jackson, A. U.; Tuomilehto, J.; Collins, F. S.; Boehnke, M. and Mohlke, K. L. (2008): Common variants near MC4R are associated with fat mass, weight and risk of obesity, Nat Genet 40 [6], pp. 768-75.

Lorincz, M. C.; Dickerson, D. R.; Schmitt, M. and Groudine, M. (2004): Intragenic DNA methylation alters chromatin structure and elongation efficiency in mammalian cells, Nat Struct Mol Biol 11 [11], pp. 1068-75.

Lundberg, K. S.; Shoemaker, D. D.; Adams, M. W.; Short, J. M.; Sorge, J. A. and Mathur, E. J. (1991): High-fidelity amplification using a thermostable DNA polymerase isolated from Pyrococcus furiosus, Gene 108 [1], pp. 1-6.

MachereyNagel (2010): Plasmid DNA Purification - NucleoBond® Xtra Midi/Maxi User Manual.

Macleod, D.; Ali, R. R. and Bird, A. (1998): An alternative promoter in the mouse major histocompatibility complex class II I-Abeta gene: implications for the origin of CpG islands, Mol Cell Biol 18 [8], pp. 4433-43.

Maes, H. H.; Neale, M. C. and Eaves, L. J. (1997): Genetic and environmental factors in relative body weight and human adiposity, Behav Genet 27 [4], pp. 325-51.

Makino, S.; Kaji, R.; Ando, S.; Tomizawa, M.; Yasuno, K.; Goto, S.; Matsumoto, S.; Tabuena, M. D.; Maranon, E.; Dantes, M.; Lee, L. V.; Ogasawara, K.; Tooyama, I.; Akatsu, H.; Nishimura, M. and Tamiya, G. (2007): Reduced neuron-specific expression of the TAF1 gene is associated with X-linked dystonia-parkinsonism, Am J Hum Genet 80 [3], pp. 393-406.

Martin, A.; Troadec, C.; Boualem, A.; Rajab, M.; Fernandez, R.; Morin, H.; Pitrat, M.; Dogimont, C. and Bendahmane, A. (2009): A transposon-induced epigenetic change leads to sex determination in melon, Nature 461 [7267], pp. 1135-8.

Martinowich, K.; Hattori, D.; Wu, H.; Fouse, S.; He, F.; Hu, Y.; Fan, G. and Sun, Y. E. (2003): DNA methylation-related chromatin remodeling in activity-dependent BDNF gene regulation, Science 302 [5646], pp. 890-3.

Maunakea, A. K.; Nagarajan, R. P.; Bilenky, M.; Ballinger, T. J.; D'Souza, C.; Fouse, S. D.; Johnson, B. E.; Hong, C.; Nielsen, C.; Zhao, Y.; Turecki, G.; Delaney, A.; Varhol, R.; Thiessen, N.; Shchors, K.; Heine, V. M.; Rowitch, D. H.; Xing, X.; Fiore, C.; Schillebeeckx, M.; Jones, S. J.; Haussler, D.; Marra, M. A.; Hirst, M.; Wang, T. and Costello, J. F. (2010): Conserved role of intragenic DNA methylation in regulating alternative promoters, Nature 466 [7303], pp. 253-7.

Mauras, N.; Delgiorno, C.; Kollman, C.; Bird, K.; Morgan, M.; Sweeten, S.; Balagopal, P. and Damaso, L. (2010): Obesity without established comorbidities of the metabolic syndrome is associated with a proinflammatory and prothrombotic state, even before the onset of puberty in children, J Clin Endocrinol Metab 95 [3], pp. 1060-8.

Mayer, C. M.; Fick, L. J.; Gingerich, S. and Belsham, D. D. (2009): Hypothalamic cell lines to investigate neuroendocrine control mechanisms, Front Neuroendocrinol 30 [3], pp. 405-23.

Mayer, W.; Niveleau, A.; Walter, J.; Fundele, R. and Haaf, T. (2000): Demethylation of the zygotic paternal genome, Nature 403 [6769], pp. 501-2.

Mellon, P. L.; Windle, J. J.; Goldsmith, P. C.; Padula, C. A.; Roberts, J. L. and Weiner, R. I. (1990): Immortalization of hypothalamic GnRH neurons by genetically targeted tumorigenesis, Neuron 5 [1], pp. 1-10.

Meyer, C. W.; Wagener, A.; Rink, N.; Hantschel, C.; Heldmaier, G.; Klingenspor, M. and Brockmann, G. A. (2009): High energy digestion efficiency and altered lipid metabolism contribute to obesity in BFMI mice, Obesity (Silver Spring) 17 [11], pp. 1988-93.

Miki, Y.; Katagiri, T.; Kasumi, F.; Yoshimoto, T. and Nakamura, Y. (1996): Mutation analysis in the BRCA2 gene in primary breast cancers, Nat Genet 13 [2], pp. 245-7.

Millar, D. S.; Paul, C. L.; Molloy, P. L. and Clark, S. J. (2000): A distinct sequence (ATAAA)n separates methylated and unmethylated domains at the 5'-end of the GSTP1 CpG island, J Biol Chem 275 [32], pp. 24893-9.

Mills, R. E.; Bennett, E. A.; Iskow, R. C. and Devine, S. E. (2007): Which transposable elements are active in the human genome?, Trends Genet 23 [4], pp. 183-91.

Mills, R. E.; Bennett, E. A.; Iskow, R. C.; Luttig, C. T.; Tsui, C.; Pittard, W. S. and Devine, S. E. (2006): Recently mobilized transposons in the human and chimpanzee genomes, Am J Hum Genet 78 [4], pp. 671-9.

Mitalipov, S. and Wolf, D. (2009): Totipotency, pluripotency and nuclear reprogramming, Adv Biochem Eng Biotechnol 114, pp. 185-99.

Mizoguchi, Y.; Kajiume, T.; Miyagawa, S.; Okada, S.; Nishi, Y. and Kobayashi, M. (2007): Steroid-dependent ACTH-produced thymic carcinoid: regulation of POMC gene expression by cortisol via methylation of its promoter region, Horm Res 67 [5], pp. 257-62.

Monk, M.; Boubelik, M. and Lehnert, S. (1987): Temporal and regional changes in DNA methylation in the embryonic, extraembryonic and germ cell lineages during mouse embryo development, Development 99 [3], pp. 371-82.

Morgan, H. D.; Sutherland, H. G.; Martin, D. I. and Whitelaw, E. (1999): Epigenetic inheritance at the agouti locus in the mouse, Nat Genet 23 [3], pp. 314-8. URL:

http://www.ncbi.nlm.nih.gov/entrez/query.fcgi?cmd=Retrieve&db=PubMed&dopt=Citation&list_uids=10545949

Muller-Riemenschneider, F.; Reinhold, T.; Berghofer, A. and Willich, S. N. (2008): Health-economic burden of obesity in Europe, Eur J Epidemiol 23 [8], pp. 499-509.

Mummaneni, P.; Bishop, P. L. and Turker, M. S. (1993): A cis-acting element accounts for a conserved methylation pattern upstream of the mouse adenine phosphoribosyltransferase gene, J Biol Chem 268 [1], pp. 552-8.

Munzberg, H.; Huo, L.; Nillni, E. A.; Hollenberg, A. N. and Bjorbaek, C. (2003): Role of signal transducer and activator of transcription 3 in regulation of hypothalamic proopiomelanocortin gene expression by leptin, Endocrinology 144 [5], pp. 2121-31.

Muratani, K.; Hada, T.; Yamamoto, Y.; Kaneko, T.; Shigeto, Y.; Ohue, T.; Furuyama, J. and Higashino, K. (1991): Inactivation of the cholinesterase gene by Alu insertion: possible mechanism for human gene transposition, Proc Natl Acad Sci U S A 88 [24], pp. 11315-9.

Newell-Price, J. (2003): Proopiomelanocortin gene expression and DNA methylation: implications for Cushing's syndrome and beyond, J Endocrinol 177 [3], pp. 365-72.

Newell-Price, J.; King, P. and Clark, A. J. (2001): The CpG island promoter of the human proopiomelanocortin gene is methylated in nonexpressing normal tissue and tumors and represses expression, Mol Endocrinol 15 [2], pp. 338-48.

Nishihara, H.; Terai, Y. and Okada, N. (2002): Characterization of novel Alu- and tRNA-related SINEs from the tree shrew and evolutionary implications of their origins, Mol Biol Evol 19 [11], pp. 1964-72.

Norris, J.; Fan, D.; Aleman, C.; Marks, J. R.; Futreal, P. A.; Wiseman, R. W.; Iglehart, J. D.; Deininger, P. L. and McDonnell, D. P. (1995): Identification of a new subclass of Alu DNA repeats which can function as estrogen receptor-dependent transcriptional enhancers, J Biol Chem 270 [39], pp. 22777-82.

Notake, M.; Tobimatsu, T.; Watanabe, Y.; Takahashi, H.; Mishina, M. and Numa, S. (1983): Isolation and characterization of the mouse corticotropin-beta-lipotropin precursor gene and a related pseudogene, FEBS Lett 156 [1], pp. 67-71.

Ogryzko, V. V.; Schiltz, R. L.; Russanova, V.; Howard, B. H. and Nakatani, Y. (1996): The transcriptional coactivators p300 and CBP are histone acetyltransferases, Cell 87 [5], pp. 953-9.

Ohneda, K. and Yamamoto, M. (2002): Roles of hematopoietic transcription factors GATA-1 and GATA-2 in the development of red blood cell lineage, Acta Haematol 108 [4], pp. 237-45.

Okano, M.; Bell, D. W.; Haber, D. A. and Li, E. (1999): DNA methyltransferases Dnmt3a and Dnmt3b are essential for de novo methylation and mammalian development, Cell 99 [3], pp. 247-57.

Oldridge, M.; Zackai, E. H.; McDonald-McGinn, D. M.; Iseki, S.; Morriss-Kay, G. M.; Twigg, S. R.; Johnson, D.; Wall, S. A.; Jiang, W.; Theda, C.; Jabs, E. W. and Wilkie, A. O. (1999): De novo alu-element insertions in FGFR2 identify a distinct pathological basis for Apert syndrome, Am J Hum Genet 64 [2], pp. 446-61.

Ollikainen, M.; Smith, K. R.; Joo, E. J.; Ng, H. K.; Andronikos, R.; Novakovic, B.; Abdul Aziz, N. K.; Carlin, J. B.; Morley, R.; Saffery, R. and Craig, J. M. (2010): DNA methylation analysis of multiple tissues from newborn twins reveals both genetic and intrauterine components to variation in the human neonatal epigenome, Hum Mol Genet 19 [21], pp. 4176-88.

Onno, M.; Nakamura, T.; Hillova, J. and Hill, M. (1992): Rearrangement of the human tre oncogene by homologous recombination between Alu repeats of nucleotide sequences from two different chromosomes, Oncogene 7 [12], pp. 2519-23.

Painter, R. C.; Roseboom, T. J. and Bleker, O. P. (2005): Prenatal exposure to the Dutch famine and disease in later life: an overview, Reprod Toxicol 20 [3], pp. 345-52.

Pennings, S.; Allan, J. and Davey, C. S. (2005): DNA methylation, nucleosome formation and positioning, Brief Funct Genomic Proteomic 3 [4], pp. 351-61.

Plagemann, A.; Harder, T.; Brunn, M.; Harder, A.; Roepke, K.; Wittrock-Staar, M.; Ziska, T.; Schellong, K.; Rodekamp, E.; Melchior, K. and Dudenhausen, J. W. (2009): Hypothalamic proopiomelanocortin promoter methylation becomes altered by early overfeeding: an epigenetic model of obesity and the metabolic syndrome, J Physiol 587 [Pt 20], pp. 4963-76.

Ponger, L. and Li, W. H. (2005): Evolutionary diversification of DNA methyltransferases in eukaryotic genomes, Mol Biol Evol 22 [4], pp. 1119-28.

Portela, A. and Esteller, M. (2010): Epigenetic modifications and human disease, Nat Biotechnol 28 [10], pp. 1057-68.

Pritchard, L. E.; Turnbull, A. V. and White, A. (2002): Pro-opiomelanocortin processing in the hypothalamus: impact on melanocortin signalling and obesity, J Endocrinol 172 [3], pp. 411-21.

Promega (2009a): PureYield™ Plasmid Miniprep System Technical Bulletin.

Promega (2009b): Wizard® SV Gel and PCR Clean-Up System technical bulletin, http://www.promega.com/tbs/tb308/tb308.html

Promega (2010a): DNA IQ™ Casework Pro Kit for Maxwell® 16 - Technical Manual Part# TM332. URL: http://www.promega.com/tbs/tm332/tm332.pdf

Promega (2010b): Dual-Luciferase® Reporter Assay System - Technical Manual.

Promega (2010c): Maxwell® 16 DNA Purification Kits - Technical Manual Part# TM284. URL: http://www.promega.com/tbs/tm284/tm284.pdf

QIAGEN (2002): Effectene Transfection Reagent Handbook.

Qiagen (2010): Omniscript® Reverse Transcription Handbook. URL: http://www.qiagen.com/Products/Pcr/QiagenReverseTranscriptases/OmniScriptRT.aspx?r=849

Quentin, Y. (1994): A master sequence related to a free left Alu monomer (FLAM) at the origin of the B1 family in rodent genomes, Nucleic Acids Res 22 [12], pp. 2222-7.

Rakyan, V. K.; Chong, S.; Champ, M. E.; Cuthbert, P. C.; Morgan, H. D.; Luu, K. V. and Whitelaw, E. (2003): Transgenerational inheritance of epigenetic states at the murine Axin(Fu) allele occurs after maternal and paternal transmission, Proc Natl Acad Sci U S A 100 [5], pp. 2538-43.

Ravelli, G. P.; Stein, Z. A. and Susser, M. W. (1976): Obesity in young men after famine exposure in utero and early infancy, N Engl J Med 295 [7], pp. 349-53.

Razin, A. and Cedar, H. (1994): DNA methylation and genomic imprinting, Cell 77 [4], pp. 473-6.

Rees, D. A.; Hepburn, P. J.; McNicol, A. M.; Francis, K.; Jasani, B.; Lewis, M. D.; Farrell, W. E.; Lewis, B. M.; Scanlon, M. F. and Ham, J. (2002): Loss of ACTH expression in cultured human corticotroph macroadenoma cells is consistent with loss of the POMC gene signal sequence, Mol Cell Endocrinol 189 [1-2], pp. 51-7.

Reik, W. (2007): Stability and flexibility of epigenetic gene regulation in mammalian development, Nature 447 [7143], pp. 425-32.

Reik, W.; Dean, W. and Walter, J. (2001): Epigenetic reprogramming in mammalian development, Science 293 [5532], pp. 1089-93.

Reinehr, T. and Wabitsch, M. (2010): Childhood obesity, Curr Opin Lipidol 22 [1], pp. 21-5.

Riggs, A. D. (1975): X inactivation, differentiation, and DNA methylation, Cytogenet Cell Genet 14 [1], pp. 9-25.

Robertson, K. D. (2005): DNA methylation and human disease, Nat Rev Genet 6 [8], pp. 597-610.

Rodriguez-Osorio, N.; Wang, H.; Rupinski, J.; Bridges, S. M. and Memili, E. (2010): Comparative functional genomics of mammalian DNA methyltransferases, Reprod Biomed Online 20 [2], pp. 243-55.

Rougier, N.; Bourc'his, D.; Gomes, D. M.; Niveleau, A.; Plachot, M.; Paldi, A. and Viegas-Pequignot, E. (1998): Chromosome methylation patterns during mammalian preimplantation development, Genes Dev 12 [14], pp. 2108-13.

Rowold, D. J. and Herrera, R. J. (2000): Alu elements and the human genome, Genetica 108 [1], pp. 57-72.

Roy-Engel, A. M.; Carroll, M. L.; Vogel, E.; Garber, R. K.; Nguyen, S. V.; Salem, A. H.; Batzer, M. A. and Deininger, P. L. (2001): Alu insertion polymorphisms for the study of human genomic diversity, Genetics 159 [1], pp. 279-90.

Rubin, C. M.; VandeVoort, C. A.; Teplitz, R. L. and Schmid, C. W. (1994): Alu repeated DNAs are differentially methylated in primate germ cells, Nucleic Acids Res 22 [23], pp. 5121-7.

Sambrook, J and Russel, DW (2001): Molecular Cloning: A Laboratory Manual, 3rd. ed., Cold Spring Harbor Laboratory Press, New York, ISBN: 978-0879695774.

Sanger, F.; Air, G. M.; Barrell, B. G.; Brown, N. L.; Coulson, A. R.; Fiddes, C. A.; Hutchison, C. A.; Slocombe, P. M. and Smith, M. (1977): Nucleotide sequence of bacteriophage phi X174 DNA, Nature 265 [5596], pp. 687-95.

Santos, F.; Hendrich, B.; Reik, W. and Dean, W. (2002): Dynamic reprogramming of DNA methylation in the early mouse embryo, Dev Biol 241 [1], pp. 172-82.

Santos, K. F.; Mazzola, T. N. and Carvalho, H. F. (2005): The prima donna of epigenetics: the regulation of gene expression by DNA methylation, Braz J Med Biol Res 38 [10], pp. 1531-41.

Schmid, C. W. (1991): Human Alu subfamilies and their methylation revealed by blot hybridization, Nucleic Acids Res 19 [20], pp. 5613-7.

Schwartz, M. W.; Woods, S. C.; Porte, D., Jr.; Seeley, R. J. and Baskin, D. G. (2000): Central nervous system control of food intake, Nature 404 [6778], pp. 661-71.

Seidah, N. G.; Benjannet, S.; Hamelin, J.; Mamarbachi, A. M.; Basak, A.; Marcinkiewicz, J.; Mbikay, M.; Chretien, M. and Marcinkiewicz, M. (1999): The subtilisin/kexin family of precursor convertases. Emphasis on PC1, PC2/7B2, POMC and the novel enzyme SKI-1, Ann N Y Acad Sci 885, pp. 57-74.

Sen, S. K.; Han, K.; Wang, J.; Lee, J.; Wang, H.; Callinan, P. A.; Dyer, M.; Cordaux, R.; Liang, P. and Batzer, M. A. (2006): Human genomic deletions mediated by recombination between Alu elements, Am J Hum Genet 79 [1], pp. 41-53.

Shaikh, T. H.; Roy, A. M.; Kim, J.; Batzer, M. A. and Deininger, P. L. (1997): cDNAs derived from primary and small cytoplasmic Alu (scAlu) transcripts, J Mol Biol 271 [2], pp. 222-34.

Shen, L.; Kondo, Y.; Guo, Y.; Zhang, J.; Zhang, L.; Ahmed, S.; Shu, J.; Chen, X.; Waterland, R. A. and Issa, J. P. (2007): Genome-wide profiling of DNA methylation reveals a class of normally methylated CpG island promoters, PLoS Genet 3 [10], pp. 2023-36.

Shen, M. R.; Batzer, M. A. and Deininger, P. L. (1991): Evolution of the master Alu gene(s), J Mol Evol 33 [4], pp. 311-20.

Sherf, B.A.; Navarro, S.L.; Hannah, R.R. and Wood, K.V. (1996): Dual-Luciferase™ Reporter Assay: An advanced co-reporter technology integrating firefly and renilla luciferase assays, Promega Notes Magazine 57.

Shimada, F.; Taira, M.; Suzuki, Y.; Hashimoto, N.; Nozaki, O.; Tatibana, M.; Ebina, Y.; Tawata, M.; Onaya, T. and et al. (1990): Insulin-resistant diabetes associated with partial deletion of insulin-receptor gene, Lancet 335 [8699], pp. 1179-81.

Shuman, S. (1994): Novel approach to molecular cloning and polynucleotide synthesis using vaccinia DNA topoisomerase, J Biol Chem 269 [51], pp. 32678-84.

Siegfried, Z.; Eden, S.; Mendelsohn, M.; Feng, X.; Tsuberi, B. Z. and Cedar, H. (1999): DNA methylation represses transcription in vivo, Nat Genet 22 [2], pp. 203-6.

Siepel, A. (2009): Phylogenomics of primates and their ancestral populations, Genome Res 19 [11], pp. 1929-41.

Singer, M. F. (1982): SINEs and LINEs: highly repeated short and long interspersed sequences in mammalian genomes, Cell 28 [3], pp. 433-4.

Singh, S. M.; Murphy, B. and O'Reilly, R. L. (2003): Involvement of gene-diet/drug interaction in DNA methylation and its contribution to complex diseases: from cancer to schizophrenia, Clin Genet 64 [6], pp. 451-60.

Smit, A. F. (1999): Interspersed repeats and other mementos of transposable elements in mammalian genomes, Curr Opin Genet Dev 9 [6], pp. 657-63.

Smit, A. F. and Riggs, A. D. (1996): Tiggers and DNA transposon fossils in the human genome, Proc Natl Acad Sci U S A 93 [4], pp. 1443-8.

Solomon, S. (1999): POMC-derived peptides and their biological action, Ann N Y Acad Sci 885, pp. 22-40.

Sorek, R.; Ast, G. and Graur, D. (2002): Alu-containing exons are alternatively spliced, Genome Res 12 [7], pp. 1060-7.

Speliotes, E. K.; Willer, C. J.; Berndt, S. I.; Monda, K. L.; Thorleifsson, G.; Jackson, A. U.; Allen, H. L.; Lindgren, C. M.; Luan, J.; Magi, R.; Randall, J. C.; Vedantam, S.; Winkler, T. W.; Qi, L.; Workalemahu, T.; Heid, I. M.; Steinthorsdottir, V.; Stringham, H. M.; Weedon, M. N.; Wheeler, E.; Wood, A. R.; Ferreira, T.; Weyant, R. J.; Segre, A. V.; Estrada, K.; Liang, L.; Nemesh, J.; Park, J. H.; Gustafsson, S.; Kilpelainen, T. O.; Yang, J.; Bouatia-Naji, N.; Esko, T.; Feitosa, M. F.; Kutalik, Z.; Mangino, M.; Raychaudhuri, S.; Scherag, A.; Smith, A. V.; Welch, R.; Zhao, J. H.; Aben, K. K.; Absher, D. M.; Amin, N.; Dixon, A. L.; Fisher, E.; Glazer, N. L.; Goddard, M. E.; Heard-Costa, N. L.; Hoesel, V.; Hottenga, J. J.; Johansson, A.; Johnson, T.; Ketkar, S.; Lamina, C.; Li, S.; Moffatt, M. F.; Myers, R. H.; Narisu, N.; Perry, J. R.; Peters, M. J.; Preuss, M.; Ripatti, S.; Rivadeneira, F.; Sandholt, C.; Scott, L. J.; Timpson, N. J.; Tyrer, J. P.; van Wingerden, S.; Watanabe, R. M.; White, C. C.; Wiklund, F.; Barlassina, C.; Chasman, D. I.; Cooper, M. N.; Jansson, J. O.; Lawrence, R. W.; Pellikka, N.; Prokopenko, I.; Shi, J.; Thiering, E.; Alavere, H.; Alibrandi, M. T.; Almgren, P.; Arnold, A. M.; Aspelund, T.; Atwood, L. D.; Balkau, B.; Balmforth, A. J.; Bennett, A. J.; Ben-Shlomo, Y.; Bergman, R. N.; Bergmann, S.; Biebermann, H.; Blakemore, A. I.; Boes, T.; Bonnycastle, L. L.; Bornstein, S. R.; Brown, M. J.; Buchanan, T. A.; Busonero, F.; Campbell, H.; Cappuccio, F. P.; Cavalcanti-Proenca, C.; Chen, Y. D.; Chen, C. M.; Chines, P. S.; Clarke, R.; Coin, L.; Connell, J.; Day, I. N.; Heijer, M.; Duan, J.; Ebrahim, S.; Elliott, P.; Elosua, R.; Eiriksdottir, G.; Erdos, M. R.; Eriksson, J. G.;

Facheris, M. F.; Felix, S. B.; Fischer-Posovszky, P.; Folsom, A. R.; Friedrich, N.; Freimer, N. B.; Fu, M.; Gaget, S.; Gejman, P. V.; Geus, E. J.; Gieger, C.; Gjesing, A. P.; Goel, A.; Goyette, P.; Grallert, H.; Grassler, J.; Greenawalt, D. M.; Groves, C. J.; Gudnason, V.; Guiducci, C.; Hartikainen, A. L.; Hassanali, N.; Hall, A. S.; Havulinna, A. S.; Hayward, C.; Heath, A. C.; Hengstenberg, C.; Hicks, A. A.; Hinney, A.; Hofman, A.; Homuth, G.; Hui, J.; Igl, W.; Iribarren, C.; Isomaa, B.; Jacobs, K. B.; Jarick, I.; Jewell, E.; John, U.; Jorgensen, T.; Jousilahti, P.; Jula, A.; Kaakinen, M.; Kajantie, E.; Kaplan, L. M.; Kathiresan, S.; Kettunen, J.; Kinnunen, L.; Knowles, J. W.; Kolcic, I.; Konig, I. R.; Koskinen, S.; Kovacs, P.; Kuusisto, J.; Kraft, P.; Kvaloy, K.; Laitinen, J.; Lantieri, O.; Lanzani, C.; Launer, L. J.; Lecoeur, C.; Lehtimaki, T.; Lettre, G.; Liu, J.; Lokki, M. L.; Lorentzon, M.; Luben, R. N.; Ludwig, B.; Manunta, P.; Marek, D.; Marre, M.; Martin, N. G.; McArdle, W. L.; McCarthy, A.; McKnight, B.; Meitinger, T.; Melander, O.; Meyre, D.; Midthjell, K.; Montgomery, G. W.; Morken, M. A.; Morris, A. P.; Mulic, R.; Ngwa, J. S.; Nelis, M.; Neville, M. J.; Nyholt, D. R.; O'Donnell, C. J.; O'Rahilly, S.; Ong, K. K.; Oostra, B.; Pare, G.; Parker, A. N.; Perola, M.; Pichler, I.; Pietilainen, K. H.; Platou, C. G.; Polasek, O.; Pouta, A.; Rafelt, S.; Raitakari, O.; Rayner, N. W.; Ridderstrale, M.; Rief, W.; Ruokonen, A.; Robertson, N. R.; Rzehak, P.; Salomaa, V.; Sanders, A. R.; Sandhu, M. S.; Sanna, S.; Saramies, J.; Savolainen, M. J.; Scherag, S.; Schipf, S.; Schreiber, S.; Schunkert, H.; Silander, K.; Sinisalo, J.; Siscovick, D. S.; Smit, J. H.; Soranzo, N.; Sovio, U.; Stephens, J.; Surakka, I.; Swift, A. J.; Tammesoo, M. L.; Tardif, J. C.; Teder-Laving, M.; Teslovich, T. M.; Thompson, J. R.; Thomson, B.; Tonjes, A.; Tuomi, T.; van Meurs, J. B.; van Ommen, G. J.; Vatin, V.; Viikari, J.; Visvikis-Siest, S.; Vitart, V.; Vogel, C. I.; Voight, B. F.; Waite, L. L.; Wallaschofski, H.; Walters, G. B.; Widen, E.; Wiegand, S.; Wild, S. H.; Willemsen, G.; Witte, D. R.; Witteman, J. C.; Xu, J.; Zhang, Q.; Zgaga, L.; Ziegler, A.; Zitting, P.; Beilby, J. P.; Farooqi, I. S.; Hebebrand, J.; Huikuri, H. V.; James, A. L.; Kahonen, M.; Levinson, D. F.; Macciardi, F.; Nieminen, M. S.; Ohlsson, C.; Palmer, L. J.; Ridker, P. M.; Stumvoll, M.; Beckmann, J. S.; Boeing, H.; Boerwinkle, E.; Boomsma, D. I.; Caulfield, M. J.; Chanock, S. J.; Collins, F. S.; Cupples, L. A.; Smith, G. D.; Erdmann, J.; Froguel, P.; Gronberg, H.; Gyllensten, U.; Hall, P.; Hansen, T.; Harris, T. B.; Hattersley, A. T.; Hayes, R. B.; Heinrich, J.; Hu, F. B.; Hveem, K.; Illig, T.; Jarvelin, M. R.; Kaprio, J.; Karpe, F.; Khaw, K. T.; Kiemeney, L. A.; Krude, H.; Laakso, M.; Lawlor, D. A.; Metspalu, A.; Munroe, P. B.; Ouwehand, W. H.; Pedersen, O.; Penninx, B. W.; Peters, A.; Pramstaller, P. P.; Quertermous, T.; Reinehr, T.; Rissanen, A.; Rudan, I.; Samani, N. J.; Schwarz, P. E.; Shuldiner, A. R.; Spector, T. D.; Tuomilehto, J.; Uda, M.; Uitterlinden, A.; Valle, T. T.; Wabitsch, M.; Waeber, G.; Wareham, N. J.; Watkins, H.; Wilson, J. F.; Wright, A. F.; Zillikens, M. C.; Chatterjee, N.; McCarroll, S. A.; Purcell, S.; Schadt, E. E.; Visscher, P. M.; Assimes, T. L.; Borecki, I. B.; Deloukas, P.; Fox, C. S.; Groop, L. C.; Haritunians, T.; Hunter, D. J.; Kaplan, R. C.; Mohlke, K. L.; O'Connell, J. R.; Peltonen, L.; Schlessinger, D.; Strachan, D. P.; van Duijn, C. M.; Wichmann, H. E.; Frayling, T. M.; Thorsteinsdottir, U.; Abecasis, G. R.; Barroso, I.; Boehnke, M.; Stefansson, K.; North, K. E.; McCarthy, M. I.; Hirschhorn, J. N.; Ingelsson, E. and Loos, R. J. (2010): Association analyses of 249,796 individuals reveal 18 new loci associated with body mass index, Nat Genet 42 [11], pp. 937-48.

Spiegelman, B. M. and Heinrich, R. (2004): Biological control through regulated transcriptional coactivators, Cell 119 [2], pp. 157-67.

St Clair, D.; Xu, M.; Wang, P.; Yu, Y.; Fang, Y.; Zhang, F.; Zheng, X.; Gu, N.; Feng, G.; Sham, P. and He, L. (2005): Rates of adult schizophrenia following prenatal exposure to the Chinese famine of 1959-1961, JAMA 294 [5], pp. 557-62.

Steegers-Theunissen, R. P.; Obermann-Borst, S. A.; Kremer, D.; Lindemans, J.; Siebel, C.; Steegers, E. A.; Slagboom, P. E. and Heijmans, B. T. (2009): Periconceptional maternal folic acid use of 400 microg per day is related to increased methylation of the IGF2 gene in the very young child, PLoS One 4 [11], p. e7845.

Stein, R.; Gruenbaum, Y.; Pollack, Y.; Razin, A. and Cedar, H. (1982a): Clonal inheritance of the pattern of DNA methylation in mouse cells, Proc Natl Acad Sci U S A 79 [1], pp. 61-5.

Stein, R.; Razin, A. and Cedar, H. (1982b): In vitro methylation of the hamster adenine phosphoribosyltransferase gene inhibits its expression in mouse L cells, Proc Natl Acad Sci U S A 79 [11], pp. 3418-22.

Straussman, R.; Nejman, D.; Roberts, D.; Steinfeld, I.; Blum, B.; Benvenisty, N.; Simon, I.; Yakhini, Z. and Cedar, H. (2009): Developmental programming of CpG island methylation profiles in the human genome, Nat Struct Mol Biol 16 [5], pp. 564-71.

Strout, M. P.; Marcucci, G.; Bloomfield, C. D. and Caligiuri, M. A. (1998): The partial tandem duplication of ALL1 (MLL) is consistently generated by Alu-mediated homologous recombination in acute myeloid leukemia, Proc Natl Acad Sci U S A 95 [5], pp. 2390-5.

Stunkard, A. J.; Foch, T. T. and Hrubec, Z. (1986): A twin study of human obesity, JAMA 256 [1], pp. 51-4.

Takahashi, H.; Hakamata, Y.; Watanabe, Y.; Kikuno, R.; Miyata, T. and Numa, S. (1983): Complete nucleotide sequence of the human corticotropin-beta-lipotropin precursor gene, Nucleic Acids Res 11 [19], pp. 6847-58.

Talens, R. P.; Boomsma, D. I.; Tobi, E. W.; Kremer, D.; Jukema, J. W.; Willemsen, G.; Putter, H.; Slagboom, P. E. and Heijmans, B. T. (2010): Variation, patterns, and temporal stability of DNA methylation: considerations for epigenetic epidemiology, FASEB J 24 [9], pp. 3135-44.

Tanaka, Y.; Yamashita, R.; Suzuki, Y. and Nakai, K. (2010): Effects of Alu elements on global nucleosome positioning in the human genome, BMC Genomics 11, p. 309.

Tang, W. Y. and Ho, S. M. (2007): Epigenetic reprogramming and imprinting in origins of disease, Rev Endocr Metab Disord 8 [2], pp. 173-82.

Tate, P. H. and Bird, A. P. (1993): Effects of DNA methylation on DNA-binding proteins and gene expression, Curr Opin Genet Dev 3 [2], pp. 226-31.

Thorleifsson, G.; Walters, G. B.; Gudbjartsson, D. F.; Steinthorsdottir, V.; Sulem, P.; Helgadottir, A.; Styrkarsdottir, U.; Gretarsdottir, S.; Thorlacius, S.; Jonsdottir, I.; Jonsdottir, T.; Olafsdottir, E. J.; Olafsdottir, G. H.; Jonsson, T.; Jonsson, F.; Borch-Johnsen, K.; Hansen, T.; Andersen, G.; Jorgensen, T.; Lauritzen, T.; Aben, K. K.; Verbeek, A. L.; Roeleveld, N.; Kampman, E.; Yanek, L. R.; Becker, L. C.; Tryggvadottir, L.; Rafnar, T.; Becker, D. M.; Gulcher, J.; Kiemeney, L. A.; Pedersen, O.; Kong, A.; Thorsteinsdottir, U. and Stefansson, K. (2009): Genome-wide association yields new sequence variants at seven loci that associate with measures of obesity, Nat Genet 41 [1], pp. 18-24.

Tobi, E. W.; Lumey, L. H.; Talens, R. P.; Kremer, D.; Putter, H.; Stein, A. D.; Slagboom, P. E. and Heijmans, B. T. (2009): DNA methylation differences after exposure to prenatal famine are common and timing- and sex-specific, Hum Mol Genet 18 [21], pp. 4046-53.

Tost, J.; Jammes, H.; Dupont, J. M.; Buffat, C.; Robert, B.; Mignot, T. M.; Mondon, F.; Carbonne, B.; Simeoni, U.; Grange, G.; Kerjean, A.; Ferre, F.; Gut, I. G. and Vaiman, D. (2006): Non-random, individual-specific methylation profiles are present at the sixth CTCF binding site in the human H19/IGF2 imprinting control region, Nucleic Acids Res 34 [19], pp. 5438-48.

Trasler, J.; Deng, L.; Melnyk, S.; Pogribny, I.; Hiou-Tim, F.; Sibani, S.; Oakes, C.; Li, E.; James, S. J. and Rozen, R. (2003): Impact of Dnmt1 deficiency, with and without low folate diets, on tumor numbers and DNA methylation in Min mice, Carcinogenesis 24 [1], pp. 39-45.

Tsukada, T.; Watanabe, Y.; Nakai, Y.; Imura, H.; Nakanishi, S. and Numa, S. (1982): Repetitive DNA sequences in the human corticotropin-beta-lipotrophin precursor gene region: Alu family members, Nucleic Acids Res 10 [5], pp. 1471-9.

Turker, M. S. (1999): The establishment and maintenance of DNA methylation patterns in mouse somatic cells, Semin Cancer Biol 9 [5], pp. 329-37.

Turker, M. S. (2002): Gene silencing in mammalian cells and the spread of DNA methylation, Oncogene 21 [35], pp. 5388-93.

Turker, M. S. and Bestor, T. H. (1997): Formation of methylation patterns in the mammalian genome, Mutat Res 386 [2], pp. 119-30.

Ullu, E. and Tschudi, C. (1984): Alu sequences are processed 7SL RNA genes, Nature 312 [5990], pp. 171-2.

Urdinguio, R. G.; Sanchez-Mut, J. V. and Esteller, M. (2009): Epigenetic mechanisms in neurological diseases: genes, syndromes, and therapies, Lancet Neurol 8 [11], pp. 1056-72.

Vaissiere, T.; Sawan, C. and Herceg, Z. (2008): Epigenetic interplay between histone modifications and DNA methylation in gene silencing, Mutat Res 659 [1-2], pp. 40-8.

Vasicek, T. J.; Zeng, L.; Guan, X. J.; Zhang, T.; Costantini, F. and Tilghman, S. M. (1997): Two dominant mutations in the mouse fused gene are the result of transposon insertions, Genetics 147 [2], pp. 777-86.

Vertino, P. M.; Yen, R. W.; Gao, J. and Baylin, S. B. (1996): De novo methylation of CpG island sequences in human fibroblasts overexpressing DNA (cytosine-5-)-methyltransferase, Mol Cell Biol 16 [8], pp. 4555-65.

Vidaud, D.; Vidaud, M.; Bahnak, B. R.; Siguret, V.; Gispert Sanchez, S.; Laurian, Y.; Meyer, D.; Goossens, M. and Lavergne, J. M. (1993): Haemophilia B due to a de novo insertion of a human-specific Alu subfamily member within the coding region of the factor IX gene, Eur J Hum Genet 1 [1], pp. 30-6.

Waddington, Conrad Hal (1957): The Strategy of The Genes, George Allen & Unwin, London.

Wagener, A.; Schmitt, A. O.; Aksu, S.; Schlote, W.; Neuschl, C. and Brockmann, G. A. (2006): Genetic, sex, and diet effects on body weight and obesity in the Berlin Fat Mouse Inbred lines, Physiol Genomics 27 [3], pp. 264-70.

Wallace, M. R.; Andersen, L. B.; Saulino, A. M.; Gregory, P. E.; Glover, T. W. and Collins, F. S. (1991): A de novo Alu insertion results in neurofibromatosis type 1, Nature 353 [6347], pp. 864-6.

Walsh, C. P.; Chaillet, J. R. and Bestor, T. H. (1998): Transcription of IAP endogenous retroviruses is constrained by cytosine methylation, Nat Genet 20 [2], pp. 116-7.

Walter, J. and Paulsen, M. (2003): Imprinting and disease, Semin Cell Dev Biol 14 [1], pp. 101-10.

Wang, J.; Liu, R.; Hawkins, M.; Barzilai, N. and Rossetti, L. (1998): A nutrient-sensing pathway regulates leptin gene expression in muscle and fat, Nature 393 [6686], pp. 684-8.

Wang, Y. and Lobstein, T. (2006): Worldwide trends in childhood overweight and obesity, Int J Pediatr Obes 1 [1], pp. 11-25.

Waterland, R. A. (2009a): Early environmental effects on epigenetic regulation in humans, Epigenetics 4 [8], pp. 523-5.

Waterland, R. A. (2009b): Is epigenetics an important link between early life events and adult disease?, Horm Res 71 Suppl 1, pp. 13-6.

Waterland, R. A. and Jirtle, R. L. (2003): Transposable elements: targets for early nutritional effects on epigenetic gene regulation, Mol Cell Biol 23 [15], pp. 5293-300.

Waterland, R. A.; Kellermayer, R.; Laritsky, E.; Rayco-Solon, P.; Harris, R. A.; Travisano, M.; Zhang, W.; Torskaya, M. S.; Zhang, J.; Shen, L.; Manary, M. J. and Prentice, A. M. (2011): Season of conception in rural gambia affects DNA methylation at putative human metastable epialleles, PLoS Genet 6 [12], p. e1001252.

Waterland, R. A.; Travisano, M.; Tahiliani, K. G.; Rached, M. T. and Mirza, S. (2008): Methyl donor supplementation prevents transgenerational amplification of obesity, Int J Obes (Lond) 32 [9], pp. 1373-9.

Weaver, I. C.; Cervoni, N.; Champagne, F. A.; D'Alessio, A. C.; Sharma, S.; Seckl, J. R.; Dymov, S.; Szyf, M. and Meaney, M. J. (2004): Epigenetic programming by maternal behavior, Nat Neurosci 7 [8], pp. 847-54.

Whitelaw, N. C. and Whitelaw, E. (2006): How lifetimes shape epigenotype within and across generations, Hum Mol Genet 15 Spec No 2, pp. R131-7.

Whitfeld, P. L.; Seeburg, P. H. and Shine, J. (1982): The human pro-opiomelanocortin gene: organization, sequence, and interspersion with repetitive DNA, DNA 1 [2], pp. 133-43. URL: http://www.ncbi.nlm.nih.gov/entrez/query.fcgi?cmd=Retrieve&db=PubMed&dopt=Citation&list_uids=6299668

WHO (2000): Obesity: preventing and managing the global epidemic. Report of a WHO consultation, World Health Organ Tech Rep Ser 894, pp. i-xii, 1-253.

Widiker, S.; Karst, S.; Wagener, A. and Brockmann, G. A. (2010): High-fat diet leads to a decreased methylation of the Mc4r gene in the obese BFMI and the lean B6 mouse lines, J Appl Genet 51 [2], pp. 193-7.

Wikberg, J. E. (1999): Melanocortin receptors: perspectives for novel drugs, Eur J Pharmacol 375 [1-3], pp. 295-310.

Wilson, A. S.; Power, B. E. and Molloy, P. L. (2007): DNA hypomethylation and human diseases, Biochim Biophys Acta 1775 [1], pp. 138-62.

Wilson, V. L. and Jones, P. A. (1983): DNA methylation decreases in aging but not in immortal cells, Science 220 [4601], pp. 1055-7.

Wilson, V. L.; Smith, R. A.; Ma, S. and Cutler, R. G. (1987): Genomic 5-methyldeoxycytidine decreases with age, J Biol Chem 262 [21], pp. 9948-51.

Wolff, G. L.; Kodell, R. L.; Moore, S. R. and Cooney, C. A. (1998): Maternal epigenetics and methyl supplements affect agouti gene expression in Avy/a mice, FASEB J 12 [11], pp. 949-57.

Wolffe, A. P. and Matzke, M. A. (1999): Epigenetics: regulation through repression, Science 286 [5439], pp. 481-6.

Wong, A. H.; Gottesman, II and Petronis, A. (2005): Phenotypic differences in genetically identical organisms: the epigenetic perspective, Hum Mol Genet 14 Spec No 1, pp. R11-8.

Woods, S. C.; Seeley, R. J.; Porte, D., Jr. and Schwartz, M. W. (1998): Signals that regulate food intake and energy homeostasis, Science 280 [5368], pp. 1378-83.

Xie, H.; Wang, M.; Bonaldo Mde, F.; Rajaram, V.; Stellpflug, W.; Smith, C.; Arndt, K.; Goldman, S.; Tomita, T. and Soares, M. B. (2010): Epigenomic analysis of Alu repeats in human ependymomas, Proc Natl Acad Sci U S A 107 [15], pp. 6952-7.

Xie, H.; Wang, M.; Bonaldo Mde, F.; Smith, C.; Rajaram, V.; Goldman, S.; Tomita, T. and Soares, M. B. (2009): High-throughput sequence-based epigenomic analysis of Alu repeats in human cerebellum, Nucleic Acids Res 37 [13], pp. 4331-40.

Xing, J.; Witherspoon, D. J.; Ray, D. A.; Batzer, M. A. and Jorde, L. B. (2007): Mobile DNA elements in primate and human evolution, Am J Phys Anthropol Suppl 45, pp. 2-19.

Xu, B.; Goulding, E. H.; Zang, K.; Cepoi, D.; Cone, R. D.; Jones, K. R.; Tecott, L. H. and Reichardt, L. F. (2003): Brain-derived neurotrophic factor regulates energy balance downstream of melanocortin-4 receptor, Nat Neurosci 6 [7], pp. 736-42.

Yach, D.; Stuckler, D. and Brownell, K. D. (2006): Epidemiologic and economic consequences of the global epidemics of obesity and diabetes, Nat Med 12 [1], pp. 62-6.

Yamada, Y.; Watanabe, H.; Miura, F.; Soejima, H.; Uchiyama, M.; Iwasaka, T.; Mukai, T.; Sakaki, Y. and Ito, T. (2004): A comprehensive analysis of allelic methylation status of CpG islands on human chromosome 21q, Genome Res 14 [2], pp. 247-66.

Yang, W.; Kelly, T. and He, J. (2007): Genetic epidemiology of obesity, Epidemiol Rev 29, pp. 49-61.

Yasuda, T.; Masaki, T.; Kakuma, T. and Yoshimatsu, H. (2004): Hypothalamic melanocortin system regulates sympathetic nerve activity in brown adipose tissue, Exp Biol Med (Maywood) 229 [3], pp. 235-9.

Yaswen, L.; Diehl, N.; Brennan, M. B. and Hochgeschwender, U. (1999): Obesity in the mouse model of pro-opiomelanocortin deficiency responds to peripheral melanocortin, Nat Med 5 [9], pp. 1066-70.

Yates, P. A.; Burman, R. W.; Mummaneni, P.; Krussel, S. and Turker, M. S. (1999): Tandem B1 elements located in a mouse methylation center provide a target for de novo DNA methylation, J Biol Chem 274 [51], pp. 36357-61.

Ye, L.; Li, X.; Kong, X.; Wang, W.; Bi, Y.; Hu, L.; Cui, B. and Ning, G. (2005): Hypomethylation in the promoter region of POMC gene correlates with ectopic overexpression in thymic carcinoids, J Endocrinol 185 [2], pp. 337-43.

Yoder, J. A.; Soman, N. S.; Verdine, G. L. and Bestor, T. H. (1997a): DNA (cytosine-5)-methyltransferases in mouse cells and tissues. Studies with a mechanism-based probe, J Mol Biol 270 [3], pp. 385-95.

Yoder, J. A.; Walsh, C. P. and Bestor, T. H. (1997b): Cytosine methylation and the ecology of intragenomic parasites, Trends Genet 13 [8], pp. 335-40.

Youngson, N. A. and Whitelaw, E. (2008): Transgenerational epigenetic effects, Annu Rev Genomics Hum Genet 9, pp. 233-57.

Zhu, Z. Z.; Hou, L.; Bollati, V.; Tarantini, L.; Marinelli, B.; Cantone, L.; Yang, A. S.; Vokonas, P.; Lissowska, J.; Fustinoni, S.; Pesatori, A. C.; Bonzini, M.; Apostoli, P.; Costa, G.; Bertazzi, P. A.; Chow, W. H.; Schwartz, J. and Baccarelli, A. (2010): Predictors of global methylation levels in blood DNA of healthy subjects: a combined analysis, Int J Epidemiol.

8 Appendix

8.1 List of figures

8.2 List of tables

8.3 List of abbreviations

Abbreviation	
ACTH	Adrenocorticotropic hormone
ADCY3	Adenylate cyclase 3
AgRP	Agouti-related peptide
ARC	Nucleus arcuatus
A^{vy}	'Viable yellow agouti' allele of the agouti gene
Axin^{Fu}	'Axin fused' allele
BamHI	Restriction enzyme with recognition site 5'-G'GATCC-3'
BDNF	Brain-derived neurotropic factor
BFMI860	Mouse strain, considered as predisposed for obesity
BMI	Body Mass Index
bp	Base pair(s)
BSA	Bovine serum albumin
^{m}C	Methylated Cytosine
C57BL/6	Mouse strain, considered as lean wild type strain
ChIP	Chromatin immunoprecipitation assays
CGI	CpG island
CPE	Carboxypeptidase E
CpG	5'-Cytosine-Guanine-3' dinucleotide
DMEM	Dulbecco`s Modified Eagle Medium
DNA	Deoxyribonucleic acid
DPZ	Deutsches Primaten Zentrum GgöttGöttingen
DTT	Dithiothreitol
EDTA	Ethylenediaminetetraacetic acid
EMSA	Electrophoretic mobility shift assay
Ep300 gene	E1A binding protein p300
EtBr	Ethidium bromide
Exo	ExonucleaseI
GPCR	G protein-coupled receptor
GT1-7	Murine hypothalamic tumor cell line with neuronal morphology
H_2O	Deionized water
H_2O_{HPLC}	Water in HPLC-quality
HhaI	HhaI methyltransferase with target site 5'-GCGC-3'
HpaII	HpaII methyltransferase with target site 5'-CCGG-3'
kD	Kilodalton
LB	Lysogeny broth (also known as Luria broth); a nutritionally rich medium
Ma	Million annos
MC1R	Melanocortin-1-Receptor
	Melanocortin-4-Receptor
MCS	Multiple cloning site

MSH	Melanocyte-stimulating hormone
NcoI	Restriction enzyme with recognition site 5’-C'CATGG-3’
NMRI	Mouse strain, considered as wild type
NPY	Neuropeptide Y
ObR	Leptin receptor (also known as LepR)
OD	Optical density
PBC	Peripheral Blood Cells
PBS	Phosphate buffered saline
PC1	Protein convertases 1
PC2	Protein convertases 2
pCpGL	Luciferase-containing plasmid vector with a CpG-free backbone
PCR	Polymerase Chain Reaction
POMC	(Pre-)Proopiomelanocortin
PVN	Nucleus paraventricularis
RNA	Ribonucleic acid
SAP	Shrimp Alkaline Phosphatase
SNP	Single Nucleotide Polymorphism
SssI	CpG methyltransferase with target site 5’-CG-3’
STAT	Signal Transducer and Activator of Transcription
T4	Enterobacteria phage T4
Taq	Taq polymerase; after the thermophilic bacterium Thermus aquaticus
TBE buffer	Tris/Borate/EDTA buffer
TOPO vector	Vector with DNA topoisomerase I activity
TrkB	Tropomyosin Related Kinase B
TSS	Transcription start site
UV	Ultraviolet light, wavelength = 10 – 400 nm
WT	Wild type
X-gal	5-bromo-4-chloro-3-indolyl- beta-D- galactopyranoside

Eigenständigkeitserklärung

Ich, Mona Mischke, erkläre hiermit, dass ich die Arbeit mit dem Titel ‚DNA Methylation of the POMC Gene: Ontogenetic, Phylogenetic, and Functional Aspects' selbstständig und ausschließlich unter Verwendung der angegebenen Hilfsmittel angefertigt habe. Des Weiteren erkläre ich meine Kenntnisnahme der dem angestrebten Verfahren zugrunde liegenden Promotionsordnung. Ich habe mich anderwärts nicht um einen Doktorgrad beworben und bin nicht im Besitz eines entsprechenden Doktorgrades.

Berlin, den Unterschrift